Ecophysiological Investigation of UV-B Tolerance of Beech Saplings (*Fagus sylvatica* L.)

Réka LÁPOSI* – Szilvia VERES – Ilona MÉSZÁROS

Department of Botany, University of Debrecen, Debrecen, Hungary

Abstract – Our work aimed to reveal UV-B sensitivity of beech both in field, and in outdoor conditions. We examined the role of UV-B radiation in activation of photoprotective mechanisms in photoinhibition and photodamage of photosynthetic apparatus under hight light intensity. Our results indicate that under natural irradiances increase of carotenoid content - especially xantophyll cycle pigments - and xantophyll cycle activity resulted in not only by visible light but also by UV-B radiation. These pigments have important role in photoprotective processes of photosynthetic apparatus. Amount of these pigments decreased under UV-B exclusion, increased under UV-B exposure, similarly to the UV-B absorbing compounds, which responded susceptibly to changes of UV-B level. These results may suggest that high UV-B tolerance of beech is due to the considerable flavonoid accumulation, which may explain practically unaltered physiological activity of photosynthetic apparatus under UV-B exposition, as these compounds have antioxidant capacity, thus they can reduce lipid peroxidation and damage of photosynthetic apparatus.

enhanced UV-B / UV-B exclusion / photosynthetic pigments / chlorophyll fluorescence / UV-B absorbing compounds

Kivonat – A bükk (*Fagus sylvatica* L.) UV-B érzékenységének ökofiziológiai vizsgálata. Munkánk során az UV-B sugárzás (természetes és emelt szintű) hatásait vizsgáltuk egy hazai erdőalkotó fafaj, a bükk újulatainak ökofiziológiai válaszreakcióira termőhelyi feltételek között és szabadföldi kísérletben. Tanulmányoztuk, hogy a levelekben a fényvédő mechanizmusok aktiválásában, illetve az intenzív napsugárzás alatt fellépő fotoszintézis gátlásban és a fotoszintetikus apparátus károsodásában a látható tartomány mellett milyen mértékben játszik szerepet a természetes UV-B sugárzás. Vizsgáltuk azt is, hogy az emelt szintű UV-B sugárzással szemben milyen a bükk levelekben a fotoszintetikus apparátus védelmét ellátó mechanizmusok hatékonysága.

Eredményeink azt mutatják, hogy természetes fényviszonyok között a fényvédő karotinoidok, ezen belül a xantofill-ciklus pigmentjeinek mennyisége és a ciklus aktivitása nemcsak a látható fény, hanem az UV-B sugárzás hatására is változik. UV-B megvonásnál a levelekben csökkent a mennyiségük, emelt szintű UV-B hatására nőtt, ahogyan az megfigyelhető volt a flavonoid típusú vegyületek esetében is, amelyek a legérzékenyebben reagáltak az UV-B szint megváltozására, és mivel UV-B szűrő képességük mellett antioxidáns tulajdonsággal is rendelkeznek így a fotoszintetizáló szövetek aktivitása viszonylag változatlan maradt.

emelt szintű UV-B sugárzás / UV-B megvonás / fotoszintetikus pigmentek / klorofill fluoreszcencia / UV-B szűrő pigmentek

* Corresponding author: laposir@karolyrobert.hu; H-4032 DEBRECEN, Egyetem tér 1.

1 INTRODUCTION

Owing to the drastic decrease of stratospheric ozone layer in the last two decades studies rightly focused on examination of the potential destructive and inhibiting effects of UV-B radiation (Madronich et al. 1998). In spite of the efforts to restrict the production of ozone depleting substances in the 1990s, thinning of the stratospheric ozone layer and increased penetration of UV-B radiation to the Earth surface will continue. The annually averaged global ozone loss is approximately 3%, but it is not equable over the two hemisphere (McKenzie et al. 2003). Severe declines will occur in years 2010-2019 in the northern hemisphere, that may result up to 50-60% increase in UV-B radiation in springtime (Schindell et al. 1998). Beside ozone depletion UV-B radiation reaching the Earth's surface is influenced by global climate change (clouds, snow-cover), air pollutants, aerosols furthermore slowing ozone recovery due to the warming of troposphere (McKenzie et al. 2003).

UV-B radiation is an important stress factor for plants, which can have direct and indirect effects on the genetic system, the photosynthetic apparatus, and membrane lipids (Björn 1996). UV-B may also play an important ecological role in altering plant growth and competitive ability, with a resultant impact on plant community composition (Sullivan 2005). These indirect effects include changes in the susceptibility of plants to attack by insects and pathogens in both agricultural and natural ecosystems, and changes in nutrient cycling (Caldwell et al. 1998).

Few studies have been carried out on temperate, angiosperm tree species under natural conditions, in spite of that long lived trees may be the most impacted by the changing present-day levels of UV-B radiation owing to the permanent exposure and the accumulation of the effects (Johanson et al. 1995). Plants under field conditions have to cope with several stress factors. Protective mechanisms of well adapted species (to high light intensity, high temperature, water deficit etc.) may be effective against increasing UV-B radiation (Mészáros et al. 2001). However plant species - moreover populations - vary greatly in their response to UV-B: negative, neutral as well as positive effects on plant performance have been reported, which suggest that some plant species may be well adapted to UV-B radiation while others are not. Furthermore the plant response to UV-B seems to depend on experimental set up, treatment regimes and duration (Searles et al. 2001).

Our work aimed to examine possible harmful effects of present and enhanced UV-B radiation on ecophysiological responses of beech (*Fagus sylvatica* L.) both in field, and in outdoor conditions. European beech is one of the major tree species in natural plant associations in Central Europe, and it is characterized by substantial capacity to acclimate to high light intensities. We examined the role of UV-B radiation in activation of photoprotective mechanisms (xantophyll cycle), furthermore in photoinhibition and photodamage of photosynthetic apparatus under hight light intensity. We also studied under enhanced UV-B the efficiency of photoprotective mechanisms in beech leaves, which provide defence for photosynthetic apparatus. In both experimental sites our attention was focused on indicators of UV-B sensitivity and tolerance (Smith et al. 2000), namely changes of photosynthetic pigment composition (chlorophylls and carotenoids), chlorophyll fluorescence parameters of dark and light adapted leaves, and accumulation of UV-B absorbing compounds. We also examined activity of photoprotective xantofill cycle, furthermore changes of water content in leaves, mesophyll succulence index and specific leaf mass, which indicate alterations in leaf anatomy.

2 MATERIALS AND METHODS

2.1 UV-B exclusion in the forest site

Field studies were performed in a beech forest site ("Rejtek Research Site", Bükk Mountains, NE Hungary), where in 1981 a part of the 80 years old forest has been clear-cut for research purposes. In order to examine effects of ambient UV-B radiation in the clear-cut area before budding time beech branches were covered with perforated polyester plastic film, which manipulated the spectral balance of natural irradiance, that is UV-B/PAR ratio considerably decreased. This treatment provided comparable growing conditions for shoots and leaves. Effects of UV-B exclusion (90%<) were determined on seedlings growing in the clear-cut area, and in parallel with it comparative measurements were carried out in the southern exposured forest edge and forest interior.

2.2 Outdoor UV-B manipulation in the Botanical Garden

The experiments on UV-B exposure and exclusion have been performed in an outdoor experimental site at the Botanical Garden of Debrecen University. Two year old beech seedlings were planted into 4 l plastic containers and were burried to 30 cm depth in the sandy soil of 1.5×1.5 m plots. A set of the plants were exposed to enhanced UV-B radiation besides the natural radiation using timer-controlled UV-B supplementation system (fluorescent tubes type UV-B 313, Q-Panel, Cleveland, USA). The tubes were wrapped with 0.1mm cellulose acetate filter (Courtaulds, Chemicals, Derby, UK) to eliminate UV-C radiation and it was changed weekly. In the control plot plants recieved only natural solar radiation. Plants were exposed to UV-B radiation at three intensity levels following daily fluctuation of natural irradiance. Midday maximum of extra UV-B was approximately 40% higher (+80 □W cm-2) than the ambient level. Concerning the experimental conditions in other UV-B studies it can be regarded as a moderatly elevated UV-B dose (McLeod 1997).

For UV-B exclusion seedlings were placed under a roof-shaped tent covered with polyester film. The northern part of the frame was uncovered by foil and slits were left in order to provide adequate air circulation. During the experiments (2000-2002) the water supply of the seedlings was equal in all plots. UV-B supplementation and exclusion treatments started before budding stage and it ran to September.

2.3 Chlorophyll fluorescence measurements

In vivo chlorophyll *a* fluorescence was measured with a portable PAM 2000 fluorometer (WALZ Germany) after 20 min dark adaptation period. Fast (F_0, F_m, F_v/F_m) and slow ($\Delta F/F_m'$, NPQ, RFD) chlorophyll fluorescence induction parameters were calculated by the equations of Schreiber et al. (1994). Slow chlorophyll fluorescence induction was analysed by saturation pulse method after 5 minutes illumination of the leaves with two different actinic light intensities (200 and 1000 μmol m^{-2} s^{-1}).

2.4 Photosynthetic pigments and UV-B absorbing compounds

Photosynthetic pigments were extracted from the leaves with 80% acetone. Absorbances of pigment extract were measured at 470; 646,8; 663,2 nm with Shimadzu UV/VIS 1601 spectrophotometer. Equations of Wellburn (1994) were used to calculate the chlorophyll *a* and *b* concentrations. Carotenoid composition was analyzed by reverse phase HPLC (UV/VIS HPLC, Jasco, Japan; Eluenses: ethylacetate, acetonitrile: water 9:1; Column: Nucleosil C18, 5μ) method (Mészáros et al. 1995) with application of zeaxanthin standard. Chlorophyll content was expressed on dry weight (mg g^{-1}), carotenoids and xanthophyll cycle pigments were

expressed on chlorophyll content (mmol mol^{-1} chl a+b). The de-epoxidation state of xanthophyll cycle (Demmig-Adams - Adams 1992) was calculated as

DEEPS = (zeaxanthin+0.5×antheraxanthin)/violaxanthin+antheraxanthin+zeaxanthin).

Accumulation of UV-B absorbing compounds in leaves was determined spectrophotometrically from acidified methanol extract (Day 1993). Flavonoid accumulation was expressed as cumulative absorbance of leaf extract at 280-300 nm related to leaf dry weight (g), fresh weight (g) and leaf unit area (cm^2) suggested by Qi et al. (2003).

Actual water content of leaves was determined by thermogravimetric method, after drying at 85 ^oC till weight ceaselessness. Water content of samplings were expressed on fresh leaf weight (WC%). Mesophyll succulence was determined by chlorophyll and water content (gH_2O mg^{-1} chl).

2.5 Statistical analysis

Effects of UV-B exclusion and enhanced UV-B were evaluated by one-way ANOVA. Multiple range tests (95% confidence intervals method) were performed to assess differences between the treatments and to indentify homogenous groups (LSD, Tukey-b rest). Significant differences were determined at *P≤0.05, **P≤0.01, ***P≤0.001. Effects of different light conditions on photosynthesis physiological parameters were analysed using multivariate statistical methods. Classification methods (discriminant analysis) were used for reconnaisance of the similarity using SPSS 11.0 software.

3 RESULTS

3.1 Effects of UV-B exclusion in field and in outdoor experiment

In field it could be generally observed that under UV-B exclusion leaves had lower chlorophyll *a/b* ratio, total carotenoid content, amount of photoprotective xantophyll cycle pigments, mesophyll succulence and accumulation of UV-B absorbing compounds. Moreover in young leaves activity of the xantophyll cycle (DEEPS) was also lower than in leaves under natural irradiances. We have shown that significant effects of UV-B exclusion was considerable on young leaves in contrast to the results from the whole growing season, because during senescence differences between leaves under UV-B exclusion and ambient UV-B might be reduced (Láposi et al. 2002). Besides well-known daily changes of some parameters (chlorophyll and water content, DEEPS, F_v/F_m) we also obtained an increase in VAZ/total carotenoid ratio parallel with a decrease in β-carotene/total carotenoid ratio in beech leaves, moreover flavonoid content of leaves was also higher at noon. Daily changes of some parameters were different under UV-B exclusion and under ambient UV-B. In UV-B excluded beech leaves midday decrease of chlorophyll and water content were less expressed, but increase of flavonoid content and decrease of F_v/F_m were larger extent than in leaves under ambient UV-B. UV-B exclusion did not affect daily changes of other examined physiological parameters in beech leaves *(Figure 1).*

From May to September we obtained less extent of decrease in chlorophyll and water content (thus increase in mesophyll succulence) in leaves under UV-B exclusion compared to the leaves under ambient UV-B. Furthermore under UV-B exclusion we have found that midday maximum of DEEPS in beech leaves decreased during the growing season *(Figure 2).*

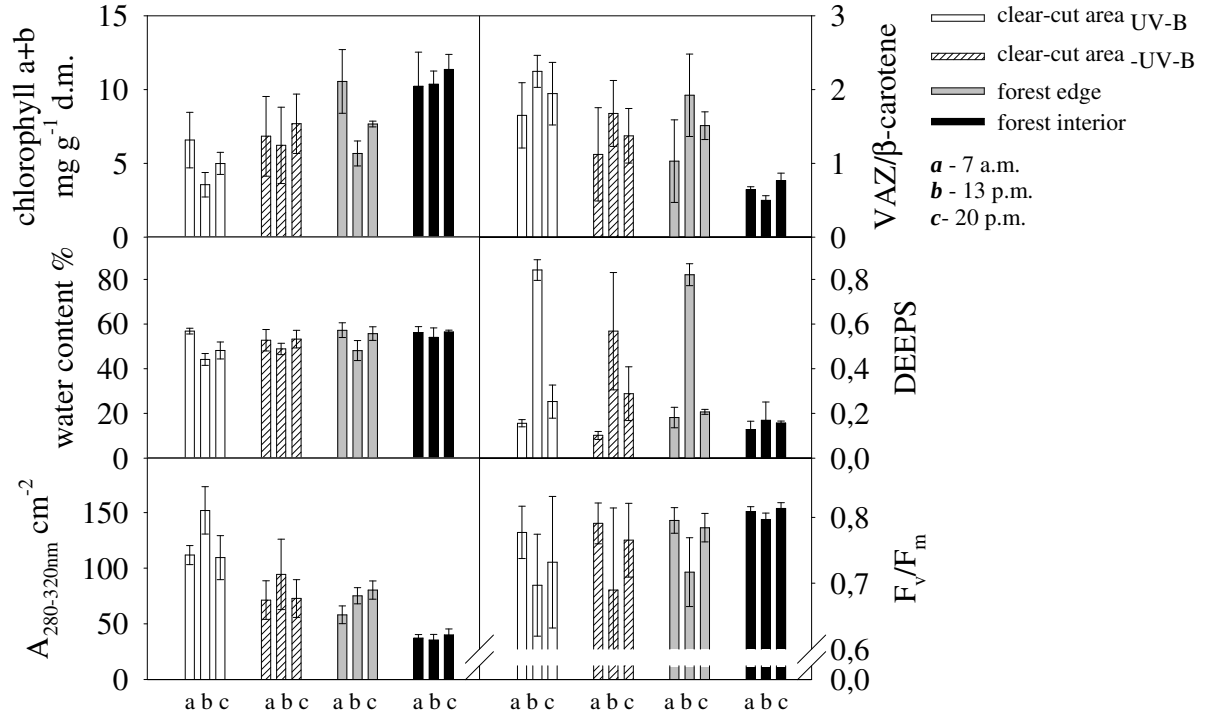

Figure 1. Daily changes of measured parameters of beech leaves in the field experiment (Rejtek Research Site, 08/07/2002) (n=6±SD).

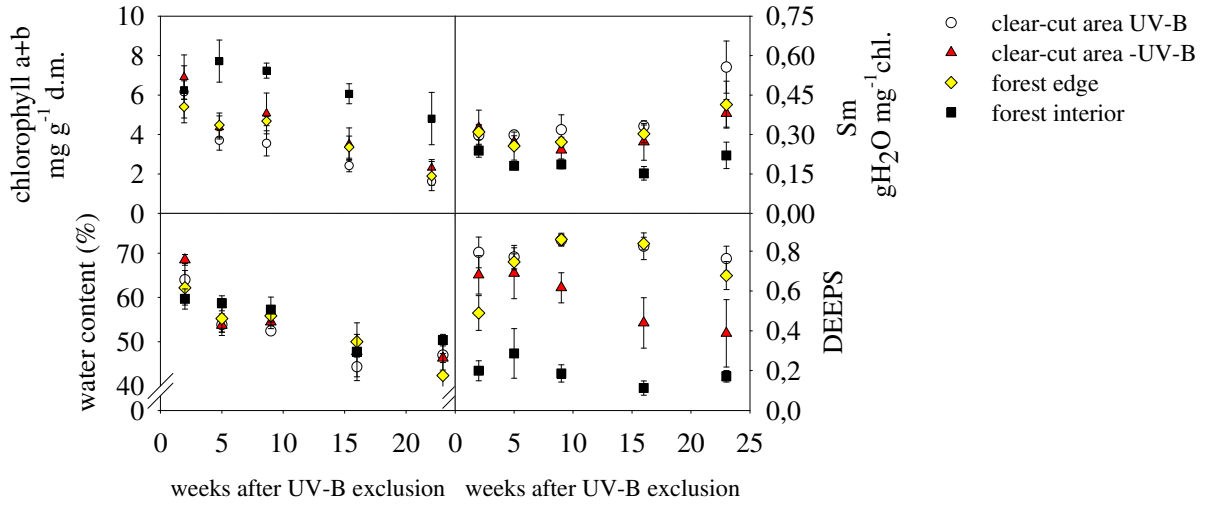

Figure 2. Seasonal changes of midday values of measured parameters in the field experiment (Rejtek Research Site, 2000) (n=3-6±SD).

In outdoor experiment effects of UV-B exclusion were non significant on the photosynthetic pigment composition and photochemical activity of beech leaves, but at noon the amount of UV-B absorbing compounds was lower than in leaves under ambient UV-B (Láposi et al. 2002). It was very hard to establish obvious significant changes on basis of dark adapted chlorophyll fluorescence parameters. In field beech leaves under UV-B exclusion had higher basal (F_0) and maximal fluorescence (F_m), furthermore higher maximal photochemical efficiency of PSII (F_v/F_m) based on morning values, which probably caused by higher amount

of chlorophyll in leaves. At noon under high light intensity differences decreased between leaves under different light climate *(Figure 1).* In outdoor experiment differences between morning and midday values of F_m and F_v/F_m decreased during growing season especially under UV-B exclusion *(Figure 3).*

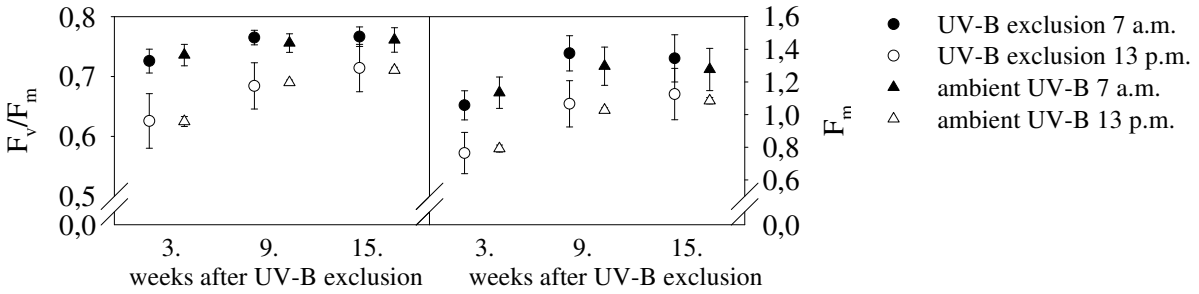

Figure 3. Daily and seasonal changes of maximal chlorophyll fluorescence (Fm) and maximal photochemical efficiency of PSII (Fv/Fm) in beech leaves in the outdoor experiment (Botanical Garden, 2002) (n=30-78±SE)

On basis of chlorophyll fluorescence parameters of light adapted leaves we have found that beech leaves under UV-B exclusion had lower actual photochemical efficiency ($\Delta F/F_m'$) and non photochemical fluorescence quenching (NPQ) in both experimental sites. NPQ and $\Delta F/F_m'$ were significantly negatively correlated, demonstrating the competition of the photochemical and non-photochemical processes *(Figure 4).*

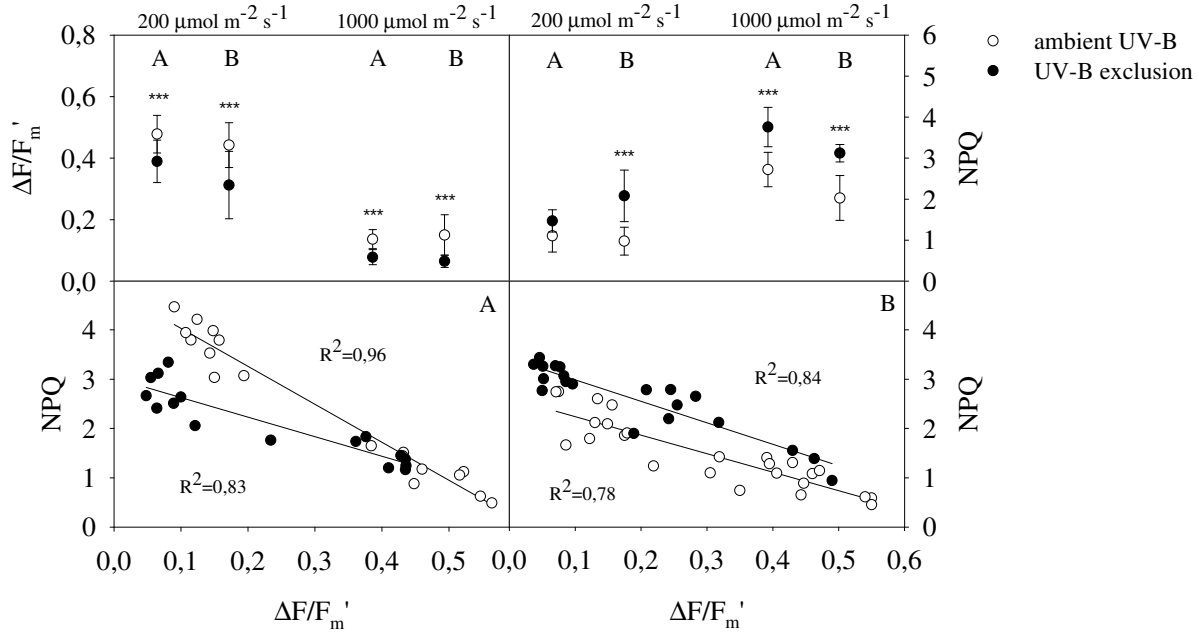

Figure 4. Chlorophyll fluorescence parameters of light adapted leaves after 3 months of treatments. (A-Rejtek Research Site, 2002; B-Botanical Garden, 2002) (n=7-13±SD).

3.2 Effects of enhanced UV-B radiation in outdoor experimental conditions

Results of discriminant analysis on basis of photosynthetic pigment composition and parameters of slow chlorophyll fluorescence induction show clear difference between leaves under ambient UV-B and UV-B exposition, while on basis of parameters of fast chlorophyll fluorescence induction leaves under different light climate were widely similar (Láposi et al. 2005). Under UV-B exposition beech leaves had lower chlorophyll and water content, higher chlorophyll *a*/b ratio, higher flavonoid and total carotenoid content (especially vaz-pool), and at noon activity of xantofill cycle (DEEPS) was also higher than leaves in the control plot (Láposi et al. 2001).

UV-B treatment did not influence significantly either basal (F_0) and maximal fluorescence (F_m), or maximal photochemical efficiency of PSII (F_v/F_m) *(Table 2).* However in beech leaves difference between morning and midday values were higher under UV-B exposure, moreover in the end of the growing season midday value of F_v/F_m was lower in the treated leaves than in the control leaves (Láposi et al. 2005). Actual photochemical efficiency ($\Delta F/F_m'$) of UV-B treated beech leaves was lower, non photochemical fluorescence quenching (NPQ) was higher than in the control leaves, while vitality index (RFD) was not affected by enhanced UV-B *(Table 1).*

*Table 1. Effects of enhanced UV-B radiation on the chlorophyll fluorescence parameters of beech leaves in the outdoor experiment. Means±SD from the three experiments are given (n=13-399). Data were tested by one-way ANOVA (*P≤0.05, ** P≤0.01, *** P≤0.001) (UV-B_{amb}: ambient UV-B; UV-B_{enh}: enhanced UV-B).*

		2000			2001			2002	
		UV-B_{enh}	UV-B_{amb}		UV-B_{enh}	UV-B_{amb}		UV-B_{enh}	UV-B_{amb}
F_0	ns	0,35±0,04	0,34±0,04	ns	0,32±0,02	0,32±0,03	ns	0,31±0,03	0,31±0,03
F_v/F_m	ns	0,77±0,02	0,77±0,02	ns	0,76±0,04	0,76±0,04	ns	0,72±0,06	0,72±0,06
F_m	ns	1,55±0,21	1,53±0,21	ns	1,38±0,21	1,37±0,24	*	1,16±0,23	1,11±0,21
RFD	ns	3,32±0,8	3,24±0,76	***	2,79±0,4	3,32±0,48	***	2,68±0,52	3,20±0,76
$\Delta F/F_m'$	***	0,26±0,17	0,29±0,19	ns	0,32±0,19	0,34±0,19	ns	0,30±0,19	0,33±0,19
NPQ	**	2,25±1,08	2,08±1,2	***	2,01±1,04	1,51±0,85	ns	1,87±1,12	1,55±0,8

Seasonal decrease of values of these parameters was more considerable in the UV-B treated leaves compared to the control leaves (Láposi et al. 2005). Results of discriminant analysis based on measured physiological parameters show that beech leaves under different light climate (ambient UV-B and UV-B exclusion) were more different from each other in field - where other stress factors also occured - than in outdoor conditions.

In outdoor conditions discriminant analysis also detected a clear difference between UV-B exclusion and UV-B exposition, while leaves under ambient UV-B were more similar to leaves under enhanced UV-B than to reduced UV-B which emphasize the effects of present-day UV-B levels *(Table 2).*

Table 2. Classification results of discriminant analysis (%) based on the measured ecophysiological parameters of leaves developed under different light conditions (UV-B_{amb}: ambient UV-B; UV-B_{enh}: enhanced UV-B; UV-B_{exc}: UV-B exclusion; FE: forest edge; FI: forest interior).

		Beech forest site (2002)				Outdoor experimental station (2002)			
		clear-cut area		FE	FI		$UV\text{-}B_{enh}$	$UV\text{-}B_{amb}$	$UV\text{-}B_{exc}$
		$UV\text{-}B_{amb}$	$UV\text{-}B_{exc}$						
Photosynthetic pigments *(n=36-46)*	$UV\text{-}B_{amb}$	88.9	0	11.1	0	$UV\text{-}B_{enh}$	83.3	16.7	0
	$UV\text{-}B_{exc}$	11.1	88.9	0	0	$UV\text{-}B_{amb}$	22.7	63.6	13.6
	FE	0	0	88.9	11.1	$UV\text{-}B_{exc}$	0	16.7	83.3
	FI	0	0	0	100.0				
UV-B absorbing compounds *(n=72-92)*	$UV\text{-}B_{amb}$	83.3	5.6	11.1	0	$UV\text{-}B_{enh}$	83.3	16.7	0
	$UV\text{-}B_{exc}$	16.7	44.4	16.7	22.2	$UV\text{-}B_{amb}$	15.9	47.7	36.4
	FE	0	33.3	61.1	5.6	$UV\text{-}B_{exc}$	12.5	12.5	75.0
	FI	0	0	0	100.0				
Fast chlorophyll fluorescence parameters *(n=298-311)*	$UV\text{-}B_{amb}$	61.0	14.6	17.1	7.3	$UV\text{-}B_{enh}$	35.5	36.8	27.6
	$UV\text{-}B_{exc}$	20.0	25.9	22.4	31.8	$UV\text{-}B_{amb}$	22.2	42.2	35.6
	FE	29.6	14.1	35.2	21.1	$UV\text{-}B_{exc}$	14.9	33.3	51.7
	FI	0	6.8	8.2	84.9				
Slow chlorophyll fluorescence parameters *(n=58-69)*	$UV\text{-}B_{amb}$	83.3	5.6	11.1	0	$UV\text{-}B_{enh}$	75.0	20.8	4.2
	$UV\text{-}B_{exc}$	18.8	50.0	31.3	0	$UV\text{-}B_{amb}$	29.2	62.5	8.3
	FE	8.3	8.3	83.3	0	$UV\text{-}B_{exc}$	4.8	9.5	85.7
	FI	0	0	0	100.0				

4 DISCUSSION

Some parameters, such as photosynthetic pigment composition, chlorophyll fluorescence, levels of UV-B absorbing compounds and specific leaf mass are known as useful indicators of UV-B tolerance or sensitivity, but display rapid responses to UV-B (and PAR), and often increase or decrease within hours (Smith et al. 2000). In our experiments photosynthetic pigment composition, leaf water content and flavonoid content altered parallel with diurnal light cycle due to not only changes of intensity of photoprotective processes, but also photodamage and resynthesis of some pigments (for example chlorophylls). Due to the higher sensitivity of chlorophyll *b*, than chlorophyll *a* (Tevini et al. 1981) increase of the chlorophyll *a/b* ratio could be observed in UV-B radiation. Activity of the xanthophyll cycle also alter in close positive correlation with diurnal light intensity, as it is an important protective mechanism against photoinhibition and photodamage of PSII (Long et al. 1994). Hader et al. (2004) described that photoinhibition (decrease of F_v/F_m) at noon under high irradiances caused by not only PAR but also UV-B radiation. The total amount of VAZ pigments, as well as the de-epoxidation index, is a good indicator of stress situations in trees as they increase in response to several environmental stress factors (Demmig-Adams - Adams, 1992). Our results show that under enhanced UV-B photoinhibition of PSII, activity of xantofill cycle (DEEPS) was higher than in leaves under ambient UV-B. In chloroplasts of higher plants it was found that the de-epoxidation of violaxanthin to zeaxanthin is inhibited upon UV-B exposure (Pfündel et al. 1992), but in field it has smaller importance. In our experiments we observed that enhanced UV-B did not inhibit the activity of xanthophyll cycle in beech leaves, or rather the activity and the pool size increased at noon. In both experimental conditions increases of the VAZ-pool resulted in increases of antheraxanthin and zeaxanthin. Beside the operation of

xanthophyll cycle, protection against photoinhibition can be increased by zeaxanthin synthesis from β-carotene via hydroxylation (Demmig-Adams - Adams, 2002).

The most frequent response to enhanced UV-B radiation is a production of UV-B absorbing compounds (Searles et al. 2001), in particular flavonoids. Flavonoids have been shown to prevent UV-B induced DNA damage (Koostra 1994), and to have free-radical scavenging activity (Barabás et al. 1998), thus offering additional protection to either the photosynthetic apparatus, or membrane lipids. In our experiments these pigments responded the most susceptibly to changes of UV-B level. Amount of these pigments decreased under UV-B exclusion, increased under UV-B exposure in beech leaves.

Our results reveal that beech seedlings are indeed affected by UV-B, even under the present radiation conditions, moreover UV-B exclusion affected to the measured ecophysiological parameters more considerably than enhanced (+40%) UV-B. According to discriminant analysis UV-B affected principally the protective mechanisms, particularly photosynthetic pigment composition and flavonoid content. At the same time photochemical activity of leaves - namely parameters of fast chlorophyll fluorescence induction - were less affected. It indicates that beech may be enable to cope with increasing UV-B due to the adaptation ability to the present-day levels of UV-B radiation. Changes in flavonoid accumulation, as well as in carotenoid content (especially xanthophyll cycle pigments) after UV-B exclusion or UV-B exposition show that beech seedlings have effective protective mechanisms to aviod strong damage of the most important metabolism processes, thus photochemical efficiency of photosynthetic apparatus could remain relatively unaffected under changing UV-B levels.

Acknowledgments: This work was supported financially by OTKA (37961 és 43646) and EU INCO COPERNICUS Program (IC15-CT98-0126).

REFERENCES

BARABÁS, K.N. – SZEGLETES, Z. – PESTENÁCZ, A. – FÜLÖP, K. – ERDEI, L. (1998): Effects of excess of UV-B irradiation on the antioxidant defence mechanisms in wheat (*Triticum aestivum* L.) seedlings. J Plant Physiol. 153: 146-153.

BJÖRN, L.O. (1996): Effects of ozone depletion and increased UV-B on terrestrial ecosystems. Int. J. Environ. Stud. 51: 217-243.

CALDWELL, M.M. – BJÖRN, L.O. – BORNMAN, J.F. – FLINT, S.D. – KULANDAIVELU, G. – TERAMURA, A.H. – TEVINI, M. (1998): Effects of increased solar ultraviolet radiation on terrestrial ecosystems. J. Photochem. Photobiol. B: Biology 46: 40-52.

DAY, T.A. (1993): Relating UV-B radiation screening effectiveness of foliage to absorbing compound concentration and anatomical characteristics in a divers group of plants. Oecologia 95: 542-550.

DEMMIG-ADAMS, B. – ADAMS, W.W.III. (1992): Photoprotection and other responses of plants to high light stress. Ann. Rev. Plant Physiol. Plant Mol. Biol. 43: 599-626.

DEMMIG-ADAMS, B. – ADAMS, W.W. III. (2002): Antioxidants in photosynthesis and human nutrition. Science 298: 2149-2153.

HADER, D-P. – LEBERT, M. – HELBLING, E.W. (2004): Variable fluorescence in the filamentous Patagonian rhodophytes, Callithamnion gaudichaudii and Ceratium sp. under solar radiation. J. Photochem. Photobiol. B. Biol. 73: 87-99.

JOHANSON, U. – GEHRKE, C. – BJÖRN, L.O. – CALLAGHAN, T.V. (1995): The effects of enhanced UV-B radiation on the growth of dwarf shrubs in a subarctic heathland. Funct. Ecology 9: 713-719.

KOOSTRA, A. (1994): Protection from UV-B-induced DNA damage by flavonoids. Plant Mol. Biol. 26: 771-774.

LÁPOSI, R. – VERES, S. – MILE, O. – MÉSZÁROS, I. (2005): Effects of supplemental UV-B radiation on the photosynthesis-physiological properties and flavonoid content of beech seedlings *(Fagus sylvatica* L.) in outdoor conditions. Acta Biologica Szegediensis 49: 151-153.

LÁPOSI, R. – MÉSZÁROS, I. – VERES, S. – MILE, O. (2002): Photosynthetic ecophysiological properties of beech (*Fagus sylvatica* L.) under exclusion of the ambient UV-B radiation. Acta Biologica Szegediensis 46: 243-245.

LÁPOSI, R. – MÉSZÁROS, I. – VERES, Sz. – MILE, O. (2001): Effects of UV-B radiation on photosynthesis-physiological properties of *Fagus sylvatica* L. and *Fraxinus angustifolia vahl.ssp. pannonica* Soó et Simon. Acta Biol. Debrecina, 23: 65-68.

LONG, S.P. – HUMPHRIES, S. – FALKOWSKI, P.G. (1994): Photoinhibition of photosynthesis in nature. Ann. Rev. Plant Physiol. Plant Mol. Biol. 45: 633-662.

MADRONICH, S. – MCKENZIE, R.L. – BJÖRN, L.O. – CALDWELL, M.M. (1998): Changes in biologically active ultraviolet radiation reaching the Earth's surface. J. Photochem. Photobiol. B: Biol. 46: 5-19.

MCKENZIE, R.L. – BJÖRN, L.O. – BAIS, A. – ILYASD, M. (2003): Changes in biologically active ultraviolet radiation reaching the Earth's surface. Photochem. Photobiol. Sci. 2: 5-15.

MCLEOD, A.R. (1997): Outdoor supplementation systems for studies of the effects of increased UV-B radiation. Plant Ecol. 128: 78-92.

MÉSZÁROS, I. – LÁPOSI, R. – VERES, S. – BAI, E. – LAKATOS, G. – GÁSPÁR, A. – MILE, O. (2001): Effects of supplemental UV-B and drought stress on photosynthetic activity of sessile oak (*Quercus petraea* L.). PS2001 Proceedings of 12th International Congress on Photosynthesis. CSIRO Publ., (ISBN:0643 067116), S3-036.

MÉSZÁROS, I. – TÓTH, R.V. – VERES, S. – VÁRADI, G. (1995): Changes in leaf xanthophyll cycle pool and chlorophyll fluorescence of beech forest species and their sun/shade adaptation. In: Mathis, P., (ed.) Photosynthesis: from Light to Biosphere. Kluwer Acad. Publ., Dordrecht, IV: 143-146.

PFÜNDEL, E. – PAN, R.S. – DILLEY, R.A. (1992): Inhibition of violaxanthin de-epoxidation by ultraviolet-B radiation in isolated chloroplasts and intact leaves. Plant Physiol. 98: 1372–1380.

QI, Y. – BAI, S. – HEISLER, G.M. (2003): Changes in ultraviolet-B and visible optical properties and absorbing pigment concentrations in pecan leaves during a growing season. Agricultural and Forest Meteorology, 120: 229-240.

SMITH, A.M. – ORMROD, D.P. – LIVINGSTON, N.J. – MISRA, S. (2000): The interaction of Ultraviolet-B Radiation and Water Deficit in Two *Arabidopsis thaliana* Genotypes. Ann. Bot. 85: 571-575.

SCHREIBER, U. – BILGER, W. – NEUBAUER, C. (1994) Chlorophyll fluorescence as a nonintrusive indicator for rapid assessment of *in vivo* photosynthesis. Ecol. Studies. 100: 49-70.

SEARLES, P.S. – FLINT, S.D. – CALDWELL, M.M. (2001): A meta-analysis of plant field studies simulating stratospheric ozone depletion. Oecologia 127: 1-10.

SHINDELL, D.T. – RIND, D. – LONERGAN, P. (1998): Increased stratospheric ozone losses and delayed enetual recovery owing to increasing greenhouse-gas concentration. Nature 392: 589-592.

SULLIVAN, J.H. (2005): Possible impacts of changes in UV-B radiation on North American trees and forests. Environmental Pollution, 137: 380-389.

TEVINI, M. – IWANZIK, M.W. – THOMA, U. (1981): Some effects of enhanced UV-B radiation on the growth and pigment composition of plants. Planta 153: 388-394.

WELLBURN, A.R. (1994): The spectral determination of chlorophylls a and b, as well as total carotenoids, using various solvents with spectrophotometers of different resolution Plant Physiol. 144: 307-313.

Acta Silv. Lign. Hung., Vol. 4 (2008) 17-27

Recent Trends of Tree Growth in Relation to Climate Change in Hungary

Zoltán SOMOGYI*

Hungarian Forest Research Institute (ERTI), Budapest, , Hungary

Abstract – The paper addresses two related issues. One is whether, and how, growth patterns of stand mean height have changed in Hungary in the last few decades, and the other is whether recently observed increases in mean annual temperature might have caused changes in growth trends. Changes in tree growth were investigated for beech (*Fagus sylvatica*), sessile oak (*Quercus petraea*) and Turkey oak (*Quercus cerris*) by comparing stand mean heights over age using data from the forest inventories of 1981 and 2001, and for sessile oak using stand mean height data from permanent sample plots since 1961. Tree growth was found to have accelerated for each species mentioned, with Turkey oak showing the largest acceleration. To study the second issue, stand mean height was related to elevation, wich in turn was related to mean annual temperature and precipitation. For these analyses, too, data of many thousands of stands in the forest inventory was used. Stand mean height was found to increase with decreasing elevation, i.e. with increasing mean annual temperature, for each of the three species. As the annual precipitation and air humidity decreases with decreasing elevation, it was concluded that increases of mean annual temperature could positively have affected tree growth in the last few decades. However, this effect is expected to be soon limited by water availability.

climate change / tree growth / beech / sessile oak / Turkey oak

Kivonat – A fanövekedés és a klímaváltozás néhány összefüggése Magyarországon. A tanulmány két, egymással összefüggő kérdést elemez. Az egyik az, hogy vajon felgyorsult-e a fák magassági növekedése az elmúlt évtizedekben, a másik pedig az, hogy e gyorsulást okozhatta-e a hőmérséklet növekedése? A fanövekedés-gyorsulást egyrészt az Országos Erdőállomány Adattár 1981-es, illetve 2001-es erdőrészlet-adataiból bükkre, kocsánytalan tölgyre és cserre levezetett kor-magasság görbék összehasonlításával vizsgáltuk, másrészt pedig hosszúlejáratú fatermési kísérleti területek adatainak trendelemzésével kocsánytalan tölgyre. Mindegyik esetben a növekedés gyorsulása volt kimutatható; leginkább a cser növekedése gyorsult fel. E gyorsulás okainak vizsgálatához összefüggést kerestünk az Országos Erdőállomány Adattár található sokezer erdőrészlet tengerszint feletti magassága és a fák átlagmagassága között. Kimutattuk, hogy az átlagmagasság – minden egyéb tényezőt állandónak tekintve – nőtt a tengerszint feletti magasság csökkenésével, ami megfelel az átlaghőmérséklet növekedésének. Mivel a csapadék éves mennyisége csökken a tengerszint feletti magasság csökkenésével, ezért azt a következtetést vontuk le, hogy az elmúlt évtizedek magasabb hőmérséklete valóban intenzívebb növekedéssel párosult. A jövőben a hőmérséklet-növekedés hatását azonban várhatóan korlátozni fogja a rendelkezésre álló víz abszolút vagy relatív csökkenése.

klímaváltozás / növekedésgyorsulás / bükk / kocsánytalan tölgy / cser

* som9013@helka.iif.hu; H-1023 Budapest, Frankel L. u. 42-44

1 INTRODUCTION

In its most recent assessment report, IPCC (2007) suggested that a „global assessment of data since 1970 has shown it is likely that anthropogenic warming has had a discernible influence on many physical and biological systems". Based on data, models and scientific reasoning, the report also stressed that, „globally, commercial timber productivity rises modestly with climate change in the short- to medium-term with large regional variability around the global trend".

For Europe, Nabuurs et al. (2002) suggested, based on model simulation, that increment could grow by 18% by 2030, and slow down on a longer term. Solberg et al. (2003) suggested increased wood production in Western Europe, but a decreased production in Eastern Europe. Finally, Schroeter (2004) also suggested increased forest growth in most parts of Europe, especially in Northern Europe.

With respect to tree growth, these findings could sometimes be expected as a consequence of the recent warming in Europe. However, without evidence that is based on measured data it is not entirely clear how and to what extent tree growth may change due to climate change.

Since tree growth is not only a biological process, but also affects the economic, social and environmental aspects of forestry, and since it can be measured relatively cheaply and accurately (as compared to most characteristics of ecosystems, such as food chain), one of the first consequences of climate change to study in Hungary was tree growth (Mátyás 1994, Somogyi 1998.a-c, Somogyi 2001, Makkonen-Spiecker-Somogyi 2000).

Another reason of the interest in tree growth is that its patterns seemed to have changed throughout Europe over a decade ago, and studies were conducted, even without considering climate change, that were widely publicized. Kuusela (1994) was among the firsts to show, by analysing the forestry statistics of the European countries, that the standing volume and current increment had considerably increased during the previous 40 years, although the amount of harvest had also increased. This study was followed by that of Spiecker et al. (1996) who, in addition to studying the issue whether tree growth could have increased or not, also attempted to address why it could have happened. The studies included analyses of forest inventory data, but also data from scientific studies such as permanent sample plots and tree ring analyses where accuracy is of high importance. The synthesis of the results suggested a more or less accelerated tree growth rate in most parts of Europe.

In Hungary, tree growth was not suspected to have changed in the 1980's (Király 1986), however, several case studies applied the hypothesis that it might have changed (Somogyi 1998a-c, Makkonen-Spiecker-Somogyi 2000, Tóth 1998, Szabados 2007). The results suggested that a large-scale study was necessary.

In this paper, which reports on the results of this study, two main questions are focused on:

I. Is there any indication of a recent change in the growth pattern at the country level?
II. Could the recent climate change result in changes in tree growth?

These questions cannot directly be answered, therefore, operative questions, two for each questions above, were formulated, also considering all available data. These are the following:

I(a) What was the growth trend like of three important tree species, i.e. beech, sessile oak and Turkey oak between 1981-2001 using forest inventory data of the National Forestry Database (NFD)?
I(b) What was the growth trend of sessile oak like in permanent sample plots?

II(a) Could any relationships be found between tree growth rate and site characteristics that are strongly affected by mean annual temperature?

II(b) In case there are such relationships, could the increase of temperature between 1981-2001 be shown to bring about the observed tree growth change (under I above) during the same period?

2 METHODS AND DATA

The above questions required different methods, assumptions and data, therefore, they are detailed in relation to the questions themselves. The same applies later for the results.

I. Recent tree growth trends

Of all possible measures, tree height was analysed to detect trends as it was available in each dataset, and it strongly correlates with site. The heights or height growths of the same species were compared in different years or time periods with the assumption that, within the limits of sample errors and the errors of the measurements, the same site brings about the same height growth. It is the same to say that, if site has changed, it affected height growth.

Another main element of our approach was that all anayses were done using all data available in the country, i.e., using the largest sample size, by which the effects of local differences of site, forest management etc. of the samples, that could have affected the results, could be minimized.

Question number I(a) was analysed using stand data from the NFD for sessile oak (*Quercus petraea* Liebl., SO), common beech (Fagus sylvatica L., CB), and Turkey oak (*Quercus cerris* L., TO). Only those stands were included where the water available for the roots only included water from precipitation (i.e., stands under the influence of floods were excluded). For all these stands and for all species in the stands, and for both 1981 and 2001, age, species ratio (by crown projection), origin (seed, coppice), mean stand height, mean stand diameter, standing volume, as well as site characteristics (see below) were queried from the NFD. From the mean stand height and age data, age-height curves were developed for both 1981 and 2001, and these curves were compared using regression and correlation techniques.

Question number I(b) was analysed using data from the SO permanent sample plots of the Hungarian Forest Research Institute. Here, too, the mean stand height data were plotted against age. In this analysis, different number of data per sample plot could be used depending on when observations started on the sample plot (the difference of the age of the stand between two consecutive measurements of the same sample plots is usually between 5-10 years). The sample plots included silvicultural experiments where a range of thinning intensities was experimented with. Including all plots of the experiments, often with different stand densities, was based on the assumption that, within wide ranges, thinning does not affect mean stand height. Intensive thinnings, which might have increased mean stand height causing mean stand height to tend lower, only occurred during the 1960'-1970's, and stands became much denser later. Thus, including these experiments could not result in the increase of the observed mean stand height growth, rather, it could only reduce any observed increase of height growth.

II. Site - tree height and site change – tree growth relationships

When studying the effects of climate change, two important climatic factors to analyse are temperature and precipitation. Unfortunately, these data were not directly available as they are not measured and stored in forestry databases, and were not available at an appropriate density from other (e.g. meteorology) databases, either. On the other hand, we suspected that relationships may exist across large areas, i.e. at the average of many stands, between these climatic factors and two measures that are assessed for each stand in Hungary: elevation and forest climate type. Elevation (EL) is measured, and stored in the NFD, for each stand at the nearest hundred m. Concerning forest climate types (FCT), four types are used in standard site assessment based on the occurrence of main tree species which is thought to correlate well with the joint effects of all climatic factors. These four types, named after the main indicator tree species themselves, are Common Beech Type (CBT), Hornbeam-Sessile oak Type (HST), Turkey Oak Type (TOT), and Forest Steppe Type (FST). According to Mátyás-Czimber (2000), the difference between the mean July monthly temperature of CBT and HST is 0.9 degrees ºC, whereas that of HST and TOT is 0.2 ºC, and the difference between the mean annual precipitation of CBT and HST is 32 mm, whereas that of HST and TOT is 86 mm.

In the present study, multiple regression techniques were used to detect relationships between mean stand height on one hand, and EL and FCT on the other, to address question number II(a). The regression analyses were made by FCT so that, within each FCT, further categories were created using other standard site parameters available in the NFD: aspect, soil type, rooting depth, as well as physical soil characteristics. However, due to limited data availability, only those categories were considered where tree growth was limited by the amount of precipitation, and where a number of stands was available that could allow to perform statistical tests. Of all possible combinations of the above site characteristics, 84 site categories were studied. Based on the relationships found, simple relationships between temperature and tree growth were developed, using a simple meta-analysis of the results by all site categories, for the three tree species of question number I.

Finally, in analysing question number II(b), the relationships found under II(a) were used to estimate how much increase of tree growth could be attributed to the observed increase of mean annual temperature between 1981-2001. Using the above relationships, predictions were also made in several scenarios of possible future increase of temperature.

3. RESULTS

I. Recent growth trends

I(a) Several thousands of mean stand height data were available for all three tree species from the NFD (not shown in the figures below). The second order polinomial age-height curves fitted for these data for 1981 and 2001, which should overlap, show significant differences for a range of age classes (*Figure 1*).

A more detailed analysis of differences by age classes, as well as FCT and origin (*Table 1*) shows more detailed tests of significance. The more categories we have, the less is of course the number of stands in a category, therefore, the less is the chance to find significant differences, and indeed, less significant differences were found, and non significant catagories were found, too. There are also categories where the mean height is lower in 2001 than in 1981. However, overall, the 2001 mean heights were generally larger than the 1981 mean heights in the same species, site and origin categories (*Table 1*). In the latter, „main" means stands where the given species is a main species, i.e. its species ratio is more than 50%, whereas „mixed" means stands where the species ratio is less than 50%. Dark cells

indicate significantly higher mean heights of the same age (in 2001), light gray colors indicate non-significantly higher mean stand heights, whereas middle gray colors indicate non-significant lower mean heights. There were no significant lower mean stand heights in 2001 than in 1981. White cells indicate classes with not enough number of stands in the respective category.

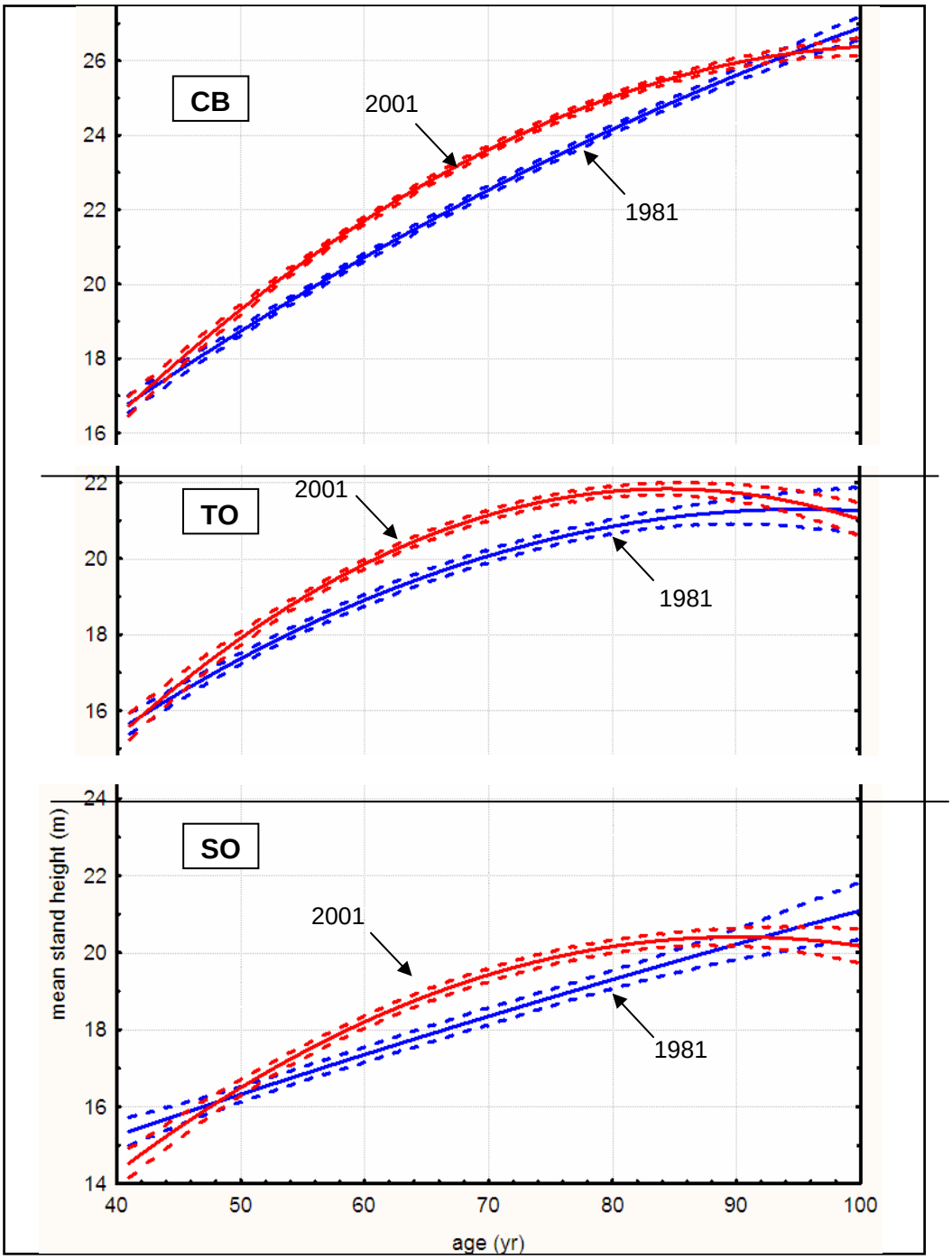

Figure 1. Second-order polinomial age–mean stand height curves, based on data (not shown in the figure) from the NFD, for species SO, TO and CB for 1981 (continuous line) and 2001 (continuous line), together with the confidence bands of 95% probability (dashed lines).

Table 1. The difference between the mean stand heights in 2001 and 1981 by age class for SO, TO and CB species by the origin (seed or coppice) and species ratio categories.

Origin	Mixing	Age class (year) 41-50	51-60	61-70	71-80	81-90	91-100	101-110	111-120
SO									
seed	main			2,57	0,50		-0,42	0,83	0,23
	mixed	0,37	-0,24	-0,78	-0,36	0,26	0,23	0,06	0,04
coppice	main		3,38	0,98	2,66	2,27	1,59	1,35	1,33
	mixed		2,04	0,02	1,98	1,27	1,68	0,23	3,30
CB									
seed	main			1,23	0,25	4,71	1,28	0,65	0,00
	mixed		0,10	3,03	1,21	2,30	0,09	1,19	2,35
coppice	main					5,70	3,80	1,11	2,75
	mixed			0,25	2,46	2,35	2,45	0,59	5,27
TO									
seed	main			-0,99	0,10	1,04	0,59	1,49	3,38
	mixed		0,16	0,52	0,09	1,24	0,53	1,03	1,32
coppice	main		1,64	0,40	1,12	2,09	3,49	3,03	6,21
	mixed		2,53	-0,28	2,45	1,83	2,43	1,76	2,17

I(b) Data from SO permanent sample plots were grouped so that one group contained measurements that were taken before 1990, and the other group contained measurements that were taken after 1990. A second-order polinomial curve was fitted to both datasets (*Figure 2*).

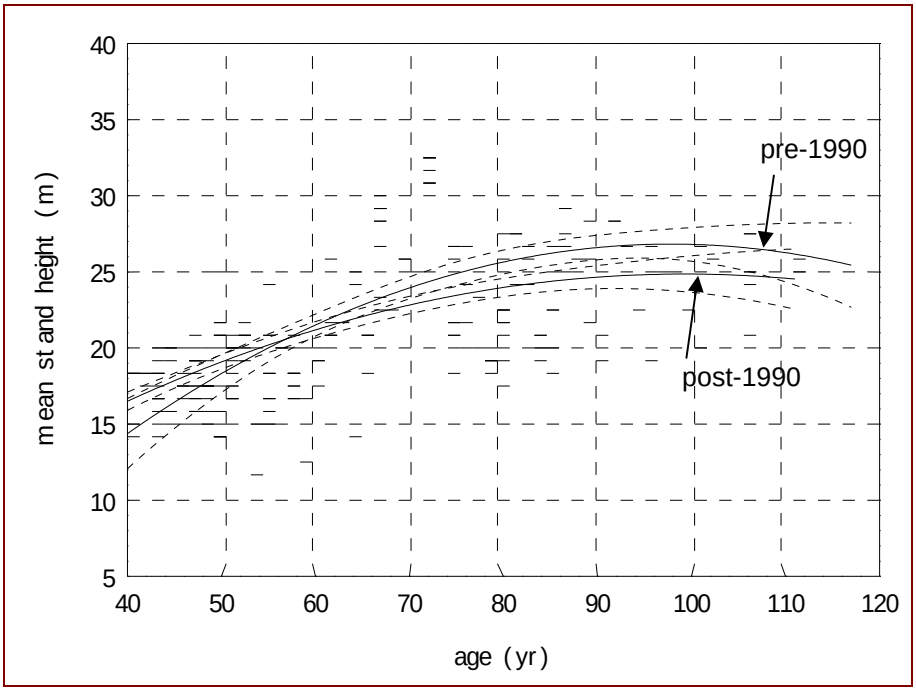

Figure 2. Second order polinomial fits to mean stand height data of SO permanent sample plots for pre-1990 measurements (thick continuous line) and post-1990 ones (thin continuous line), together with confidence bands of 95% probability (dashed lines).

In general, the curve fitted to the post-1990 measurements goes higher than the one fitted to the pre-1990 measurements. Significant differences were found between ages 75-95 years.

II. Site-tree growth relationships

II(a) The relationships between elevation and mean stand height was modeled using linear regression models with the data from the NFD. The basic assumption was that *ceteris paribus*, i.e. everything else (species, FCT, soil type, aspect) being the same, mean stand height is determined by the elevation. The linear model was developed for all possible species and site combinations between 300-600 m a.s.l where we had enough data. The regression coefficients (i.e. the coefficients of the slope of the linear line) varied between -1.6 and 0.8 and represented a normal distribution (*Figure 3*). The full confidence interval of 95% probability is found in the negative range for each tree species, and the mean value of the regression coefficients is a negative number, i.e. -0.499 for CB, -0.57 for TO and -0.29 for SO. It thus seems that generally, although with a high deviation, elevation has a discernible effect on mean stand height, and mean stand height decreases with the decrease of the elevation.

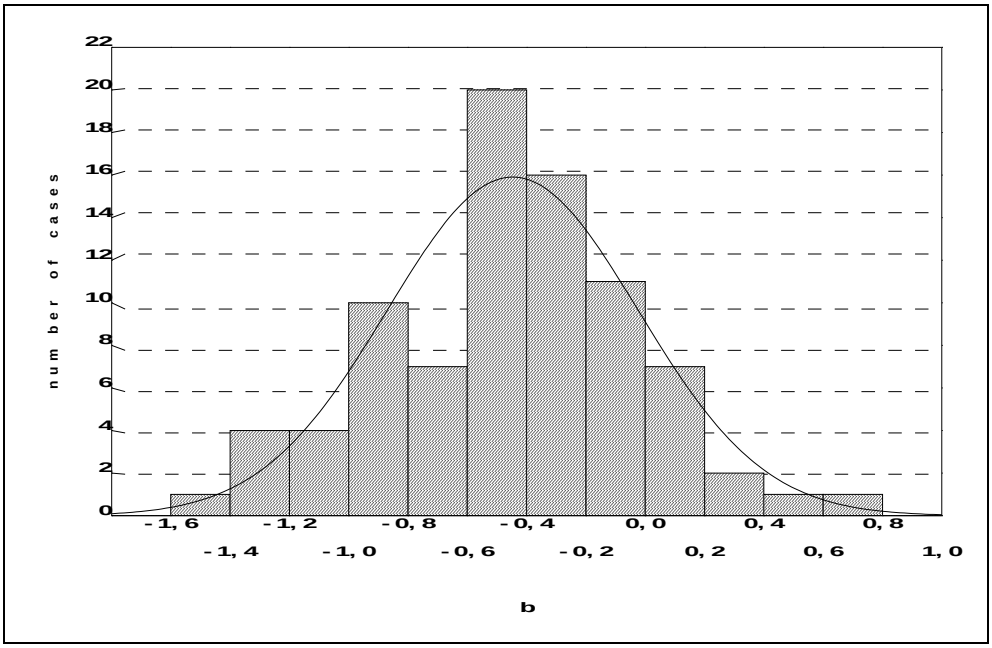

*Figure 3. The distribution of the regression coefficients (b) of the linear model: mean stand height = a + b * elevation for all species taken together and for all possible site categories, for elevations between 300-600 m (N = 84; mean value = -0.454, and the confidence band is found between -0.545 and -0.362). Similar distributions were found, with different mean values, by species (see text).*

Relationships between FCT and mean stand height was also modeled by species, as well as main soil types, using second-order age-height polinomial curves. *Figure 4* demonstrates that, for SO and on typical brown forest soil types, significant differences exist between the age-height curves of the different FCTs. The differences by FCT are more expressed than those by the elevation. However, standard deviation is usually high, and, although differences are often found, the number of stands by a site class is usually not enough to find significant differences. Generally, trees grow highest in the CBT, they grow lower in the HOT, and lowest in the TOT (there are very few occurrences of the three species studied in the FOS forest climate type).

We note here that it may seem paradoxical that mean stand height decreases with the decrease of the elevation, but it increases with the FCT when moving from TOT towards CBT (CBT is usually found at higher elevation than TOT). However, elevation is only one factor that determines FCT, thus, moving along elevation and FCT is not equivalent to moving along the same axis but in opposite directions, rather, elevation and FCT are different dimensions of the same niche. In any event, we do not have a coherent theory on how FCT affects tree growth, and further studies are needed to identify the effects of the various factors in relation to FCT that may affect tree growth.

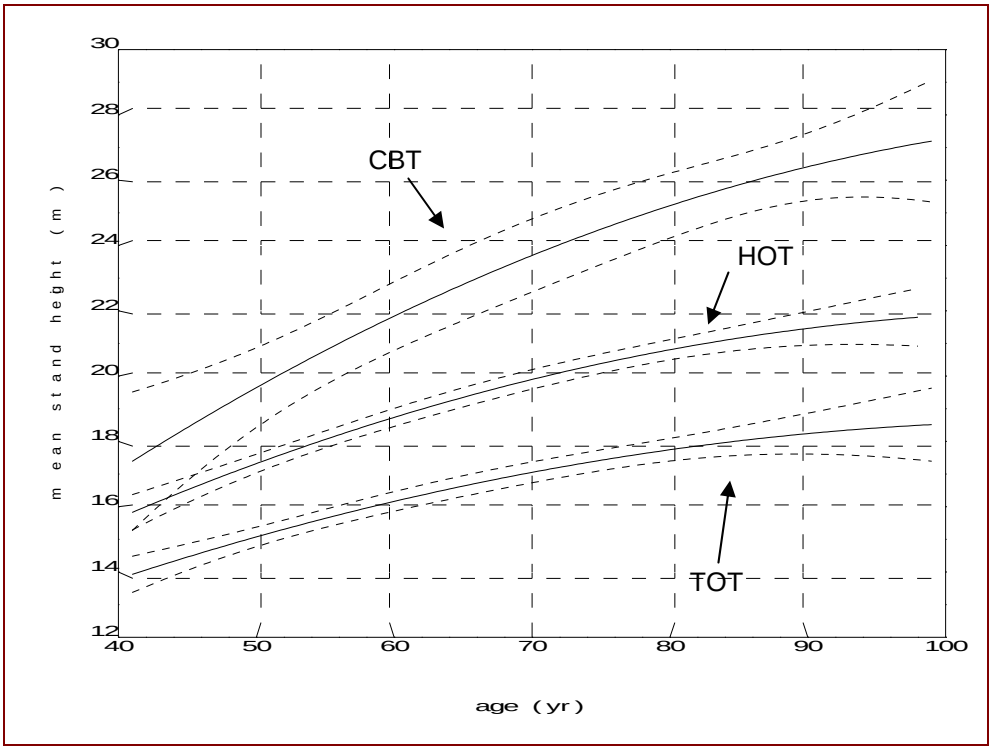

Figure 4. Age-height curves (continuous lines) by FCT for SO stands on typical brown forest soils and in Southern aspects. Dashed lines represent confidence bands of 95% probability. The upper lines are fitted to data of stands in CBT (the data are not shown in the figure), the lines in the middle are for HOT, and the lower lines are for TOT.

II(b) We have estimated what increase of height growth could occur, by applying the relationships of the II(a) analysis, assuming an increase of temperature of 1.0 ºC that was observed in Hungary between 1981 and 2001. We also estimated what would happen in the future in case of a further temperature increase of 0.5 and 2.0 ºC. (Note that these increases are the same or higher than the differences between the mean annual temperatures of the various forest climate types that were mentioned above, see Mátyás-Czimber 2000.)

As a first step, it is necessary to define growth increase potential. It is

- a long-term average increase of the tree height growth
- if mean annual temperature increased in the long term by X ºC (i.e., if the mean temperature stabilized after an X ºC increase),
- and if all other factors that influence tree growth remained the same, including e.g. the amount of precipitation.[1]

[1] According to our current knowledge about the precipitation, it will decrease somewhat in Hungary. However, even with the same amount of annual precipitation, it can occur that the precipitation becomes a growth limiting factor according to Liebig's law of the minimum. This, however, does not have any major effect on the conclusions of our study

In the second step, we must convert elevation to temperature. In Hungary, the mean annual temperature changes by 0.5-0.6 ºC by every 100 m change of elevation, and this change can be assumed linear. In the third step, if the linear model under II(a) above is applied to the mentioned temperature changes than we get an average potential tree height growth increase of 0.45 m for every 100 m increase of the elevation. Formulated in yet another way, every 0.1 ºC increase of mean temperature (across all age and site classes and for all tree species studied) is equivalent to a height growth increase of 0.07 m. The species specific values are the following: CB, 0.1 m/0.1 ºC, SO, 0.05 m/0.1 ºC, and TO, 0.1 m/0.1 ºC. Finally, using these values and assuming three scenarios of temperature increase, the potential tree height growth increase values can be calculated for all tree species (*Table 2*).

Table 2. Tree growth increase potentials (for its definition see text above) in three scenarios of temperature increase by tree species, calculated from the linear model under II(a) and all assumptions and calculations under II(b) above.

Tree species	Mean increase of tree height (m) if the increase of mean temperature is (ºK)		
	0.5	1	2
Common beech (CB)	0.5	1	2
Sessile oak (SO)	0.25	0.5	1
Turkey oak (TO)	0.5	1	2

4. DISCUSSION

The results of the study of recent growth trends (questions number Ia and b) suggest that tree growth has recently increased in Hungary. The study involved many data (and all data available) that eliminated the errors of individual tree height measurements. We also checked whether there were any changes in the methodology of mean stand and individual tree height measurements during the forest inventories between 1981 and 2001, however, according to information that we received from the National Forest Service, which runs the forest inventories, there were no such changes. Thus, we concluded that there is high confidence that tree height growth has indeed increased.

Concerning site-growth relationships (question number IIa) it must be stressed that both temperature and precipitation are very complex factors, and neither any mean value (annual, monthly, or for the „vegetation season"), nor totals, minimum or maximum values (again for a year, a month or for the vegetation season) are enough to fully predict tree growth, even if any of these factors are Liebig-minimum values at least for a certain period of time. The application of the elevation, a data that is available in the NFD, as a temperature-proxy has the advantage that no such means, totals, minima or maxima were used but a complex, although proxy, variable that integrates all of these, both for temperature, as well as for precipitation.

With the decrease of elevation, the mean annual temperature increases and the amount of precipitation decreases, which means that using the elevation as a proxy will only show the effect of temperature in the increase of tree growth, and the decrease of the precipitation may only result in an underestimation of this tree growth increase (i.e., we get a conservative estimate for the temperature – tree growth increase relationship). It is, however, clear that we only identified statistical (correlational) relationships between temperature increase and tree growth increase, and not causal relationships.

We applied the *ceteris paribus* principle for each other tree growth limiting factor that were available in the NFD. This means e.g. that, when studying the possible effects of the

elevation, we only involved data of those stands that had the same other characteristics, such as tree species, FCT and soil type. Again, many other factors that could not be included in the analysis, such as the amount of photosintetically active radiation and the like, do cause tree growth to change in directions opposite to temperature (e.g., they decrease tree growth when temperature increases), thus, ignoring them only leads to an underestimation, or conservative estimation, of the possible effects of warming.

As mentioned before, tree growth was modeled using tree height which is age dependent. The effects of age on the regression coefficients in *Figure 3* could sometimes be shown, however, it could not be shown in other cases. This does not mean that the elevation, or the related mean annual temperature, do not affect growth, it only means that, in addition to the elevation, age, aspect etc., there may be other factors that affect growth, or we did not have enough data in certain species-site categories.

Concerning the effects of the elevation and the FCT, the latter showed stronger correlation to growth than the elevation. This may be explained by the fact that the FCT is a more complex indicator of all factors affecting growth than the elevation. But because FCT is not only defined by the temperature, and because no direct relationship is known between FCT and temperature, we could not use it to predict the increase of tree growth in relation to the change of temperature. On the other hand, FCT is defined by the very occurrence of the species themselves, however, the occurrence of a species does not only depend on the requirements of these species to the physical environment, but also on the competition of these and other species with overlapping niche elements, therefore, it can occur that a characteristic species of a FCT grows better in another FCT (e.g. SO in the CBT, *Figure 4*).

In any event, further analyses will be required, using geographical information systems, to better understand the relationships between the elevation and tree height growth. Many site type combinations could be defined using the site characteristics that are available in the NFD. We did not analyse all these combinations, but not only because many of these characteristics may not have strong relationships with tree growth, but because our intention was to establish relationships at the country level. These relationships are most probably not linear, and depend on age and many other factors that could not be involved in the analyses.

When studying the possible effects of the temperature on tree growth in various scenarios (question number II(b)), the estimated increase of tree growth corresponds well with the observed changes between 1981-2001, thus, we concluded that the observed increase of temperature in the country recently could give rise to the observed changes in the tree growth. We, however, again stress that we only studied statistical correlations, not causal effects.

Finally, we note that the rate of increase of volume growth that may be a resultant of the increase of tree height growth will probably not justify a substantial increase of the annual allowable cut. Also, as a consequence of Liebig's law of the minimum, a further increase of tree growth due to a further increase of temperature may not happen at all (Mátyás–Nagy 2005, Mátyás, 2006). According to IPCC (2007), globally, the wood production could only be increased slightly in the short- and medium-term up to a further 1-3 ºC temperature increase. This is because the trees' requirements to water will increase at a speed that is higher than the speed of the temperature increase, and, according to the current predictions, the amount of summer precipitation is likely to decrease, and is going to limit tree growth accross large areas as the amount of precipitation is already close to the limiting amount. It can be assumed that both trees, as well as forest management may only have a few more years, possibly a few decades, to successfully adjust and adapt to the effects of climate change.

Acknowledgments: The study was made possible by the „Klímaerdő" NKFP project led by prof. Cs. Mátyás. Data from the NFD was provided by the State Forest Service. The sessile oak permanent sample plots were managed and measured by many people, first of all prof. Rezső Solymos, A. Béky, J. Bogyai, as well as J. Balikó.

REFERENCES

IPCC (2007): Working Group II Contribution to the Intergovernmental Panel on Climate Change Fourth Assessment Report Climate Change 2007: Climate Change Impacts, Adaptation and Vulnerability. Summary for Policymakers, April 6th, 2007. http://www.ipcc.ch.

JÁRÓ, Z. (1973): Erdészeti termőhelyfeltárás, termőhelyvizsgálat (műszaki irányelvek). [Forest site survey and site evaluation – technical standards] In: Danszky, I. (szerk.): Erdőművelés. [Silviculture] Mezőgazdasági Könyvkiadó Vállalat, Budapest. 853-868. (in Hungarian)

KIRÁLY, L. (1986): Élőfakészlet, fakitermelés, fapusztulás, növedék. [Standing volume, Utilization, Forest decline, Increment] Budapest, kézirat. (Manuscript in Hungarian)

KUUSELA, K. (1994): Forest resources in Europe 1950-1990. European Forest Institute Research Report No. 1. Cambridge University Press, Cambridge, UK.

MAKKONEN-SPIECKER, K. – SOMOGYI, Z. (2000): Az európai erdők felgyorsult növekedéséről - egy európai kutatási program eredményei és visszhangja. [On the accelerated increment of European forests – results and echo of a European reearch project] Erdészeti Kutatások 89: 73-80. (in Hungarian)

MÁTYÁS, CS. (1994): Modeling climate-change effects with provenance test data. Tree Physiology 14: 797-804.

MÁTYÁS CS. (2006): Migratory, genetic and phenetic response potential of forest tree populations facing climate change. Acta Silvatica et Ligniaria, 2: 33-46

MÁTYÁS, CS. – CZIMBER, K. (2000): Zonális erdőtakaró mezoklíma szintű modellezése: lehetőségek a klímaváltozás haásainak előrejelzésére. II. [Mesoclimate-level modeling possibilities of zonal forest cover.] Erdő és klíma konferencia kiadványa (Debrecen, 2000. július 7-9.), 83-97. (in Hungarian)

MÁTYÁS CS. – NAGY L. (2005): Genetic potential of plastic response to climate change. Tag.Ber., Forum Genetik und Wald, (ed. M. Konnert) Teisendorf, 55-69.

Nabuurs, G.J., – PUSSINEN, A. – KARJALAINEN, T. – ERHARD, M. – KRAMER, K. (2002): Stemwood volume increment changes in European forests due to climate change – a simulation study with the EFISCAN model. Glob. Change Biology, 8: 304-316.

SCHRÖTER, D. et al. (2004): The ATEAM final report 2004 - Detailed report related to overall project duration. Advanced Terrestrial Ecosystem Analysis and Modelling, a project funded under the 5th framework Programme of the European Union, pp. 139. http://www.pik-potsdam.de/ateam/.

SOLBERG, B. – MOISEYEV, A. – KALLIO, A.K. (2003): The economic impacts of accelerating forest growth in Europe. Forest Policy Econ. 5: 157-171. (in Hungarian)

SOMOGYI, Z. (1998a): Gyorsuló fanövekedési trendek Európában I. [Accelerated tree growth in Europe. I] Erdészeti Lapok CXXXIII. 1: 6-7. (in Hungarian)

SOMOGYI, Z. (1998b): Gyorsuló fanövekedési trendek Európában II. [Accelerated tree growth in Europe. II.] Erdészeti Lapok CXXXIII. 2: 37-38. (in Hungarian)

SOMOGYI, Z. (1998c): Gyorsuló fanövekedési trendek Európában III. [Accelerated tree growth in Europe. III.] Erdészeti Lapok CXXXIII. 3: 65-66. (in Hungarian)

SPIECKER, H. – MIELIKÄINEN, K. – KÖHL, M. – SKOVSGAARD, J. P. (ed.) 1996. Growth trends in European forests. European Forest Institute Research Report No. 5. Springer.

SZABADOS, I. (2007): Időjárási fluktuáció hatása a produkcióra dendrokronológiai kutatások alapján. Erdő-klíma V. NYME, Sopron. (in Hungarian)

SZALAI, S. – SZENTIMREY, T. (2002): Melegedett-e Magyarország éghajlata a XX. században? Beszámoló a 2000. évi tevékenységről. [Has the climate of Hungary become warmer?] OMSZ, Budapest. 3-14. (in Hungarian)

TÓTH, J. (1998): Hozzászólás Dr. Somogyi Zoltán: "Gyorsuló fanövekedési trendek Európában I., II. és III. c. cikkéhez. [Contribution to the papers Accelerated tree growth in Europe. I-III. by Z. Somogyi] Erdészeti Lapok. (in Hungarian)

Acta Silv. Lign. Hung., Vol. 4 (2008) 29-38

Effects of Artificial Regeneration Methods on Mortality, Growth and Shape of Oak Seedlings in a Central – European Oak-Hornbeam Stand

Tamás TOBISCH *

Department of Ecology and Silviculture, Hungarian Forest Research Institute, Budapest, Hungary

Abstract – This paper analyses the results of an artificial regeneration experiment carried out in an oak-hornbeam stand. The effects of initial seedling density (10200, 14300, 35700 stems per hectare), spacing geometry (140 cm x 70 cm, 240 cm x 40 cm), chemical (with Erunit and Nabu) and mechanical weeding of pedunculate (*Quercus robur*) and sessile oak (*Quercus petraea*) were examined at the age of eight years. The mortality of *Q. robur* seedlings was independent of the initial density but that of *Q. petraea* increased with it. Height and diameter growth of both species significantly decreased with the density, and the values of the diameter-to-height ratios (DHR) became smaller as the density increased. At approximately the same seedling density the mortality was lower but the seedlings were shorter, thinner and the values of DHR were smaller if the distance between stems was much lower than that between rows. Mechanical or chemical weeding did not affect considerably seedling mortality, growth or shape in any of the spacing types.

weeding / *Quercus petraea* / *Quercus robur* / seedling development / seedling survival / spacing

Kivonat – Mesterséges felújítási eljárások hatása az újulat öngyérülésére, növekedésére és alakjára egy közép-európai gyertyános-tölgyesben. A tanulmány egy gyertyános-tölgyesben végrehajtott mesterséges felújítási kísérlet eredményeit mutatja be. Kocsányos (*Quercus robur*) valamint kocsánytalan tölgy (*Quercus petraea*) esetében a felújítás nyolcadik évében vizsgáltam a kiindulási csemeteszámnak (10200, 14300, 35700 db/ha), a hálózat geometriájának (140 cm x 70 cm, 240 cm x 40 cm) valamint vegyszeres (Erunit és Nabu vegyszerekkel) és mechanikus ápolásoknak a hatását. A kocsányos tölgy öngyérülése nem függött a kiindulási csemeteszámtól, ugyanakkor a kocsánytalan tölgyé a csemeteszámmal emelkedett. A csemeteszám emelkedésével a magassági növekedés ill. a vastagodás mindkét fafaj esetében csökkent, és a csemeték nyurgábbá váltak. Megközelítőleg azonos kiindulási csemeteszám mellett a tőtávolság csökkentésével (és így a sortávolság növelésével) az újulat öngyérülése csökkent, ugyanakkor a csemeték magassága és vastagsága is csökkent, valamint felnyurgultak. A mechanikus ill. a vegyszeres ápolás egyik hálózati típus esetében sem befolyásolta jelentősen a csemeték növekedését ill. alakját.

ápolás / *Quercus petraea* / *Quercus robur* / újulat fejlődése / újulat mortalitása / ültetési hálózat

* tobischt@erti.hu; H-1023 BUDAPEST, Frankel Leó út 42-44.

1 INTRODUCTION

One of the most important periods in the life of managed forests is the regeneration. It determines the subsequent development of the growing stand (Ovington – MacRae 1960). Thus, the regeneration technique must be chosen with special care from ecological and economical points of view.

The costs of regeneration strongly correlate with the biological aspects of the applied technique. Methods less suitable for seedling survival and development are more expensive while planting must be repeated and the regeneration period is longer. Costs of seeds or seedlings are possibly high if regenerating artificially. Thus, determining the optimal seed or seedling number is of great importance. To do this, four questions must be answered: How does seedling density influence 1. the mortality and 2. the growth of the developing stand as well as in long-term 3.the shape and 4. the wood structure of the individual trees?

In artificial oak regenerations, wide spacing with low number of seedlings was often applied in Central Europe (Weaver – Spiecker 1993). However, using high number of seeds or seedlings with closer distance between stems can be more advantageous from three points of view (Varga 1966, Savill and Spilsbury 1991):

1. the canopy of the growing stand closes faster so weed competition decreases sooner;
2. the shape of the seedlings may become better while forking is inhibited due to the shading of the neighbouring seedlings;
3. there is a greater supply for natural or artificial selection.

Furthermore, smaller distances between stems can facilitate height growth to some extent in the case of some species (Fekete 1938, Szodfridt 1959). It is also clear that more seedlings can utilize site productivity better as long as spacing is not too dense which leads to a greater intraspecific competition and consequently to slower seedling growth (Szodfridt 1959, Harmath 1961, Solymos 1983, Harkai 1987, Kolb – Steiner 1990). Other disadvantages of denser spacing are its obviously higher costs and technical difficulties with silvicultural treatments (weeding, cleaning; Varga 1966). The effects of spacing on oak seedling survival and growth are still poorly known.

Costs of weeding can be high at both artificial and natural regeneration. At the beginning of regeneration herbs can influence survival and growth of seedlings in two main ways (Magyar 1933): by shading (competition for light) and by root competition (competition for water; Harmer et al. 2005, Harmer – Morgan 2007). Thus, chemical or mechanical weeding can facilitate seedling survival and growth of oak as well as those of other tree species (Ovington – MacRae 1960, Jarvis 1964, Csesznák 1980, Kolb et al. 1990, Kolb – Steiner 1990, Collet – Frochot 1996, Collet et al. 1996, Chaar et al. 1997, Collet et al. 1997, Collet et al. 1998, Kelly 2002, Coll et al. 2003). There is an important difference between the chemical and mechanical protection. While in the former case usually the whole plant dies with its root system, in the latter in most cases only the above-ground part is killed. In this way shading effect decreases but root competition does not. So seedling growth may remain inhibited (Davies 1985, Löf 2000). On the other hand, weed competition does not hinder seedling development by all means (Madsen 1995). Furthermore, in some cases even the total protection from root competition of herbs did not lead to higher seedling growth intensity (Szappanos 1969).

Weeding experiments of oak were usually quite short-term analyzing data of 1-4 years (Szappanos 1969, Collet and Frochot 1996, Collet et al. 1996, Chaar et. al 1997, Collet et al. 1997, Löf 2000). Some studies (Collet et al. 1998, Kelly 2002) were longer-term, but the combined effects of different weeding treatments and spacing types were not examined.

The aim of the present study is to determine the effects of different spacing types and weeding treatments on oak seedling survival and growth simultaneously in a sessile oak–

hornbeam and a pedunculate oak–hornbeam stand: How do spacing geometry, initial seedling density, mechanical and chemical weeding influence the mortality, growth and shape (lankiness) of the seedlings?

2 MATERIALs AND METHODS

2.1 Study area

The study stand (subcompartment Káld 46 B, approximately 11.1 ha, 47°09'N, 17°00'E) is growing on rusty brown forest soil, 200 m above sea level. The climate is characterized by a diagram (*Figure 1*). The whole study area was fenced against game in 1994.

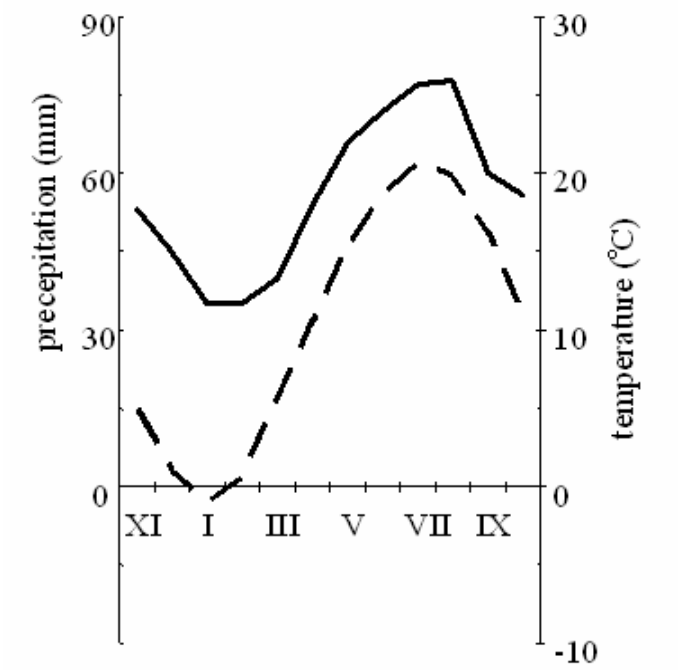

Figure 1. Climate diagram for characterizing the study stand. Monthly precipitation (solid line) and temperature (broken line) were measured at two nearby meteorological stations, Káld and Pápa, respectively from 1901 to 1950. Source: Kakas (1967).

The parent stand consisted of sessile oak (32% according to the data of the Hungarian National Forest Service), turkey oak (*Quercus cerris*, 24%), hornbeam (*Carpinus betulus*, 24%) and pedunculate oak (*Quercus robur*, 20%) before starting the regeneration. The closure of the parent stand was approximately 95%. At this time the stand was nudum (i.e. the ground vegetation was very sparse).

In the initial stage of regeneration high cover of fleabane (*Erigeron canadensis*) was characteristic. Later on thistle species (*Cirsium sp.*) and *Erigeron annuus* proliferated. From the third year bushgrass (*Calamagrostis epigeios*) occurred in high abundance. Finally, by the fifth year the cover of blackberry (*Rubus spp.*) has reached high values in some spots endangering seedling survival and growth.

2.2 Silvicultural treatments

The whole stand was divided into 12 blocks of approximately identical size (*Figure 2*). Blocks No. 1-2, 5-8, 11-12 are included in the present study.

No site preparation was applied on the study area before planting. One year-old seedlings of *Quercus robur and Q. petraea* were planted in different spacing types in the spring of 1995 (*Table 1*). One of the applied densities (14300 stems per hectare) is that which is recommended by Danszky (1963) for oak-hornbeam stands growing in this region of Hungary.

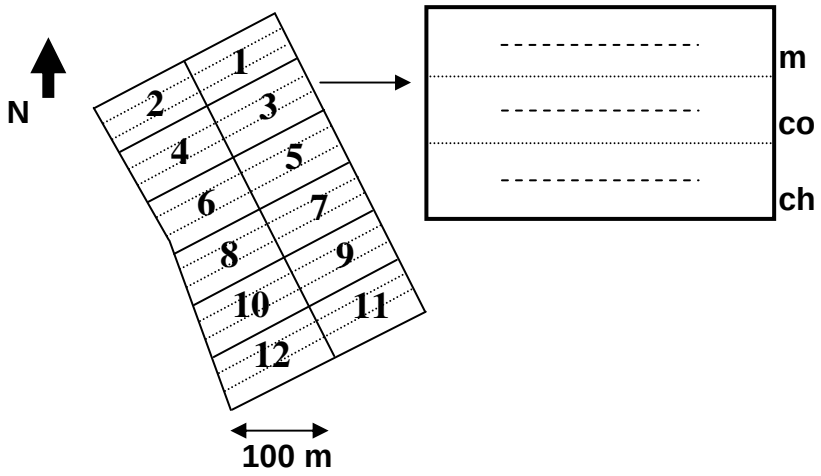

Figure 2. Experiment design. The study stand was divided into 12 blocks of approximately identical size. Each block consists of three plots in which different weeding treatments (mechanical weeding – m; control – co; chemical weeding – ch) were applied. Seedlings were sampled along 50 m long transects (broken line) in the middle of each plot.

Table 1. Spacing types of artificial regeneration. dist. – distance; Q. rob. – Quercus robur; Q. pet. – Quercus petraea

Blocks	Species	Row dist. (cm)	Stem dist. (cm)	No. stems per hectare
1.	Q. rob.	140	70	10200
2.	Q. pet.	140	70	10200
5.	Q. rob.	240	40	10400
6.	Q. pet.	240	40	10400
7.	Q. rob.	140	50	14300
8.	Q. pet.	140	50	14300
11.	Q. rob.	140	20	35700
12.	Q. pet.	140	20	35700

At the beginning of the regeneration all blocks but No. 11 and No. 12 were sprayed with Erunit. Afterwards, every block was divided into three plots in accordance with the applied weeding method (one control plot, one plot weeded chemically and one plot weeded mechanically). Seedlings of goat willow (*Salix caprea*) and aspen (*Populus tremula*) were cut in all plots in 1999. In the plots weeded mechanically the above-ground biomass of the competing vegetation was removed in July 1997 and in July 1998.

Chemical weeding was carried out by chemicals Erunit and Nabu in March 1997 and in June 1998, respectively. The second treatment was not performed in blocks No. 1 and No. 2 due to unfavourable weather conditions. Because of the high cover of bushgrass Nabu must have been sprayed in blocks No. 11 and No. 12 in May 1997. Erunit inhibits the germination of mono- and dicotyledons alike for three-four months. One liter Erunit contains 300 g acetochlor, 200 g atrazine and 30 g antidote AD-67. The applied concentration was 7 l/ha. Nabu kills monocotyledons selectively. The agent of Nabu is sethoxydim (12.5%). Nabu was sprayed in

concentration of 4 l/ha. Both chemicals can reduce root competition. In 2000 woody species were weeded out in all plots. Afterwards, further weeding treatments were not necessary.

2.3 Sampling

Sampling was carried out in 2003 and started with a pilot sampling to analyze the effect of sample size on the value of the mean of the dependent variables (seedling height and diameter). That is, much more seedlings were sampled in some chosen plots (on which the variance of seedling height and that of seedling diameter were the highest according to visual estimation) than the estimated required minimum. From the data the fluctuation of the mean value with increasing sample size was determined. The sampling size from which the fluctuation was smaller than 5% was considered as the required minimum sample size. Based on the obtained data heights and diameters at breast height of all seedlings were measured along 50 m long transects in the middle of each plot (*Figure 2*) except for plots of blocks No. 6, No. 11 and No. 12. In the latter plots transects were divided into 10 m long sections due to the high number of seedlings. Heights and diameters at breast height of all seedlings were measured along the two end and the middle sections.

Table 2a. Effects of initial seedling number on mortality, growth and shape of Q. robur seedlings at row distance of 140 cm. The age of the regeneration was 8 years.

Weeding	No. stems per hectare	n	Mortality (%)	h (cm)	d (mm)	(d/h) x 10^{-3}
me	10200	53	26	380** (89)	34.5** (14.3)	8.8 (3.0)
me	14300	78	22	330 (61)	27.1 (10.9)	8.0 (2.3)
me	35700	112	25	243** (73)	16.6** (9.9)	6.2** (2.8)
co	10200	62	13	342 (73)	28.9 (11.5)	8.2 (2.1)
co	14300	73	27	344 (75)	28.0 (11.2)	7.8 (2.3)
co	35700	121	19	262** (77)	16.3** (9.9)	5.6** (2.5)
ch	10200	48	33	350** (74)	31.2** (13.1)	8.6** (2.4)
ch	14300	74	26	291 (84)	21.8 (11.5)	6.9 (2.6)
ch	35700	120	20	279 (83)	16.5** (9.8)	5.4** (2.5)

Table 2b. Effects of initial seedling number on mortality, growth and shape of Q. petraea seedlings at row distance of 140 cm. The age of the regeneration was 8 years.

Weeding	No. stems per hectare	n	Mortality (%)	h (cm)	d (mm)	(d/h) x 10^{-3}
me	10200	53	26	345** (79)	31.0** (12.8)	8.6** (2.7)
me	14300	73	27	275 (81)	19.7 (11.3)	6.5 (2.9)
me	35700	102	32	250* (76)	16.1* (10.4)	5.8* (2.7)
co	10200	53	26	346** (66)	30.1* (12.1)	8.4 (2.3)
co	14300	72	28	303 (84)	24.7 (13.5)	7.5 (3.0)
co	35700	95	37	269** (68)	17.4** (9.7)	5.9** (2.4)
ch	10200	59	17	352** (59)	31.2** (10.2)	8.7** (2.0)
ch	14300	83	17	269 (77)	19.7 (10.6)	6.8 (2.6)
ch	35700	80	47	247* (76)	14.9** (8.3)	5.7** (2.4)

Quotients in the last column are the averages of quotients calculated for each seedling. Standard deviations are showed in parentheses. Plots in which 14300 seedlings were planted were compared to the two other plots in the case of each weeding treatment. If the difference was significant it is indicated only at data of the two latter plots. h – average height of the seedlings; d – average diameter at breast height of the seedlings; me – plots weeded mechanically; co – control plots; ch – plots weeded chemically; *Q. rob.* – *Quercus robur*; *Q. pet.* – *Quercus petraea*; * - $p<0.05$; ** - $p<0.01$.

2.4 Data analysis

The shape of the seedlings was characterized with the quotient of the diameter and the height (d/h). Since both diameter and height were expressed in meter the quotient has no dimension. Data was evaluated with analysis of variance using BIOMstat 3.3 program (2002). For checking normality and homogeneity of variances the Kolmogorov-Smirnov and F-max statistics (Hartley 1950) as well as log-anova tests (Martin – Games 1977) were used, respectively. For assumptions of parametric ANOVA could not have been met Kruskal-Wallis ANOVA was applied. The effects of weeding were studied in each block (i.e. in the case of each spacing type, *Table 1*) separately. Otherwise the interaction between weeding and spacing would have been overlooked.

3 RESULTS

3.1 Effects of seedling density at the same row distance

Considering all plots, the average mortality of pedunculate and sessile oak was similar, 21.3% and 26.4%, respectively. Mortality of pedunculate oak doesn't correlate strongly with the initial seedling number in any of the plots (*Table 2a, b*). In contrast, mortality of sessile oak seems to increase with it in every plot. Height and diameter growths as well as DHR of the seedlings decreases significantly as seedling number increases (*Table 2a, b*). These effects are similar in the cases of both oak species and all weeding types.

3.2 Effects of spacing geometry at the same seedling density

Seedling survival was higher in all but one plots in which the differences between the two distance types (distances between rows and distances between stems) were greater (*Table 3a, b*). On the other hand, seedlings of both species were significantly shorter, thinner and DHR values were higher in these plots.

Table 3a. Effects of spacing geometry on mortality, growth and shape of 8-year old Q. robur seedlings

Weeding	Spacing (cm x cm)	n	Mortality (%)	h (cm)	d (mm)	(d/h) x 10^{-3}
me	140 x 70	53	26	380 (89)	34.5 (14.3)	8.8 (3.0)
me	240 x 40	111	11	300** (70)	24.5** (12.1)	7.7* (2.8)
co	140 x 70	62	13	342 (73)	28.9 (11.5)	8.2 (2.1)
co	240 x 40	114	9	291** (75)	24.0** (11.8)	7.8 (2.8)
ch	140 x 70	48	33	350 (74)	31.2 (13.1)	8.6 (2.4)
ch	240 x 40	94	25	324 (77)	26.3* (12.3)	7.7* (2.4)

Table 3b. Effects of spacing geometry on mortality, growth and shape of 8-year-old Q. petraea seedlings

Weeding	Spacing (cm x cm)	n	Mortality (%)	h (cm)	d (mm)	(d/h) x 10^{-3}
me	140 x 70	53	26	345 (79)	31.0 (12.8)	8.6 (2.7)
me	240 x 40	66	12	288** (70)	23.4** (11.5)	7.6 (2.7)
co	140 x 70	53	26	346 (66)	30.1 (12.1)	8.4 (2.3)
co	240 x 40	66	12	305** (73)	23.7** (11.4)	7.3* (2.5)
ch	140 x 70	59	17	352 (59)	31.2 (10.2)	8.7 (2.0)
ch	240 x 40	48	36	299** (69)	23.9** (12.3)	7.5**(2.4)

Standard deviations are showed in parentheses. Significance level is indicated only at the data of plots of spacing 240 cm x 40 cm. For abbreviations see *Table 2*. * - $p<0.05$; ** - $p<0.01$.

3.3 Effects of weeding

Weeding did not improve seedling survival of any of the two oak species in any of the spacing types (*Table 4*). On the contrary, in some blocks survival of pedunculate oak seemed to decrease due to weeding. Seedling growth was not promoted considerably either by mechanical or chemical weeding. In some blocks (No. 7, No. 8, No. 11 and No. 12; *Table 4*) seedlings, which were weeded ("w-seedlings") are even significantly shorter and thinner than seedlings, which were not weeded. In contrast, in some other blocks (No. 1, No. 2 and No. 5) "w-seedlings" are significantly taller and thicker though most of these differences are not important from silvicultural point of view. Weeding didn't influence seedling shape practically.

Table 4. Effects of weeding on mortality, growth and shape of oak seedlings. The regeneration was 8 years old

Blocks	Weeding	n	Mortality (%)	h (cm)	d (mm)	(d/h) x 10^{-3}
1.	me	53	26	380* (89)	34.5* (14.3)	8.8 (3.0)
1.	co	62	13	342 (72)	28.9 (11.5)	8.2 (2.1)
1.	ch	48	33	350 (74)	31.2 (13.1)	8.6 (2.4)
2.	me	53	26	345 (79)	31.0 (12.8)	8.6 (2.7)
2.	co	53	26	346 (66)	30.1 (12.1)	8.4 (2.3)
2.	ch	59	17	352* (59)	31.2* (10.2)	8.7* (2.0)
5.	me	111	11	300 (70)	24.5 (12.1)	7.7 (2.8)
5.	co	114	9	291 (75)	24.0 (11.8)	7.8 (2.8)
5.	ch	94	25	324** (77)	26.3 (12.3)	7.7 (2.4)
6.	me	66	12	288 (70)	23.4 (11.5)	7.6 (2.7)
6.	co	66	12	305 (73)	23.7 (11.4)	7.3 (2.5)
6.	ch	48	36	299 (69)	23.9 (12.3)	7.5 (2.4)
7.	me	78	22	330* (61)	27.1 (10.9)	8.0 (2.3)
7.	co	73	27	344 (75)	28.0 (11.2)	7.8 (2.3)
7.	ch	74	26	291** (84)	21.8** (11.5)	6.9* (2.6)
8.	me	73	27	275 (81)	19.7* (11.3)	6.5 (3.0)
8.	co	72	28	303 (84)	24.7 (13.5)	7.5 (3.0)
8.	ch	83	17	269** (77)	19.7* (10.6)	6.8 (2.6)
11.	me	112	25	243* (73)	16.6 (10.0)	6.2* (2.8)
11.	co	121	19	262 (77)	16.3 (9.9)	5.6 (2.5)
11.	ch	120	20	279 (83)	16.5 (9.8)	5.4 (2.5)
12.	me	102	32	250* (76)	16.1 (10.4)	5.8 (2.7)
12.	co	95	37	269 (68)	17.4 (10.0)	5.9 (2.4)
12.	ch	80	47	247** (76)	14.9 (8.3)	5.7 (2.4)
All	me	648	22.6 (7.4)	228 (128)	29.2 (8.5)	7.2 (2.9)
All	co	656	21.4 (9.7)	231 (122)	30.0 (8.0)	7.1 (2.7)
All	ch	606	27.6 (10.5)	221 (122)	29.6 (8.3)	6.9 (2.7)

Plots, which were weeded were compared to the control plots. Significance level is indicated at the data of the former plots. Standard deviations are showed in parentheses. For abbreviations see *Table 2*. * - $p<0.05$; ** - $p<0.01$.

4 DISCUSSION

Higher seedling number increased mortality of sessile oak. The survival of pedunculate oak during the first eight years of the regeneration was determined by other factors not investigated in this study. On the other hand, intraspecific competition between the seedlings inhibited growth and decreased DHR. The results are in accordance with earlier experiments studying other tree species (e.g. Szodfridt 1959, Harmath 1961, Solymos 1983, Harkai1987).Spacing geometry is very important from silvicultural point of view (Varga 1966). If the distance between rows is large enough (e.g. 240 cm) weeding can be motorized easily. According to the results, however, larger distance between rows didn't compensate for smaller distance between stems at the same seedling density. Because of the small stem distance competition between the seedlings became more intense. This slowed seedling developmet and decreased DHR. On the other hand, survival of seedlings was much higher in this case. The reason for this phenomenon is not clear. These results disprove the hypothesis of Varga (1966) who concluded that applying large row and small stem distance is just as appropriate for seedling development as the application of equal distances between rows and stems.

Weeding did not improve seedling survival of any of the two oak species. This does not mean that th herb layer could not inhibit seedling development because it is possible that immediately after the weeding occasions "w-seedlings" grew faster. The only thing that is surely known is that in long-term the effects of the applied weeding treatments are negligible from silvicultural point of view. It must be taken into consideration, however, that weather conditions of 1997 were not favourable for spraying Erunit and this could have influenced the results. Presumably, because of the low precipitation of that year only a small amount of this chemical could infiltrate into the soil leading to low effectiveness of protection. Furthermore, decrease of the cover of bushgrass due to spraying Nabu promoted indirectly the proliferation of blackberry and dicotyledons of tall growth. Thus, weed competition was not reduced effectively enough by this chemical too.

Negative effects of weeding treatments observed in some blocks could be partly the consequence f weeding mistakes (e.g. accidental removal of oak seedlings in plots weeded mechanically). On the other hand, the lower cover of the herb layer in the plots weeded chemically let aspen and goat willow establish and grow.

5 CONCLUSIONS

According to the results, planting approximately 10 000 seedlings per hectare seem to be enough for the successful regeneration. Planting more seedlings slows down the growth and is more expensive. However, later on, effects of the initial seedling number on wood structure must be studied as well (Igboanugo 1990). Considering the same seedling density, from biological point of view it is more advisable to reduce the difference between row and stem distances. It is unnecessary to carry out weeding treatments every year.

The conclusions are valid primarily for stands which have similar stand structure and occur under similar site conditions as the study stands of the present experiment. However, even in these cases further research must be carried out to make the results more general.

Acknowledgements: The financial support given by Szombathely Forestry Company is greatly acknowledged. In particular, I would like to thank Miklós Monostori, the local silvicultural manager for leading the silvicultural works of the experiment. I thank János Balikó for his help in sampling and data processing as well as Zoltán Járó, Albert Béky and Zoltán Somogyi for revising the manuscript.

REFERENCES

BIOMstat 2002. Version 3.3. Exeter Software, East Setauket, USA.

CHAAR, H. – COLIN, F. – COLLET, C. (1997): Effects of environmental factors on shoot development of *Quercus petraea* seedlings. A methodological approach. For. Ecol. Manage. 97: 119-131.

COLL, L. – BALANDIER, P. – PICON-COCHARD, C. – PRÉVOSTO, B. – CURT, T. (2003): Competition for water between beech seedlings and surrounding vegetation in different light and vegetation composition conditions. Ann. For. Sci. 60: 593-600.

COLLET, C. – FROCHOT, H. (1996): Effects of interspecific competition on periodic shoot elongation in oak seedlings. Can. J. For. Res. 26: 1934-1942.

COLLET, C. – COLIN, F. – BERNIER, F. (1997): Height growth, shoot elongation and branch development of young *Quercus petraea* grown under different levels of resource availability. Ann. Sci. For. 54: 65-81.

COLLET, C. – GUEHL, J.-M. – FROCHOT, H. – FERHI, A. (1996): Effect of two forest grasses differing in their growth dynamics on water relations and the growth of *Quercus petraea* seedlings. Can. J. Bot. 74: 1562-1571.

COLLET, C. – NINGRE, F. – FROCHOT, H. (1998): Modifying the microclimate around young oaks through vegetation manipulation: Effects on seedling growth and branching. For. Ecol. Manage. 110: 249-262.

CSESZNÁK, E. (1980): Arboricidek használata az erdőfelújítás sikerének fokozásában. [Using arboricids for more successful regeneration of forests.] EFE Tud. Közlem. 1980(2): 53-58. (in Hungarian)

DANSZKY, I. (ed.) (1963): Magyarország erdőgazdasági tájainak erdőfelújítási, erdőtelepítési irányelvei és eljárásai. I. Nyugat-Dunántúl erdőgazdasági tájcsoport. [Principles and methods of regeneration and afforestation of forest regions of Hungary. I. Nyugat-Dunántúl forest region group.] Országos Erdészeti Főigazgatóság, Mezőgazdasági Könyv- és Folyóirat Kiadó Vállalat, Budapest. 265-327. (in Hungarian)

DAVIES, R.J. (1985): The importance of weed control and the use of tree shelters for establishing broadleaved trees on grass-dominated sites in England. Forestry 58: 167-180.

FEKETE, Z. (1938): A sűrűség és záródás hatása az akácegyed fejlődésére. [The influence of density and closeness on the development of locust trees.] Erdészeti Lapok 77: 8-23. (in Hungarian)

HARKAI, L. (1987): A duglászfenyő-hálózati kísérlet értékelése. [Valuation of spacing experiment with Douglas fir.] Erdészeti Kutatások 39: 33-38. (in Hungarian)

HARMATH, B. (1961): Üzemi nyárdugványozási kísérletek tág hálózatban. [Experiments on enterprise-scale propagation of poplar by cuttings in wide spacing.] Az Erdő 10: 452-456. (in Hungarian)

HARMER, R. – BOSWELL, R. – ROBERTSON, M. (2005): Survival and growth of tree seedlings in relation to changes in the ground flora during natural regeneration of an oak shelterwood. Forestry 78: 21-32.

HARMER, R. – MORGAN, G. (2007): Development of Quercus robur advance regeneration following canopy reduction in an oak woodland. Forestry 80: 137-149.

HARMER, R. – ROBERTSON, M. (2003): Seedling root growth of six broadleaved tree species grown in competition with grass under irrigated nursery conditions. Ann. For. Sci. 60: 601-608.

HARTLEY, H.O. (1950): The maximum F-ratio as a short cut test for heterogeneity of variances. Biometrika 37: 308-312.

IGBOANUGO, A.B.I. (1990): Effects of shading on shoot morphology, wood production and structure of Quercus petraea seedlings. For. Ecol. Manage. 38: 27-36.

JARVIS, P.G. (1964): The adaptibility to light intensity of seedlings of *Quercus petraea (Matt.) Liebl.* J. Ecol. 52: 545-571.

KAKAS, J. (ed.) (1967): Magyarország éghajlati atlasza, II. kötet, adattár. [Climatic atlas of Hungary, vol. II, tables.] Országos Meteorológiai Intézet, Akadémiai Kiadó, Budapest. 41-56., 125-128. (in Hungarian)

KELLY, D.L. (2002): The regeneration of *Quercus petraea* (sessile oak) in southwest Ireland: a 25-year experimental study. For. Ecol. Manage. 166: 207-226.

KOLB, T.E. – STEINER, K.C. (1990): Growth and biomass partitioning of northern red oak and yellow-poplar seedlings: effects of shading and grass root competition. For. Sci. 36: 34-44.

KOLB, T.E. – BOWERSOX, T.W. – MCCORMICK, L.H. (1990): Influences of light intensity on weeded-induced stresses of tree seedlings. Can. J. For. Res. 20: 503-507.

LÖF, M. (2000): Establishment and growth in seedlings of *Fagus sylvatica* and *Quercus robur*: influence of interference from herbaceous vegetation. Can. J. For. Res. 30: 855-864.

MADSEN, P. (1995): Effects of soil water content, fertilization, light, weed competition and seedbed type on natural regeneration of beech (*Fagus sylvatica*). For. Ecol. Manage. 72: 251-264.

MAGYAR, P. (1933): Természetes újulat és az aljnövényzet. [Natural regeneration and the ground vegetation.] Erdészeti Kutatások 35: 78-106. (in Hungarian)

MARTIN, C.G. – GAMES, P.A. (1977): Anova tests for homogeneity of variance: Nonnormality and unequal samples. J. Educ. Stat. 2: 187-206.

OVINGTON, J.D. – MACRAE, C. (1960): The growth of seedlings of *Quercus petraea*. J. Ecol. 48: 549-555.

SAVILL, P.S. – SPILSBURY, M.J. (1991): Growing oaks at closer spacing. Forestry 64: 373-384.

SOLYMOS, R. (1983): Az erdeifenyő erdősítések ültetési hálózata. [Spacing of Scots pine.] Az Erdő 32: 147-150. (in Hungarian)

SZAPPANOS, A. (1969): *A Carex pilosa* – gyertyános – kocsánytalan tölgyesek természetes újulatának darabszám- és növedékvizsgálata. [Investigations of number of pieces and increment of natural regeneration of *Carex pilosa* hornbeam – sessile oak stands.] EFE Tud. Közl. 1969(1): 21-38. (in Hungarian)

SZODFRIDT, I. (1959): Nemesnyár hálózati kísérletek. [Spacing experiments on hybrid poplars.] MTA Agrártud. Oszt. Közl. 15: 331-336. (in Hungarian)

VARGA, B. (1966): Az ültetési hálózat racionalizálására irányuló törekvések a Mátrai Erdőgazdaságban. [Efforts to rationalize spacing in Mátra Forestry Company.] Az Erdő 15: 1-5. (in Hungarian)

WEAVER, G.T. – SPIECKER, H. (1993): Silviculture of high-quality oaks: questions and future research needs. Ann. Sci. For. 50: 531-534.

Acta Silv. Lign. Hung., Vol. 4 (2008) 39-48

Changes of Frost Damage and Treeline Advance for Swiss Stone Pine in the Calimani Mts. (Eastern Carpathians, Romania)

Zoltán KERN [a*] – Ionel POPA [b]

[a] Institute for Geochemical Research, Hungarian Academy of Sciences, Budapest, Hungary
[b] Forest Research and Management Institute, Research Station for Norway Spruce Silviculture, Câmpulung Moldovenesc, Romania

Abstract -- Checking the tree-ring structure of 39 living and 9 crossdated dead samples of Swiss stone pine (*Pinus cembra* L.) collected from the upper timberline of the CalimaniMts. we have identified 59 frost rings over the past 250 years. We found concentrated occurrence of frost events in three decades: in the 1790s, 1810s and 1910s. No frost ring was observed in two bidecadal periods: 1750-1770 and 1850-1870. Out of the analysed interval 1963-2004 is the longest period without frost ring occurrence. After 1920 both frequency and severity of frost events seem to decrease compared to the prior 170 years. We determined the altitude of highest growing stone pine individuals in the Bradului Ciont–Pietrosu region in June, 2006. Individuals were sorted into tree-form or bush-like morphological groups. Mean elevation data of the groups were corrected by an estimated constant bias of GPS measurements (-30 m). Comparing the corrected values to early 20th century inventory data 65 m and 95 m upward migration was determined for treeline and boundary of bush-like occurence, respectively. The parallel results suggest that the 20th century advance of the upper forest limit was due to the decrease of frost stress at the zone of timberline.

Swiss stone pine (*Pinus cembra* L.) / late frost / timberline / frost ring / climate change

Kivonat – Cirbolyafenyők fagykárosodása és az erdőhatár változásai a Kelemen-havasokban (Keleti-Kárpátok, Románia). A Kelemen-havasok felső erdőhatárán növekvő cirbolyafenyők évgyűrűszerkezetének vizsgálata során 59 fagygyűrűt ismertünk fel. Az 1750-2004 időszakban a mintaszám elég magas, a vizsgált egyedek átlagos életkora elég stabil ahhoz, hogy a fagygyűrű észlelések előfordulási gyakoriságai alapján kijelentsük:

1) 1790-es, 1810-es és az 1910-es évtizedekben koncentráltan fordultak elő fagyesemények.
2) 1750-1770, 1850-1870 és 1963-2004 intervallumokban nem találtunk fagygyűrűt.
3) 1876-ban érintette az állományt a legdrasztikusabb fagyesemény 1750 óta.
4) 1920 után a kései fagyok erőssége és előfordulási gyakorisága is csökkenni látszik a megelőző 170 évhez képest. Ezt nem magyarázhatjuk a vizsgált egyedek átlagos életkorának emelkedésével, mert az életkor szórása is növekszik, jelezve, hogy az idős – fagytűrőbb - egyedek mellett fiatal - fagyérzékeny - példányok is vannak.

GPS segítségével 2006 júniusában meghatároztuk a legmagasabban növekvő cirbolya példányok tengerszint feletti magasságát. A bemért példányokat alak szerint két csoportba (fa alakú, bokor-szerű) soroltuk. A mért magasságokat kontrol mérések alapján korrigáltuk. A korrigált magassági adatokat a

[*] Corresponding author: kern@geochem.hu H-1112 BUDAPEST, Budaörsi út 45.

XX. század első évtizedében készített részletes felmérés adataihoz hasonlítottuk. A 2006-os fahatárra 65, az eltörpült, bokor-szerű példányokra 95 méterrel magasabb értéket kaptunk, mint amit száz évvel korábban közöltek.
Az eredemények azt sugallják, hogy a felső erdőhatár XX. sz-i előrenyomulása a fagy-stressz mérséklődésének tulajdonítható, melyet a fagyesemények intenzitásának csökkenése igazol.

Cirbolyafenyő (*Pinus cembra*) / kései fagy / erdőhatár / fahatár / klímaváltozás

1 INTRODUCTION

High mountain zonation is a prominent indicator in climate change investigations (Gottfried et al. 1994, Pauli et al. 2003). The clearest, visible boundary in mountain vegetation is the transitional belt between forest and alpine meadows. Within a mature, natural forest/meadow transition zone three further boundaries should be mentioned (Körner 1998). The upper limit of closed forest is the timberline. The discontinuous line following the altitudinal boundary of tree-form individuals is the treeline, while the uppermost virtual line above treeline where only seedlings and dwarfed individuals appear is the tree species line. The same belts are present in the taiga/tundra transition zone too.

Owing to its pronounced climatic determination this transitional zone is in the highlight of tree-ring research (Fritts 1976).

Temporal fluctuations in treeline position have been described at many sites (Luckmann – Kavanagh 1998, Esper – Schweingruber 2004, Koch et al. 2004, Nicolussi et al. 2005, Mátyás 2006).

Our investigations aim to detect the climate sensitivity of stone pine in Calimani Mts. and to evaluate its potential to reconstruct environmental history. The relationship of climate and ringwidth fluctuation is assessed in separate papers both on interannual (Kern et al. 2007) and decadal/centennial scale (Popa – Kern accepted). This paper analyses the frequency of anatomical deformations of wood related to temperature drops during the vegetation period between 1750 and 2004. In addition we present the first results from the Carpathians confirming the upward advance of upper treeline since the first decade of the 20th century.

2 MATERIAL AND METHODS

2.1 Site description

The Calimani Mts. is the highest volcanic range in the Carpathians. The central part is characterized by a northward opened caldera. Steep slopes ascend from the inner depression to the rim of the caldera, while gentle slopes descend towards the pediment. The highest peaks are mounds on the rim. The range culminates at the Pietrosu peak (2102 m asl) (*Figure 1*).

The elevated terrain at the central range hosts coniferous forest. subalpine vegetation zone grows above the timberline while patches of stony tundra with blanket of lichens can be found in the regions of the highest peaks (Nagy et al. 2006). Natural timberline (~1700 m asl) is well preserved at the steep north facing slopes where anthropogenic influence (e.g.: grazing, wood cutting) was negligible. Timberline is characterized by Norway spruce (*Picea abies* (L.) Karst) and Swiss stone pine (*Pinus cembra* L.). The local pine occurrence represents the eastern boundary of European distribution area of the species. Stone pine individuals also appear on the southern side descending toward the Mures Valley, but the largest stands are are located on the northern slopes of Rachitis Peak and Pietricele Peak (Höhn 2001). The southern side population has lower genetic variability compared to northern side one (Höhn et al. 2005).

Recent dendroecological investigations proved that temperature exerts significant positive influence on annual growth of the stone pine at the Eastern Carpathian timberline (Popa 2005, Kern et al. 2007).

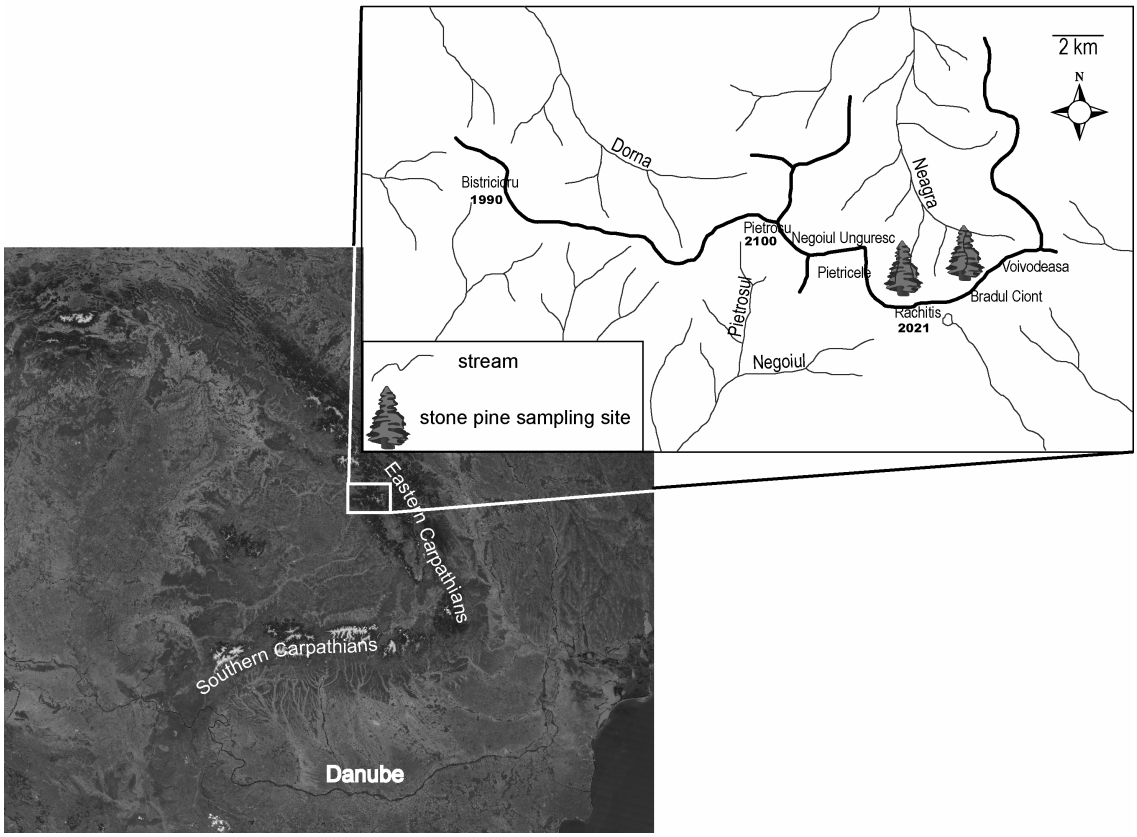

Figure 1. Location of the Calimani Mts in the Eastern Carpathians. The sketch map shows the study site within the area (MODIS image downloaded from: http://visibleearth.nasa.gov)

2.2 Sample collection and preparation

The research area is the upper timberline below the Rachitis Peak and Bradului Ciont Peak (*Figure 1*). We have collected samples from living trees and numerous dead trees lying on the ground between 2003 and 2006. Samples' surfaces were prepared by abrasive belt and polished, so the tree-ring boundaries became distinguishable under binocular microscope.

Beside classical dendroclimatological investigations occurrences of frost rings (*Figure 2)* were also recorded. Checking the tree-ring structure of 39 living and 9 reliably crossdated dead stone pine samples collected from the upper timberline of Calimani Mts. we have identified numerous frost rings (*Figure 2*).

Two characteristics were recorded for each identified frost ring:

- Calendar date of the tree ring displaying the frost ring.
- Cambial age of the tree when the frost ring has developed.

Cambial age was precisely determined by ring counting when boring hit the pith. If an extracted increment core or a hollow disk lacked the pith then the missing rings (pith-offset) were estimated by pith locator (graphics of concentric circles).

Number of trees and frost ring frequency were determined for each year. Frost ring frequency was calculated in a given year as number of frost damaged tree rings divided by the

total number of tree rings. In addition, mean age and corresponding standard deviation were also calculated year-by-year from the sample set.

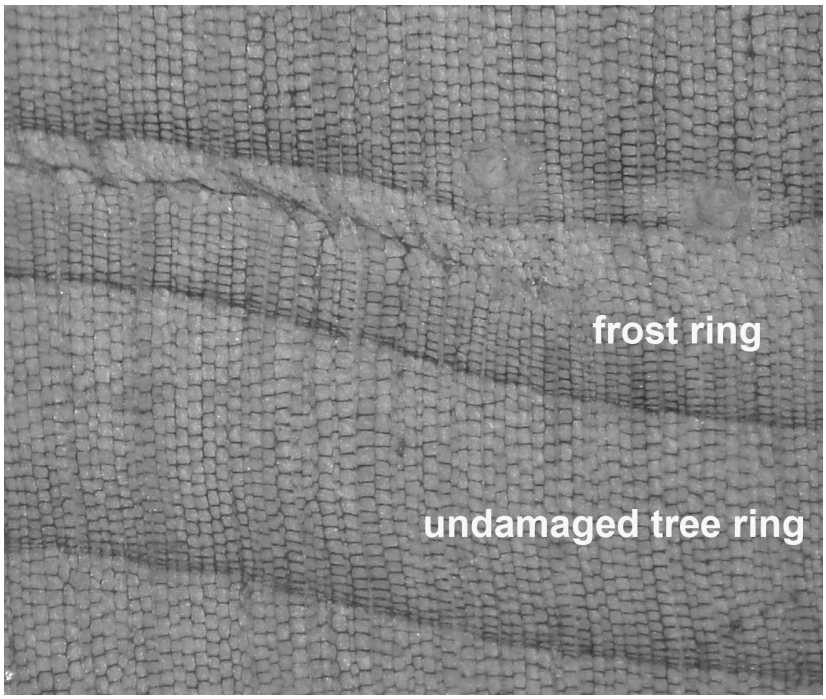

Figure 2. Undamaged vs. frost-affected tree rings as seen on a polished surface in radial transect. The characteristic deformation (frost ring) in the narrower ring is caused by collapse of cells. Note that frost ring does not necessarily extend around the entire circumference!

2.3 Altimetry

We determined the altitude of occurrence of the highest growing stone pine individuals along the Bradului Ciont–Pietrosu part of the caldera-rim in June 2006. We applied Mobile Mapper GPS reciever in mapping.

Specimens were sorted into tree-form or bush-like morphological groups in order to ease comparison between actual and early 20th century inventory data (Fekete – Blattny 1913).

Our original plan for the correction of GPS-measured elevation data by phase measurement failed due to technical difficulties. We had to apply a rather simple method to estimate the difference between the GPS-derived elevation, above ellipsoid, and the real elevation above sea level. The altitude of the Rachitis meteorological station (~2020 m asl) was measured in the mornings and in the afternoons of the work-days of mapping. The resulted elevation data scattered in the 2047.7-2052.5 m range suggesting a roughly constant, 30 m overestimation for the GPS derived elevation data. To improve precision we reduced all elevation data by 30 m in the final comparison (see *Tables 1* and *3*).

3 RESULTS

3.1 Frost rings

The final chronology covers the 1664-2004 period. We have identified in total 59 frost rings out of 6935 investigated tree rings. However frequency percentages are misleading at the low replicated beginning part of the record. Therefore, results are discussed for the 1750-2004

period only, where the number of samples exceeds 10 trees and where the major part of frost ring occurrences (57) was observed (*Figure 3*).

Mean age fluctuated between 50 and 165 yrs, standard deviation changed from 33 up to 93 yrs in the studied period.

We found concentrated occurrences of frost rings in three decades: in the 1790s, 1810s and 1910s.

No any frost ring appeared in two bidecadal periods: 1750-1770 and 1850-1870. The longest period without frost ring occurrence was between 1963 and 2004 in the analysed interval. The maximum of frost ring frequency percentage was 53% for the year of 1876 when 10 samples had a frost ring out of the 19 trees representing that year. The second prominent year was 1810 when 5 from 21 investigated trees have shown a frost ring.

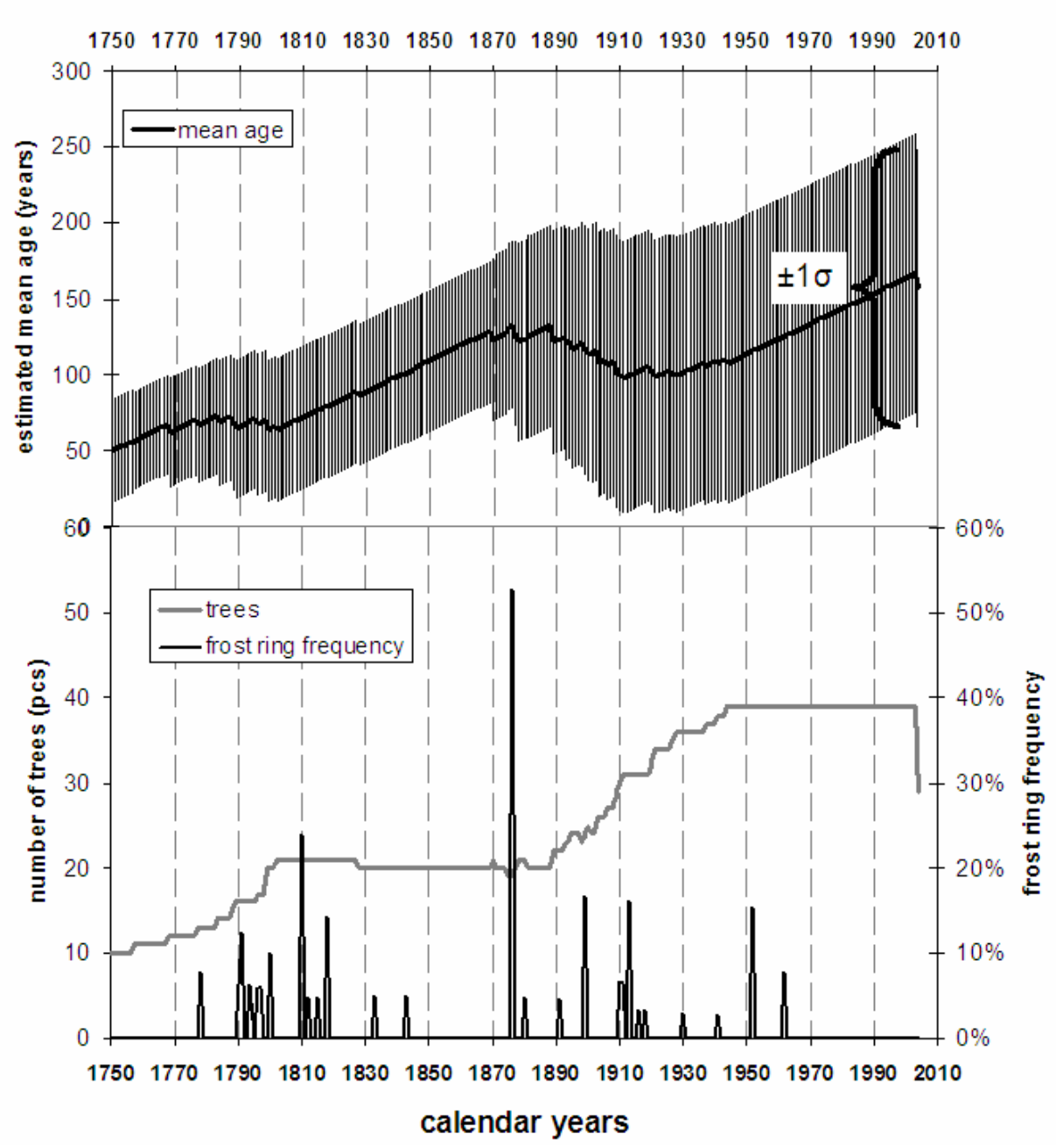

Figure 3. Fluctuation of mean age and its standard deviation (upper graph); frost ring frequency and sample number (lower graph) over the 1750-2004 period

3.2 Treeline

Two tree-form and four bush-like stone pine individuals were found in NW exposure being at highest elevation in their broader area. Arithmetic mean was calculated from individual elevation data within both groups (*Table 1*).

Table 1. Results of altimetry of tree-form and bush-like individuals in NW exposition at the highest elevations, uncorrected data (PDOP below 4 indicates precise measurement)

		Lat (°)	Lon (°)	Alt (m)	PDOP
dwarf-shape	1	47.098	25.238	1964	2.65
	2	47.098	25.238	1951	2.67
	3	47.100	25.236	1933	3.24
	4	47.104	25.259	1880	3.14
	mean			1932	
tree-shape	1	47.102	25.246	1865	2.09
	2	47.101	25.245	1868	2.05
	mean			1866	

4 DISCUSSION

4.1 Frost rings

Severity of frost events occurring in the vegetation season is evaluated from two viewpoints. The stronger the frost event, the higher the frost ring frequency in the stand and the elder specimens are affected (Popa et al. 2006).

The timberline in the Calimani Mts. has suffered the most drastic frost damage in 1876 since 1750. If our sample depth is representative for the stand, it means that frost rings developed in more than half of the trees. The frost ring containing tree ring with oldest observed cambial age (176) coincide with this event. Mature individuals older than 80 years of cambial age have been abundantly affected in that year.

Old diaries, newspapers and the meteorological yearbook reported late frost in the Carpathian region for the 19-21st May 1876 (*Table 2*). So the cold weather of those days must have caused the frost rings of stone pines (Popa et al. 2006).

The course of the pentad mean temperature anomalies (*Figure 4*) shows significantly different temporal evolution of meteorological preconditions causing the 1876 frost ring as Stahle (1991) (cited by Schweingruber 1996) found for post oak (*Quercus stellata* Wangenh.) from North America. Stahle (1991) reported above-average temperature sustained for 2 days at 10-12 days before the frost event. Our meteorological data show the highest positive anomalies one month before the frost event, which had to span more than two days because the vertex of the anomaly-curve existed for two pentads.

Except for the 1910s only single year frost events appear during the 20th century. The recent four decades without frost ring is the longest interval lacking evidence of frost lesion over the studied period. These findings indicate that after 1920 both frequency and severity of frost events seem to decrease in the region compared to the prior 170 years. The increasing estimated mean age of samples cannot explain this phenomenon because the corresponding standard deviation range widens indicating that young – frost sensitive – specimens were continuously represented in the period. It suggests that temperature drops during the vegetation period tend to show lower amplitudes becoming less effective in causing significant damage in the currently developing increment at the timberline. This experience is in agreement with the findings of Scheifinger et al. (2003). They found that the real risk of

late frost damage for plants was lower in Central Europe during the 1990s as compared to the previous four decades. In addition, examining long instrumental temperature records Moberg et al. (2000) found a progressive reduction of about 7% of inter-daily variability of daily temperature index in all-seasons between 1880 and 1998 at four European stations.

Table 2. Reports about late frosts from 1876 in the broader Carpathian region

Late frost in May 1876	Location	Altitude above sea level (m)	Observation	Reference
19-20th, May	Sopron (Hungary)	224	Grapes frozen	Réthly 1998 pp. 542-543.
20th, May	Ungvár (now Uzhgorod, Ukraine)	129	-1.6°C in the morning	
21st, May	Taktabáj (Hungary)	95	Cereals, beans, potatoes frozen	
21st, May	Jászdózsa (Hungary)	100	Heavy frost	
19-21st, May	Sárospatak (Hungary)	126	Heavy frost	Schenzl 1878 pp.105-111.
21st, May	Csíksomlyó (now Şumleu, Romania)	707	Flowering trees frozen	
21st, May	Bakonybél (Hungary)	286	Flowering trees frozen	

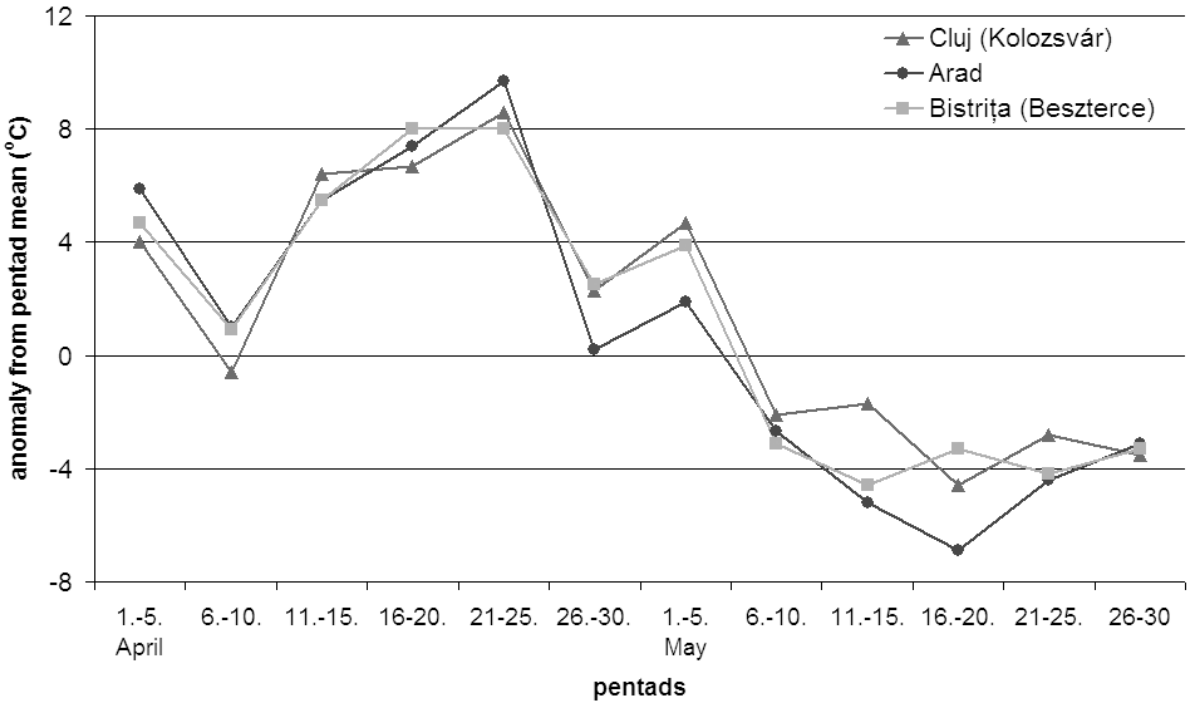

Figure 4. Anomalies of pentad mean temperature at Cluj, Arad and Bistriţa stations between 01. April–30. May, 1876 (data from Schenzl (1878))

4.2 Treeline

For the determination of the elevation change we reduced the mean elevation data of tree-form and bush-like boundaries, uniformly, by the 30 m because of the overestimation bias of GPS measurements. Comparison of treeline data from old forestry survey to present-day corrected ones (*Table 3*) indicate significant upward migration. For the treeline position and bush-like occurrence boundary 65 m and 95 m rising was determined, respectively. In a similar study, Nicolussi et al. (2005) have observed 65 m upslope advance of stone pine treeline in the Ötztal Alps for the 1850-1980 period. Koch et al. (2004) found that treeline, dominated by mountain hemlock (*Tsuga mertensiana*) and subalpine fir (*Abies lasiocarpa*), has risen ~40 m over the last 100 years in Garibaldi Park, (Coast Range Mts., British Columbia). Mátyás (2006) reports a spruce treeline elevational shift in the Southern Urals between 60 and 80 m for the 1928-2000 period. Our results are in agreement with the trend and with the order of magnitude of above-mentioned data.

There are a few possible explanations for discrepancies. First, different species might react with different dynamics. Second, we cautiously avoided sample sites with visible human disturbance (Kern – Popa, 2007) but we cannot exclude that the sites of old forest inventory had anthropogenic influence. Another potential source of error might come from methodological differences between the 20th and 21st century surveys. Elevation data of the old forestry survey were barometrically determined and graphically corrected (Fekete 1902) while GPS determines the elevation above an ellipsoid which we corrected by the above described method.

The collected data support the hypothesis that changes in the frost ring record and migration of the treeline are closely related evidences of vegetation response to a recent regional environmental change. Decreasing frequency and severity of frost events indicate decreasing frost stress accompanied with warmer vegetation season for the timberline in the subalpine zone of the Calimani Mts. The observed upslope migration of altitudinal limit of tree-form and bush-like morphological groups of Swiss stone pine during the 20th century is in agreement with decreasing frost intensity, since milder conditions above the actual forest boundary provide an opportunity to colonize the higher elevated long-time treeless terrain.

Table 3. Centennial shift in the upper limit of tree-form and bush-like occurrences of stone pine in Calimani Mts. between 1910 and 2006 (in metres)

	Altitude of upper limit for	
	tree-form	bush-like
~ 1910 (Fekete, Blattny 1913)	1771	1807
2006 (*corrected data*)	1836	1902
„migration”	+65	+95

5 CONCLUSIONS

Tree-ring structure of 48 (39 living, 9 dead) stone pine trees were analysed from a 340 years long interval (1664-2004). Detailed discussion is restricted to the post-1750 period.

The timberline of Calimani Mts. has suffered the most drastic frost event in 1876 since 1750. After 1920 both frequency and severity of frost events seem to decrease compared to the prior 170 years.

Comparing treeline data from the old forest inventory of Fekete and Blattny to present-day (2006) data indicates a significant upward shift. A difference of 65 m and 95 m was established for treeline and boundary of bush-like occurence, respectively. This value is a bit higher than other published data but is in the same order of magnitude.

The observed upslope advance of tree-form and bush-like morphological groups of stone pine during the 20th century is probably related to the decreasing frost stress above the timberline zone documented by the frost ring record. So, less severe conditions above the forest boundary provide opportunities to colonize the long-time treeless terrains.

Acknowledgement: ZK was funded by the Hungarian National Science Foundation (OTKA) projects T43666 and K67583; IP by the IDEII program, project ID65. The joint field work was financed by the bilateral cooperation project RO-37/2005. Special thanks to Miklós Kázmér and Csaba Mátyás for their comments on an earlier version of the manuscript.

REFERENCES

ESPER, J. – SCHWEINGRUBER F.H. (2004): Large-scale treeline changes recorded in Siberia. Geophysical Research Letters 31 L06202, doi: 10.1029/2003GL019178

FEKETE, Z. (1902): Magasságmérések az erdészeti növényföldrajzi megfigyeléseknél. [Altimetry techniques in forestry.] Erdészeti Kísérletek 4: 45-54. (in Hungarian)

FEKETE, L. – BLATTNY, T. (1913): Az erdészeti jelentőségű fák és cserjék elterjedése a Magyar Állam területén. [Distribution of trees and shrubs significant in forestry in Hungary.] I. vol, Selmecbánya, 793 p. (in Hungarian)

FRITTS, H. (1976): Tree rings and climate. Academic Press, London. 567 p.

GRABHERR, G. – GOTTFRIED, M. – PAULI, H. (1994): Climate effects on mountain plants. Nature 369: 448.

HÖHN, M. (2001): Pinus cembra populációk ökológiai, morfometrikai és diverzitás-vizsgálata a Kelemen-havasok területén. [Ecological, morphometrical and diversity studies on *Pinus cembra* populations in the Kelemen Mountains (East Carpathians)] Kanitzia 9: 59-72. (in Hungarian)

HÖHN, M. – ÁBRÁN, P. – VENDRAMIN, G.G. (2005): Genetic analysis of Swiss stone pine populations (*Pinus cembra* L. subsp. *cembra*) from the Carpathians using chloroplast microsatellites. Acta Silvatica & Ligniaria Hungarica,. 1: 39-47.

KERN, Z. – NAGY, B – POPA, I. (2007): A periglaciális környezet változásainak vizsgálata a Kelemen-havasokban meteorológiai adatok elemzésével a geomorfológiai és dendrokronológiai bizonyítékok tükrében. [Periglacial environment in Călimani Mts, Romania. – meteorology, geomorphology and dendrochronology.] In: Kázmér M. (ed.): Környezettörténet [Environmental history], Hantken kiadó, Budapest. 257-276. (in Hungarian)

KERN, Z. – POPA, I. (2007): Kései fagyok nyomai cirbolyafenyők évgyűrűiben a Kelemen-havasok erdőhatár övezetében, 1750 és 2004 között. [Imprints of late frosts in tree rings of stone pine at the timberline zone of the Călimani Mts, Romania between 1750 and 2004.] Erdő és Klíma V. 323-334. (in Hungarian with Engl. summary)

Koch, J. – Menounos, B. – Clague, J.J. – Osborn, G.D. (2004): ENVIRONMENTAL CHANGE IN GARIBALDI PROVINCIAL PARK, SOUTHERN COAST MOUNTAINS, BRITISH COLUMBIA. GEOSCIENCE CANADA 31 (3): 127-135.

KÖRNER, C. (1998): Worldwide positions of alpine treelines and their causes. In: Beniston, M. - Innes J. L. (eds.): The impacts of climate variability on forests. Springer. 221-239.

LUCKMAN, B. H. – KAVANAGH, T. A. (1998): Documenting the effects of recent climate change at treeline in the Canadian Rockies. In: Beniston, M. - Innes J. L. (eds.): The impacts of climate variability on forests. Springer, 121-144.

MÁTYÁS CS. (2006) Vándorló erdők. [Migrating forests] Természet Világa, 137. 10: 448-450. (in Hungarian)

MOBERG, A. – JONES, P.D. – BERGSTROM, H. – CAMUFFO, D. – COCHEO, C. – DAVIES, T.D. – DEMARÉE, G. – MAUGERI, M. – MARTIN-VIDE, J. – VERHOEVE, T. (2000): Day-to-day

temperature variability trends in 160- to 275-year-long European instrumental records. Journal of Geophysical Research 105 (D18): 22849-22868.

NAGY, B – KERN, Z. - BUGYA, É. - POPA, I. - KOHÁN, B. (2006): Changes of the periglacial environment of the Călimani Mountains since the Late Little Ice Age. 2nd International Workshop on Alpine geomorphology & Mountain hazards.16-17.

NICOLUSSI, K. – KAUFMANN, M. – PATZELT, G. – VAN DER PLICHT, J. – THURNER, A. (2005): Holocene tree-line variability in the Kauner Valley, Central Eastern Alps, indicated by dendrochronological analysis of living and subfossil logs. Vegetation History and Archeobotany 14: 221-234.

PAULI, H. – GOTTFRIED, M. – GRABHERR, G. (2003): Effects of climate change on the alpine and nival vegetation of the Alps. Journal of Mountain Ecology 7: 9-12.

POPA, I. (2005): Dendroclimatological research at Norway spruce (*Picea abies* (L.) Karst) and Swiss stone pine (*Pinus cembra* L.) from Ronda Mountains. Proceeding of the Romanian Academy series B 7 (1): 65-70.

POPA, I. – KERN, Z. – NAGY B. (2006): Frost ring: a biological indicator of widespread freezing days, and 1876 AD as a case study from the Eastern Carpathians. Proceeding of the Romanian Academy, Series B 8 (1): 55-67.

POPA, I. – KERN, Z. (submitted): Long summer temperature reconstruction inferred from tree-ring record for Eastern Carpathians. Climate Dynamics

RÉTHLY, A. (1998): Időjárási események és elemi csapások Magyarországon 1801-1900. [Meteorological events and calamities in Hungary between 1801–1900.] Vol. I. OMSZ, Budapest, 615 p. (in Hungarian)

SCHEIFINGER, H. – MENZEL, A. – KOCH, E. – PETER, CH. (2003) Trends of spring time frost events and phenological dates in Central Europe. Theoretical and Applied Climatology 74: 41-51.

SCHENZL, G. (1878): Jahrbücher der Kön. Ung. Central-Anstalt für Meteorologie und Erdmagnetismus. VI. kötet, Magyar Kir. Egyetemi Könyvnyomda, Budapest. 128 p.

SCHWEINGRUBER, F.H. (1996): Tree rings and environment. Dendroecology, Birmensdorf, Swiss Federal Institute for Forest, Snow and Landscape Research, 609 p.

STAHLE, D.W. (1990): The tree-ring record of false spring in the Southcentral USA. Dissertation, Arizona State University (manuscript)

Pre- and Postfrontal Influences on Light Trapping of Winter Moth (*Operophtera brumata* L.)

János PUSKÁS [a*] – László NOWINSZKY [b]

[a] Department of Physical Geography, Berzsenyi Dániel College, Szombathely, Hungary
[b] Department of Technology, Berzsenyi Dániel College, Szombathely, Hungary

Abstract – Light trap catches of the winter moth (*Operophtera brumata L.*) getting from the data of national light-trap network were analysed in connection with weather fronts. It is concluded, that weather fronts modify the catches of light traps according to their specific characters (main types) and according to their successions. It is worthy of attention, however, that even in those cases in which the front reduces the number of insects caught, pre- and post-frontal influences often manifest themselves in an increase of the number of collected specimens. Because of the frequency of weather fronts it would be useful to take their effects into consideration on the quantity of insects captured at light-traps. It is necessary to improve the applied method for this purpose.

weather front / light-trap / insect

Kivonat – Pre- és posztfrontális hatások a kis téliaraszoló (*Operophtera brumata* L.) fénycsapdázására. A szerzők az országos fénycsapda hálózat anyagából megvizsgálták a kis téliaraszoló (*Operophtera brumata* L.) gyűjtési eredményeit. Megállapították, hogy az egyes időjárási frontok típusuknak (közelítő és tartózkodó hideg, meleg, okklúziós, egyidejűleg tartózkodó hideg, meleg és okklúziós) megfelelően és attól függően is mindig azonosan módosítják a fénycsapdázás eredményességét, hogy milyen típus után következnek. Figyelemre méltó, hogy a front hatására csökken a befogott lepkék száma, a pre- és posztfrontális hatások sok esetben a gyűjtött egyedek számának emelkedésében nyilvánulnak meg. Az időjárási frontok gyakorisága miatt célszerű lenne hatásukat a fénycsapdázott rovarok mennyiségi értékelése során figyelembe venni, ehhez azonban az alkalmazott módszer továbbfejlesztése szükséges.

időjárási front / fénycsapda / rovar

1 INTRODUCTION

There were a few studies to examine the activities of insects in relation to several types of weather fronts. This contrasts the intensive researches in medical meteorology. Only some publications can be found in the literature dealing with the relationship of weather fronts to light-trap catches of insects. It would be very important to study this problem, because the frontal passages cause sudden and significant changes in the physical environment of living creatures. The organisms of humans or animals reply with front sensitivity symptoms to

[*] Corresponding author: pjanos@gmail.com; 9700 SZOMBATHELY, Károlyi Gáspár tér 4.

simultaneous changes of all weather factors. The exact calculation of insect population densities is only possible, if the factors influencing their flying activity are known. We can use it for the purpose of plant protecting monitoring and forecasting. The flying activity can significantly change very often, when different weather fronts come, so the number of caught individuals represents the current mass of population in different rates of their real numbers.

The connection of weather fronts and light-trap catches of insects was studied by Wéber (1959) in Hungary. According to him research on the influences of front changes is difficult for many reasons (the fronts can come after each other in a few hours intervals, fronts can pass through a country without changing the air-masses, the intensity of the same types of fronts can be different). In the course of his examination he did not try to draw general regularities, but he elaborated a graphical method to characterise the modifying influence of weather fronts on light-trap catches based on the analysis of each concrete typical event. Járfás (1979) made studies on the influence of individual weather factors instead of weather fronts, because of the above-mentioned problems. Kádár and Szentkirályi (1982, 1992) made examinations on the flight activity of ground beetles (*Coleoptera: Carabidae*) using the data of monthly Calendar of Weather Phenomena issued by the National Meteorological Service. They found significant differences between the influences of cold and warm weather fronts. We examined the flying activity of harmful insects in relation to macrosynoptic weather situations - which have close connection with weather fronts - in one of our publications (Károssy et al., 1992). No fundamental publications have been found in foreign literature dealing with the connection of weather fronts and light trap catches.

The data - produced by the national light-trap network in Hungary, which is unprecedented even at world standards - are suitable to examine the influences of weather fronts with mathematical-statistical methods.

2 MATERIAL AND METHODS

Weather fronts can be typified according to more points of view. Berkes (1961) determined 21 types of fronts for the territory of Hungary and characterised them. However their validity is questionable in space, and they do not expand to the whole country (Csizsinszky, 1964). That is why we revaluated the situations of weather fronts in Hungary. We could get these information from the synoptic maps of "Daily Weather Reports" of Hungarian National Meteorological Service (Puskás, 2001).

The light trap data of winter moth (*Operophtera brumata* L.) were analysed from the database of the national light-trap network in Hungary. The food plants of these species widespread in whole Europe are well known. The winter moth attacks not only all the deciduous trees in forests, but also the fruit-trees. The most preferred food trees are oaks, hornbeam, beech, horse chestnut, lime and European hazel (Szontagh and Tóth, 1977). The moths fly at sunset and in the evening from early October till mid-December.

Catches were collected at 18 light trap stations between 1961-1976. Total number of daily catches was 3712 representing 46290 specimens from 837 nights. Daily catches mean the collecting result at one station at one night independently of the catch size.

The location of warm-, cold- and occluded fronts were determined for each day between 1st March and 30th November for the years 1961-1976 from Daily Weather Report issued by the Hungarian National Meteorological Service. We classified the fronts on the basis of their quality and location compared to the surface of Hungary (Puskás, 2001). The following front groups were used:

1.	on-coming cold front	OCF
2.	cold front	CF
3.	on-coming warm front	OWF
4.	warm front	WF
5.	on-coming occluded front	OOF
6.	occluded front	OF
7.	on-coming warm and cold fronts	OWCF
8.	warm and cold fronts	WCF
9.	simultaneous warm, cold and occluded fronts	WCOF
10.	without fronts	W

On-coming front means that the front comes close to the border or just enters to the territory of Hungary. The first 6 front types contain only one weather front, but in the last three ones there can be found two or three fronts. The cold and warm front types are well-known, therefore we should like to show the characteristics of the other weather front types. In the case of occlusion the quick cold front will pull up to warm front line, so the two different air masses can be completely combined. There is a previous situation in type 7 and 8, because the cold front does not reach the warm one, only later can form the occlusion. We can see a complete cyclone when type 9 develops and all the different three front types are simultaneously in the Carpathian Basin.

In the course of processing we examined separately all the 9 types of front situations for those days which followed a day with no front effect including those ones when the previous silent day was proceeded a day with a front effect. We could use these front types because the fronts can pass the whole territory of the Carpathian Basin in a few hours. That is why prefrontal and postfrontal effects can follow each other during the same night.

We calculated relative catch values (RC) from daily light-trap catches for all stations, so we could process the values of different localities and dates simultaneously together. Relative catch is the quotient of the number of individuals caught during the sampling interval (1 night), and the mean catch of one generation or flight counted for the sample interval. In this way, in the case of expected mean number of individuals, the value of relative catch is 1.

After this we summarised the values of relative catches coming from different observing stations for each night. We made an average from these values for all the types of fronts. We made a comparison between the values of relative catch belonging to the front types of each day and the average values of catches on the days before and following the front to demonstrate the possible increase or decrease of collection results caused by weather fronts. We examined the days before separately if there were no any front effect and also if there were any other type of front in the territory of Hungary. We made a comparison between values of relative catches belonging to each type of weather fronts and the catches on the previous and the following nights to show the influence of fronts. We separated those previous days when there were no any front effect and those ones when fronts were in the territory of our country. We examined the differences of catches belonging to the front types on those days, which came after frontless days. These differences were compared with the expectable values. Although we examined all the effects of types and changes of weather fronts, but we did not use the results, where we did not find significant differences in catching results. We controlled the significance level of differences with t-test after the analysis of variance.

4 RESULTS

The catching success of light-traps for winter moth (*Operophtera brumata L.*) depending on weather front changes is shown in *Table 1.*

Table 1. Light-trapping of winter moth (Operophthera brumata L.) in connection with weather fronts

Days before and after night of light trapping (0 day)												
– 2			– 1			0			+ 1			+ 2	
RC	N	P	RC	N	P	RC	N	P	RC	N	P	RC	N
			Without			OCF							
1.13	115		1.42	120	**	1.18	122		0.99	125	**	1.34	133
			CF			OCF							
1.24	33	*	2.06	31	**	0.78	34	*	1.44	33		0.99	33
			Without			CF							
1.08	141		1.14	180	**	1.36	178	**	1.07	176		0.87	174
			OCF			CF							
1.28	56	**	0.71	60		0.98	66	*	0.46	60	*	0.98	58
			WF			CF							
0.96	41		1.00	39	**	1.72	47	**	0.89	44		1.16	44
			OF			CF							
1.87	12		0.64	13	**	2.39	13	**	0.62	13	**	1.59	13
			Without			OWF							
0.71	63	**	1.44	64		1.57	74	*	1.25	67		1.51	64
			CF			OWF							
0.47	10	*	1.44	13	*	0.30	14	*	1.09	15		1.59	16
			WF			OWF							
0.77	33	**	0.35	33	**	1.53	33		1.22	32		1.02	28
			Without			WF							
0.72	199		0.66	194	*	0.88	228	**	1.29	193		1.08	185
			OWF			WF							
0.82	35		1.17	37	*	0.64	37	*	1.18	43		1.2	44
			OCF			WF							
0.45	13	*	1.71	12		1.31	24	*	2.66	18		1.69	18
			Without			OF							
1.22	75		1.04	76	**	0.41	78	**	1.17	79		1.00	77
			CWF			OF							
1.32	10		2.27	11	*	0.55	11	*	0.84	11		0.71	13
			Without			OWCF							
1.04	20	*	1.72	21		1.92	22		1.34	21	*	0.92	22
			Without			WCF							
1.00	21		1.19	19	**	0.54	22		0.69	20	**	1.03	20
			CF			WCF							
1.36	23		1.52	22	**	0.71	24	*	1.35	23		1.32	22
			Without			WCOF							
1.25	31		1.13	29	**	1.83	31		2.03	28	**	0.95	25

Notes: RC = relative catches, N = number of data
Significance levels: * = $P < 0.05$, ** = $P < 0.01$

5 DISCUSSION

The on-coming cold front (OCF) is unfavourable for the catches, if it comes after a cold front (CF) or a day without front effect. The catching increase on the following and second day after it. The on-coming warm front (OWF) is also unfavourable if it comes after cold front (CF). The warm front (WF) and specially the occluded front (OC) are unfavourable, but in both cases the number of caught specimens increases on the following days. The cold front (CF) is favourable for catching, if it comes after a warm front (WF), an occluded front (OF) or a day exempt from any front effect, but the numbers of specimens caught decreases on the following night. The catching is strikingly high on those nights, when simultaneous warm-, cold- and occluded front (WCOF) effects arrive at the Carpathian Basin. The favourable effect is noticed also at the following night at that case. The number of moths caught increased, when there was a cold front (CF) or a day without front before the on-coming warm front (OWF). In this last case the catching is already high at the night before. The on-coming cold- and warm fronts (OCWF) cause also a strong rise in the number of specimens caught.

Practical utilisation of our results seem to be difficult at this moment, because the effect of front types can not unified as favourable or as unfavourable for the success of light trapping, but they are variable according to the front type on the day before. Our examinations did not justify the Wéber's (1959) observation, which experienced prefrontal effects in connection with warm fronts and postfrontal effects in connection with cold fronts. As we think the cold front hardly can mean favourable weather situation for moths. We can explain the observed high flight activity with an idea written in one of our earlier publications (Nowinszky, 1994) the developing of flying activity in cold front (CF) effects. According to our hypothesis the low values of relative catches always refer to those weather situations, when the flying activity of insects is reduced. We can not explain the high values so unanimously. The important environmental changes cause physiological changes in the body of insects. The life of adult is short that is why the unfavourable weather endangers not only the survival of the individual moth, but also the survival of the whole species. In our opinion the moths can use two strategies to prevent these effects, which hinder their normal life functions. One is an increased activity, which is expressed in the rising intensity of the flying, copulation and egg-laying. The other the opposite and the insects try to hide and to tide over the unfavourable weather situations in an inactive mode. So as we see the high catching values equally can belong to favourable and unfavourable weather situations. In those cases, where we did not known the catching results belonging to the front changing in the Table 1, we did not experience significant differences in the number of caught moths. The reason of this can be data belonging to specific front changes, and partly by the fact that some of front changes do not cause significant differences in the flying activity of moths. On the basis of the present results we can demonstrate that weather fronts and especially some types of them modify the success of light trapping. It is worthy of attention, however, that even in those cases in which the front reduces the number of insects caught, pre- and post-frontal influences often manifest themselves in an increase of the number of collected specimens. If we could explore the effects of weather fronts on the flight activity of each species we would be able to work out more exact plant protecting prognoses. For this reason we feel it very necessary to continue our research.

REFERENCES

BERKES, Z. (1961): [Types of air-masses and fronts in the Carpathian Basin] (in Hungarian). Időjárás. 5: 289-293.

CSIZSINSZKY, M. (1964): [Validity of Budapest front calendar in the territory of Hungary] (in Hungarian). National Meteorological Report about the scientific research in 1963. 2: 95-98.

JÁRFÁS, J. (1979): Forecast of harmful moth species with light-trap (in Hungarian). PhD Dissertation, Kecskemét. 127.

KÁDÁR, F. - SZENTKIRÁLYI, F. (1983): Analyse der Lichtfallenfänge der Laufkäfer (Col., Carabidae) in verschiedenen Apfelanlagen und Maisbeständen. Verh. SIEEC, 10: 150-154.

KÁDÁR, F. - SZENTKIRÁLYI, F. (1992): Influences of Weather Fronts on the Flight Activity of Ground Beetles (Coleoptera, Carabidae). Proceedings of the 4th ECE/XIII. SIEEC, Gödöllő 199: 500-503.

KÁROSSY, CS. - NOWINSZKY, L. - TÓTH, GY. - PUSKÁS, J. (1992): Flying activity of the agricultural harmful insects and the connection of macrosynoptic weather types. Boletin de la Sociedad de Lima. 105: 57-58.

NOWINSZKY, L. [ed.], (1994): Light-trapping of insects influenced by abiotic factors. Part I. Savaria University Press. 155.

PUSKÁS, J. (2001): New weather front types and catalogue for the Carpathian Basin. In. No-winszky L. [ed.]: Light trapping of insects influenced by abiotic factors. Part III. Savaria University Press, Szombathely. 87-118.

SZONTAGH, P. - TÓTH, J. (1977): Forest protecting guide (in Hungarian). Mezőgazdasági Kiadó. 211.

WÉBER, M. (1959): Influence of meteorological front changes on insects attracted by light (in Hungarian). Yearbook of Teachers' Training College Pécs. 259-275.

Acta Silv. Lign. Hung., Vol. 4 (2008) 55-59

Correlation Between Hue-angle and Colour Lightness of Steamed Black Locust Wood

László TOLVAJ [a*] – Károly NÉMETH [b]

[a] Institute of Physics, University of West Hungary, Sopron, Hungary
[b] Institute of Chemistry and Forest Site Survey, University of West Hungary, Sopron, Hungary

Abstract – Black locust (*Robinia pseudoacacia L.*) wood was steamed at wide range of temperature (75-130°C) applying long (22 days) steaming time. The colour change was monitored by CIE L*a*b* and L*h*c* colour co-ordinate systems. A wide range of colours from greenish yellow up to chocolate brown were created by steaming in function of the steaming time and temperature. In spite of this wide colour range a good linear correlation was found between the lightness and the colour hue. This linearity had little distortion only above 100°C at a long steaming time. Accordingly, this linear correlation gives the possibility to follow the colour change during steaming by measuring only the lightness.

black locust / steaming / lightness / colour hue

Kivonat – A színezeti szög és a világosság kapcsolata gőzölt akác faanyag esetében. Akác (*Robinia pseudoacacia L.*) faanyagot gőzöltünk széles hőmérséklet tartományban (75-130°C), és hosszú ideig (22 nap). A színváltozást CIE L*a*b* és L*h*c* színkoordináta rendszerekkel határoztuk meg. A gőzölési időtől és hőmérséklettől függően a sárgászöldtől a csokoládé barnáig a színek széles skáláját állítottuk elő. A színek széles skálája ellenére jó lineáris korrelációt találtunk a világosság és a színezeti szög között. Ez a linearitás csupán 100°C fölött, hosszú gőzölési időknél nem teljesült. Ez a lineáris kapcsolat lehetőséget ad a gőzölés során bekövetkező színváltozás követésére csupán a világosság mérésével.

akác / gőzölés / világosság / színezeti szög

1 INTRODUCTION

The texture of wood is one of the most marvellous natural colour harmonies (Kucera and Katuscak 1992). Ranging between yellow and red the colour of wood creates the feeling of warm (Masuda 2001), that is why wood is often used as decorative material in our milieu. The reproduction of colour in wood industry is more and more important. Nowadays the colour determination and selection occur visually in industry, but in research and hopefully in industry the future is the objective colour measurement. Many articles have been published using objective colour measurement technique in last years (Németh – Faix 1988, Bekhta –

* Corresponding author: tolla@fmk.nyme.hu; H-9400 SOPRON, Bajcsy-Zs. u. 4.

Niemz 2003, Hapla – Militz 2004, Mitsui et al 2001, 2004, Mitsui 2004). Mostly the CIE L*a*b* colour co-ordinate system is applied based on D65 light source. The colour co-ordinates are calculated from the reflexion data of the surface. This calculation is a complicated mathematical process (Németh 1984), but for computer supported colorimeters this is more simple. Correlation could be established between the co-ordinates which simplify the industrial colour measurement. It would not be necessary to calculate all tree co-ordinatees. Németh (1982) found that light wooden colour is always accompanied with close to yellow hue and dark colour usually has reddish hue.

In this study the correlation between colour hue and lightness was examined during steaming of black locust. A special attention was paid to determine the influence of temperature and steaming time because of the high temperature sensitivity of the colour change of black locust (Tolvaj et al 2004). On the basis of the results an easy method is proposed to monitor the colour change caused by steaming.

2 MATERIAL AND METHODS

For laboratory steaming black locust (*Robinia pseudoacacia L.*) wood specimens were investigated. Specimens were prepared with the size of 200x60x20 (mm) and only those without any wood defects were used for the tests. The treatment was carried out in a steam chest at 100% relative humidity with temperature values of 75-130^{o}C. Wood specimens were placed in a large pot with distilled water for conditioning the air to maintain maximum relative humidity between 75-100 ^{o}C. The pot was heated in a drying chamber to the indicated temperatures. The steaming process started with a six hours heating. The temperature was regulated automatically around the set values with a tolerance of ± 0.5^{o}C. Specimens were removed after 1; 2; 4; 6; 9; 12; 15; 18 and 22 days. The temperatures above 100°C were generated in an autoclave because of the high pressure. Specimens were removed from here after 0.5; 1; 2; 3; 4; 5 and 6 days of steaming between 105-115°C and after 0.25; 0.5; 1; 2; 3; and 6 days of steaming at 120°C and at 130°C.

Before colour measurements, the steamed wood specimens were conditioned for one month at room temperature. The specimens were then cut with a sharp circular saw through the centre parallel to the longer side and the newly prepared surfaces were used for colour measurements. For the colour measurements a MINOLTA 2002 colorimeter was used. The reflection spectrum was measured in the 400-700 nm regions. From these data, the L*, h*, c* colour co-ordinates were calculated based on the D65 light source. On each specimen, colour measurements were taken at 10 randomly chosen spots and the results were used for further analyses.

3 RESULTS AND DISCUSSION

The colour hue of wood is between 0° and 90°, where 0° represents the red colour and 90° represents the yellow colour. The full intensity range of lightness is 0-100 units, where 0 represents the total dark followed by grey up to bright white (100 units). Németh (1982) found linear relationship between lightness and colour hue examining the colour co-ordinates of different wood species. Tolvaj (1994) demonstrated the same relation within one sample if the colour change was created by steaming at 90°C in case of black locust, poplar, spruce, Scots pine and larch, the only difference among the species consist of the slope of the line.

Based on these results the temperature and steaming time dependence of the above mentioned linear relationship was investigated in the case of black locust. A wide range of colours from greenish yellow up to chocolate brown were created by steaming varying the

steaming time and temperature (Tolvaj et al 2004). The correlation between lightness and colour hue the results are presented in Fig. 1 and 2. Where the linearity is well demonstrated. The linear regression equations and the coefficients of determination are listed in Table 1. (The curved end parts in Fig. 2 were ignored.) The coefficients of determination shows high correlation between the hue and the lightness in all cases. The dots representing the nonsteamed samples are located in the top-right corner followed by the colour dots of the steamed samples towards left with growing steaming time listed in "Materials and methods". In Fig. 1 the colour parameters are presented for specimens with steaming temperatures below 100°C. The initial colour of black locust is one of the most yellow wooden colour, represented here by the 1.4 - 1.5 units of hue. With increasing temperatures the change towards red (decreasing hue values) is greater. At 75°C the decrease stops at 1.2 units, but at 95°C it goes down to 1 unit for the longest treatment time. In Fig. 2 the colour parameters are presented for specimens with steaming temperatures above 100°C. The linearity between lightness and colour hue is accentuated at short steaming times. Only exceptions are the end parts of the lines. The curves have minimum values close to 0.96 of hue independently of the steaming temperature, but they are obtained at different time values. With rising temperature this time values are decreasing rapidly, for example at 100°C this time value is 18 days but at 130°C this drops to 1 day. The chemical background of this phenomenon needs further investigations.

Table 1. The linear regression equations and the coefficients of determination (R2)

Temperature (°C)	Fitted linear function	R^2
75	y = 0.0143x + 0.4818	0.983
80	y = 0,014x + 0.47	0.997
85	y = 0,0161x + 0,319	0.9954
90	y = 0,0154x + 0,3726	0.9853
95	y = 0,0146x + 0,400	0.9968
100	y = 0.0153x + 0.3708	0.9915
105	y = 0.0144x + 0.3889	0.9986
110	y = 0.013x + 0.4607	0.9938
115	y = 0.0148x + 0.3999	0.9955
120	y = 0.0158x + 0.3321	0.9998
130	y = 0.0165x + 0.2856	0.998

The above discussed linear correlation gives the possibility to follow the colour change during steaming by measuring only the lightness. This result represents the main impact of this study. Because the lightness depends only on the Y colour component it can be measured by a proper colour filter too, avoiding the use of an expensive colorimeter. This possibility permits a fast and easy colour monitoring at steaming. But a special attention has to be paid for high steaming temperatures and long treatment times where the linearity is distorted.

4 CONCLUSIONS

A wide range of colours for black locust wood, from greenish yellow up to chocolate brown can be created by steaming using different steaming time and temperature. In spite of this wide colour range a linear correlation was found between the lightness and the colour hue. This linearity had little distortion only above 100°C and just in the case of long steaming time. The linear correlation makes possible to control the colour change during steaming by measuring only the lightness, which does not need expensive colorimeter, only using a colour filter and a detector are sufficient.

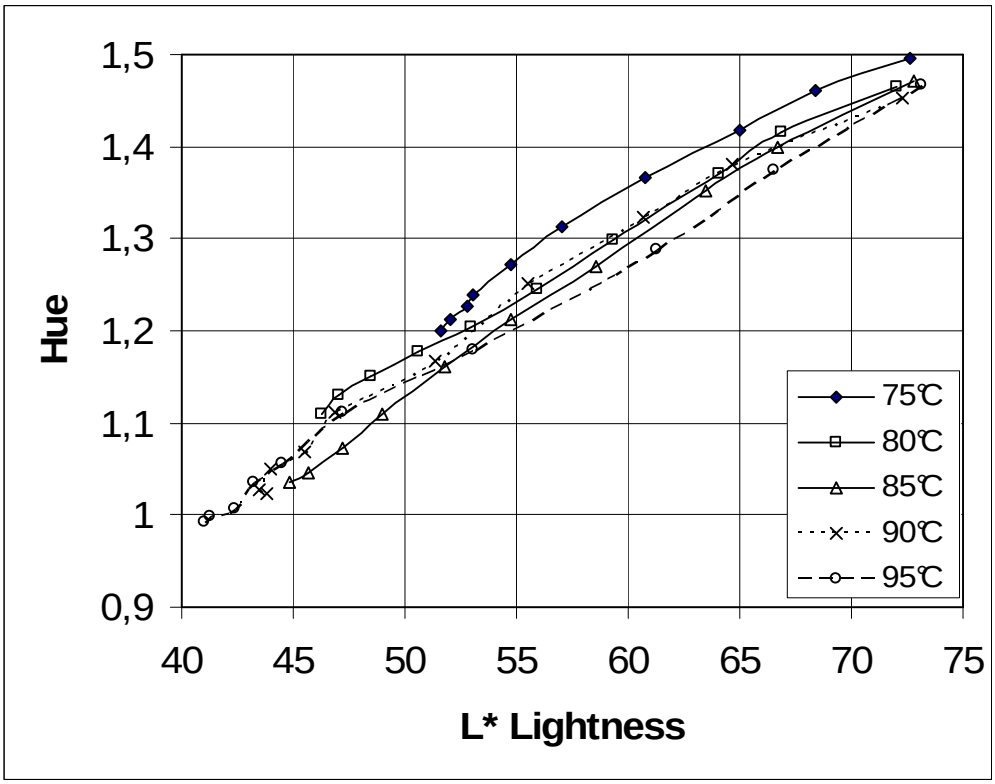

Figure 1. Correlation between lightness and hue of steamed black locust (temp. below 100°C). Colour dots of nonsteamed wood are in the right corner followed by the dots of steamed wood with increasing time

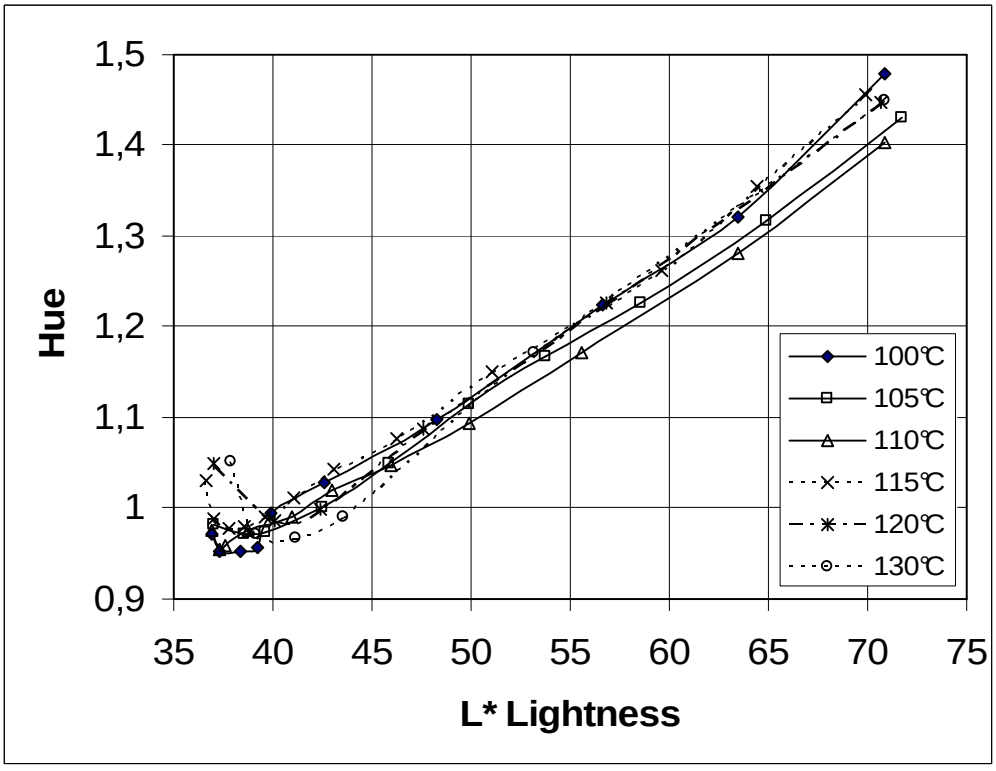

Figure 2. Correlation between lightness and hue of steamed black locust (temp. above 100°C). Colour dots of nonsteamed wood are in the right corner followed by the dots of steamed wood with increasing time

Acknowledgement: The authors thank the financial support of the Hungarian Jedlik Project.

REFERENCES

BEKHTA, P. – NIEMZ, P. (2003): Effect of High Temperature on the Change in Color, Dimensional Stability and Mechanical Properties of Spruce. Holzforschung 57: 539-546

HAPLA, F. – MILITZ, H (2004): Colour measurements and gluability investigation on red heart beech wood (*Fagus sylvatica* L.) Wood Research 49: 1-12.

KUCERA, L. – KATUSCAK, S. (1992): Das Phenomen Holzfarbe. Holz-Farbe-Gestaltung, 24. Fortsbildungkurse der Schweizerishen Arbeitsgemeinschaft für Holzforschung (SAH) in Weinfelden. (4-5 November) Zürich. 43-52.

MASUDA, M. (2001): Why human loves wood grain figure? Extraction of vision-physical characteristics deeply related to impression. ICWSF 2001 Conference (5-7 September) Ljubljana. 11-23.

MITSUI, K – TAKADA, H – SUGYAMA, M. – HASEGAWA, R. (2001): Changes in the Properties of Light-Irradiated Wood with Heat Treatment. I. Effect of Treatment Conditions on the Change in Color. Holzforschung 55: 601-605

MITSUI K (2004): Changes in the properties of light-irradiated wood with heat treatment. Part 2. Effect of light-irradiation time and wavelength. Holz als Roh und Werkstoff 62:23-30

MITSUI, K. – MURATA, A. – TSUCHIKAWA, S. – KOHARA, M. (2004): Wood Photography Using Light Irradiation and Heat Treatment. Color Research and Application 29:312-316

NÉMETH K. (1982): A fa színének értékelése a CIELAB-rendszerben. [The colour of wood in CIELAB system] Az Erdészeti és Faipari Egyetem Tudományos Közleményei (2): 125-135 (in Hungarian)

NÉMETH, K. (1984): Színmérés a faiparban IV. A CIELAB színingermérő rendszer alkalmazása Faipar 33 (5) 156-159.

NÉMETH, K. – FAIX, O. (1988): Farbmessung zur Beobachtung der Photodegradation des Holzes. Holz als Roh- und Werkstoff 46: 472

TOLVAJ, L. (1994): A faanyag optikai tulajdonságai. *In:* A faipari műveletek elmélete (Szerk.: Sitkei György) [Optical properties of wood *In:* Theories of mechanical wood processing]. Mezőgazdasági Szaktudás Kiadó, Budapest. 87-103. (in Hungarian)

TOLVAJ, L. – MOLNÁR, S. – TAKÁTS, P. – VARGA, D. (2004): Az akác (*Robinia pseudoacacia L.*) faanyag színének változása a gőzölési idő és hőmérséklet függvényében [Colour modification of black locust as a function of steaming time and temperature]. Faipar 52 (4): 9-14 (in Hungarian)

Acta Silv. Lign. Hung., Vol. 4 (2008) 61-79

Festigkeitstheorien von anisotropen Stoffen mit sprödem Bruchverhalten

Teil 1: Vergleich und Beurteilung der anisotropen Festigkeitskriterien auf Grund von theoretischen Überlegungen

József SZALAI*

Institut für Technische Mechanik und Tragwerke, Westungarische Universität, Sopron, Ungarn

Zusammenfassung – Um die Ttragfähigkeit von Konstruktionen aus anisotropen Werkstoffen beurteilen zu können, wird eine Festigkeitstheorie benötigt. Von den Festigkeitshypothesen, die im vorigen Jahrhundert aufgestellt wurden, können drei, als allgemeingültig betrachtet werden, das heisst sie können für alle Arten der Anisotropie des Werkstoffes und beliebige Spannungszustände verwendet werden. Jede dieser Theorien kann durch eine Festigkeitsoberfläche (das ist eine Hyperoberfläche im Raum der sechs Spannungskomponenten) veranschaulicht werden. Jeder Punkt dieser Fläche stellt einen Spannungszustand im Grenzzustand des Versagens dar und soll im Folgenden als Spannungspunkt bezeichnet werden. Für zähe Stoffe sind diese Oberflächen immer konvex. Es ist zu beweisen, dass diese Oberflächen für Stoffe mit sprödem Bruch auch konkave Flächenteile – im Einklang mit der Praxis – beinhalten können. Die Relationen der Festigkeitshypothesen können so umgestaltet werden, dass auf einer Seite der Bestimmungsgleichung ein Ergänzungspotential, bzw. eine zu ihm proportionale Grösse bleibt. So interpretiert, behaupten die Theorien von Mises und Tsai-Wu, dass das bis zum Bruch angehäufte Ergänzungspotential eine Konstante und somit unabhängig von der Orientierung der Hauptspannungen gegenüber der Hauptachsen der Anisotropie ist. Diese unserer physikalischen Vorstellung widersprechende Schlussfolgerung wird allein von dem Kriterium von Ashkenasi nicht gefolgt, es sagt im Gegenteil aus, dass das bis zum Bruch angehäufte Ergänzungspotential keine Konstante, sondern eine Funktion der Invarianten des Spannungszustandes und damit indirekt der Orientierung ist. Unsere Feststellungen gelten in erster Linie für das natürliche Holz und für die Holzwerkstoffe, können aber für jeden anisotropen Stoff mit sprödem Bruchverhalten zu erweitert werden.

anisotrope Festigkeitstheorien / zusammengesetzter Spannungszustand / ergänzungspotenzial von anisotropen Stoffen / technische Festigkeiten / Holz- und Holzwerkstoffe

Abstract – Strength-theories of anisotropic materials with brittle rupture. Part 1: Comparison and adjudication of anisotropic strength-criterions by virtue of theoretical considerations. The sizing of load-bearing anisotropic structures needs strength-criterion theories. Three of these hypothesises from the last century seem to be generally acceptable, so they are adaptable to all anisotropic materials in optional tensional status. A strength surface (a 6-dimensions hyper surface in the place of the stress-components) meets all theories. If they are tough materials, these surfaces can

* jkszalai@fmk.nyme.hu; H-9401 SOPRON, Pf. 132

be only convex. Demonstrable – according the tests: the bunging surfaces with brittle rupture materials can content concave parts, too. The bunging relations can be transformed having one site supplementary potential or rather proportional expressions. In this interpretation the thesises of von Mises and of Tsai-Wu affirm the supplementary potential to bunging is constant and depends not on the orientation. The not reconcilable to this approach consequence is not followed by the Ashkenasi-theory affirming the accumulated to the break supplementary potential is not constant, but depends on invariants of the stress state, mediately on orientation. These statements apply first of all to wood and wood-based materials, but can be extended to all anisotropic materials with brittle rupture.

combined stress state / brittle rupture / anisotropic strength-theories / complementary energy / engineering strengths / wood and wood based materials

Kivonat – Ridegen törő anizotrop anyagok tönkremeneteli elméletei. 1. rész: Az anizotrop tönkremeneteli kritériumok összehasonlítása és megítélése elméleti meggondolások alapján. Az anizotrop anyagú teherviselő szerkezetek méretezéséhez szükség van valamilyen tönkremeneteli elméletre. Az elmúlt században megalkotott tönkremeneteli hipotézisek közül három általános érvényűnek tekinthető jelenik meg a szakirodalomban. Ezek bármilyen jellegű anizotrópia és tetszőleges feszültségi állapot esetén alkalmazhatók. Ezen elméletek megalkotói: von Mises, R. (1928); Ashkenasi, E.K. (1966); Tsai, S.W. és Wu, E.M. (1971). Mindhárom elmélet szemléltethető egy ún. szilárdsági felülettel (ami egy hiperfelület a feszültség-komponensek hatdimenziós terében). Amennyiben egy kritikus pontban a feszültségi állapotnak megfelelő képpont rajta van a hiperfelületen, az anyag éppen a tönkremenetel határállapotában van. Ha a feszültségi képpont a felületen kívül helyezkedik el, az anyag tönkrementnek tekintendő. Szívós anyagoknál a tönkremeneteli felület mindig konvex. Bizonyítható - és a gyakorlatban is tapasztalható - hogy rideg anyagoknál a felület konkáv részeket is tartalmazhat. A szilárdsági kritériumokat megfogalmazó relációk átalakíthatók úgy, hogy az egyik oldalon kiegészítő potenciál, ill. azzal arányos mennyiség szerepeljen. Így értelmezve a von Mises- és Tsai-Wu-elméletek szerint az anyag tönkremenetelének pillanatában, a törésig felhalmozott kiegészítő potenciál a főfeszültségek orientációs helyzetétől függetlenül konstans. Ezt a fizikai elképzelésünknek ellentmondó megállapítást egyedül az Askenazi elmélet nem feltételezi. Éppen ellenkezőleg, azt mondja ki, hogy a tönkremenetelig felhalmozott kiegészítő potenciál nem állandó, hanem a feszültségi állapot első két invariánsának – s ezzel indirekt módon az orientációnak – függvénye. Megállapításaink elsősorban a természetes faanyagra és a faalapú anyagokra vonatkoznak, de minden ridegen törő anizotrop anyagra kiterjeszthetők.

anizotrop szilárdságelméletek / összetett feszültségi állapot / anizotrop anyagok kiegészítő potenciálja / technikai szilárdságok / faanyag és faalapú anyagok

1 EINLEITUNG

Die komplizierte innere Struktur und die sich dadurch ergebende Inhomogenität und Anisotropie des Holzes können bei der Bestimmung der Tragfähigkeit von Holzkonstruktionen auf Grund der für sie geltenden Normen und Vorschriften nur in sehr begrenztem Umfang berücksichtigt werden. Besondere Bedeutung erhält dieses Problem, wenn Voraussagen über die Tragfähigkeit und Sicherheit projektierter Holzkonstruktionen gefällt werden sollen.

Üblicherweise herrscht in den kritischen Punkten der zu untersuchenden Konstruktionen ein mehrachsiger Spannungszustand. Für die Beschreibung des Materialverhaltens in derartigen Fällen wurden auch für isotrope Werkstoffe Festigkeitshypothesen aufgestellt. Die Aufgabe ist in zwei Fragestellungen zu teilen. Die erste Frage: wie ändert sich die Festigkeit im Falle eines verhältnismässig einfachen Spannungszustandes (wie z.B. bei reiner Zug-, Druck- und Scherbeanspruchung) in Abhängigkeit der Orientierung. Auf Grund der Erfahrung für die Beschreibung der Elastizität ergibt sich automatisch der Gedanke, die

Festigkeit hat selbst eine Tensorqualität und der Festigkeitstensor soll mindestens vierten Ranges sein. Werden die Tensorkomponenten sorgfältig gewählt, können die zu den verschiedenen Richtungen gehörenden Normal- und Scherfestigkeiten mit Hilfe der Regel der Tensortransformation leicht bestimmt werden. Das zweite Problem heisst: wird der Bruchspannungszustand in einem mechachsigen Spannungszustand gesucht, wird eine geeignete sogenannte Festigkeits- oder Bruchhypothese gebraucht. In dem vergangenen Jahrhundert haben Forscher als Ergebnis ihrer theoretischen und praktischen Arbeit viele Festigkeitshypothesen für anisotrope Stoffe ergründet. Die Mehrzahl dieser sind nur für spezielle Spannungszustände zu verwenden. Zu Ende des Jahrhunderts haben sich jedoch einige Festigkeitshypothsen allgemeiner Gültigkeit auskristallisiert, welche von den Wissenschaftlern akzeptiert und untersucht wurden. Diese Festigkeitskriterien wurden nicht ausgesprochen für Holz, sondern für beliebige anisotrope Stoffe, in erster Linie für faserverstärkte Kunststoffe aufgestellt. Bei der Auswahl eines Bruchkriteriums soll die Art des Versagens berücksichtigt werden. Bei vielen anisotropen Stoffen wird eine grosse Formänderung und ein plastisches und verfestigendes Verhalten zugrundegelegt. Das Versagen von natürlichem Holz, Holzwerkstoffen und den meisten faserverstärkten Kunststoffen ist spröde, der Bruch erfolgt schlagartig bei einer kleinen Deformation. Die Festigkeitshypothesen sollen aus dieser Sicht geprüft werden, ob sie die zähe oder spröde Art des Versagens widerspiegeln können. Der andere Gesichtspunkt der Untersuchungen bedeutet die Analyse, ob der physikalische Inhalt der Festigkeitskriterien nicht zu irgendeinem Widerspruch führt.

Im Folgenden sollen drei Bruchhypothesen und zwar die Hypothese von Mises, die von Tsai-Wu und die von Ashkenasi untersucht werden. Es ist bemerkenswert, dass obwohl die Theorien für das Intaktbleiben bzw. Versagen ihre eigene Relation verwenden, in den für die Bestimmung der in den verschiedenen Kriterien befindlichen Koeffizienten brauchen die gleichen technischen Festigkeitswerte auftreten.

2 FESTIGKEITSTHEORIEN FÜR ANISOTROPE STOFFE

Auf Grund der Fachliteratur gilt die folgende allgemeine Polynom-Gleichung als Festigkeitskriterium (Szalai, J. 1994):

$$t_{ij}\sigma^{ij} + t_{ijkl}\sigma^{ij}\sigma^{kl} + t_{ijklmn}\sigma^{ij}\sigma^{kl}\sigma^{mn} + t_{ijklmnop}\sigma^{ij}\sigma^{kl}\sigma^{mn}\sigma^{op} + ... \le c\,, \qquad (2.1)^{\dagger}$$

$$\text{mit} \quad i,j,k,l,m,n,o,p,\ldots = 1,2,3,$$

wobei

σ^{ij} – den Tensor der wirkenden Spannungen, bzw. die Spannungskomponenten bedeute, und

t_{ij}, t_{ijkl}, t_{ijklmn}, $t_{ijklmnop}$,.... – Festigkeitstensoren 2-, 4-, 6-, 8-, ... -en Ranges, und

c – ein beliebiges Skalar sind.

Wird die Relation erfüllt, bleibt das Material stabil und es tritt kein Versagen auf. Die einzelnen Festigkeitstheorien unterscheiden sich voneinander eigentlich nur darin, welche und wie viele Glieder der Gleichung (2.1) berücksichtigt werden.

[†] Hier und auch später wird die Einstein'sche Summationsregel verwendet.

2.1 Die von Mises'sche Festigkeitstheorie

R. von Mises (1928) hat in seiner Theorie nur das zweite Glied der Gleichung (2.1) behalten. Sein Festigkeitskriterium lautet somit:

$$t_{ijkl}\sigma^{ij}\sigma^{kl} \le 1, \qquad \text{mit } i,j,k,l = L, R, T, \tag{2.2}$$

L, R, T – sind die anatomischen Hauptrichtungen des Holzes.

Nimmt man den Begriff des – von Mises vorgeschlagenen – plastisches Potentials an, ist der Festigkeitstensor vierten Ranges symmetrisch ($t_{ijkl} = t_{klij}$) und besitzt im Falle einer allgemeinen Anisotropie 21 von einander unabhängige Komponenten. Verfügt das Material über eine orthogonale Anisotropie, sinkt die Zahl der unabhängigen Komponenten auf 9. Die neun Komponenten des Holzes (oder eines orthotropen Holzwerkstoffes) können durch die experimentell bestimmbaren, sog. technischen Festigkeiten ausgedrückt werden:

$$t_{iiii} = \frac{1}{\left(f_i^{+}\right)^2} \quad \text{oder} \quad = \frac{1}{\left(f_i^{-}\right)^2}, \qquad \text{mit } i = L \text{ oder, } R \text{ oder } T, \tag{2.3/a}$$

wobei

f_i^{+} und f_i^{-} – Zug- bzw. Druckfestigkeiten in den anatomischen Hauptrichtungen, und

$$\left(t_{ijij} + t_{ijji} + t_{jiij} + t_{jiji}\right) = \frac{1}{\left(t_{ij}\right)^2}, \qquad \text{mit } i, j = L, R, \text{ oder } L, T, \text{ oder } R, T, \tag{2.3/b}$$

wobei

t_{ij} – die Scherfestigkeiten in den anatomischen Hauptebenen sind.

Die physikalische Interpretation der sog. interaktiven Festigkeitskomponenten kann zwar nicht anschaulich ausgedrückt werden, zu ihrer Bestimmung gibt es aber mehrere Ansätze. Werden die Normalfestigkeiten in der Richtung der Winkelhalbierenden zwischen den anatomischen Hauptebenen gemessen, ergeben sich für die Komponenten des Festigkeitstensors folgende Ausdrücke:

$$\left.\begin{aligned}
\left(t_{iijj} + t_{jjii}\right) &= \frac{4}{\left(f_{ij}^{k(45)+}\right)^2} - \frac{1}{\left(f_i^{+}\right)^2} - \frac{1}{\left(f_j^{+}\right)^2} - \frac{1}{\left(t_{ij}^{+}\right)^2}, \\
\left(t_{iijj} + t_{jjii}\right) &= \frac{4}{\left(f_{ij}^{k(45)-}\right)^2} - \frac{1}{\left(f_i^{-}\right)^2} - \frac{1}{\left(f_j^{-}\right)^2} - \frac{1}{\left(t_{ij}^{+}\right)^2},
\end{aligned}\right\} \tag{2.3/c}$$

mit $i, j = L, R,$ oder $L, T,$ oder $R, T,$

wobei

$f_{ij}^{k(45)+}$, $f_{ij}^{k(45)-}$ – Zug- bzw. Druckfestigkeiten in Richtung der Winkelhalbierenden gegenüberden Achsen i-j sind.

Die übrigen Komponenten des Festigkeitstensors verschwinden.

Gl. (2.1) kann als eine Hyperoberfläche im Raum der neun Spannungskomponenten gedeutet werden. Diese kann im Falle eines ebenen Spannungszustandes grafisch als Fläche leicht dargestellt werden. Im orthotropen Fall und ebenen Spannungszustand kann die Schubspannungskomponente aus der Gl. (2.2) ausgedrückt werden und ergibt:

$$\sigma^{ij} = \sqrt{\frac{1 - t_{iiii}\sigma^{ii}\sigma^{ii} - t_{jjjj}\sigma^{jj}\sigma^{jj} - (t_{iijj} + t_{jjii})\sigma^{ii}\sigma^{jj}}{t_{ijij} + t_{ijji} + t_{jiij} + t_{jiji}}} \quad , \tag{2.4}$$

mit $i, j = L, R$ oder L, T oder R, T.

Theoretisch ist diese Fläche ein Ellipsoid, dessen Hauptachsen mit den Spannungskoordinaten zusammenfallen. Am *Bild 1* wurde die Festigkeitsoberfläche von Fichtenholz (*Picea abies* Karst.) in der Ebene *L,-R* dargestellt. Die dazu verwendeten technischen Festigkeiten (Wittmann, Gy. et al. 2001) zeigt *Tabelle 1.*

Tabelle 1. Technische Festigkeiten von Fichtenholz (Picea abies Karst.) in der L-R Ebene.
Table 1. Engineering strength in the plane L-R of spruce (Picea abies Karst).

Fichtenholz		f_L^+	f_L^-	$f_{LR}^{T(45)+}$	$f_{LR}^{T(45)-}$	f_R^+	f_R^-	t_{LR}
Grösse der Strichprobe	(Stück)	315	319	292	325	302	291	-
Mittelwert	(MPa)	63,52	49,34	9,15	9,08	5,92	3,49	9,32
Absolute Streuung	(MPa)	15,00	8,87	2,62	2,32	1,67	0,78	4,01
Relative Streuung	(%)	23,62	17,98	28,59	25,54	28,18	22,37	42,99

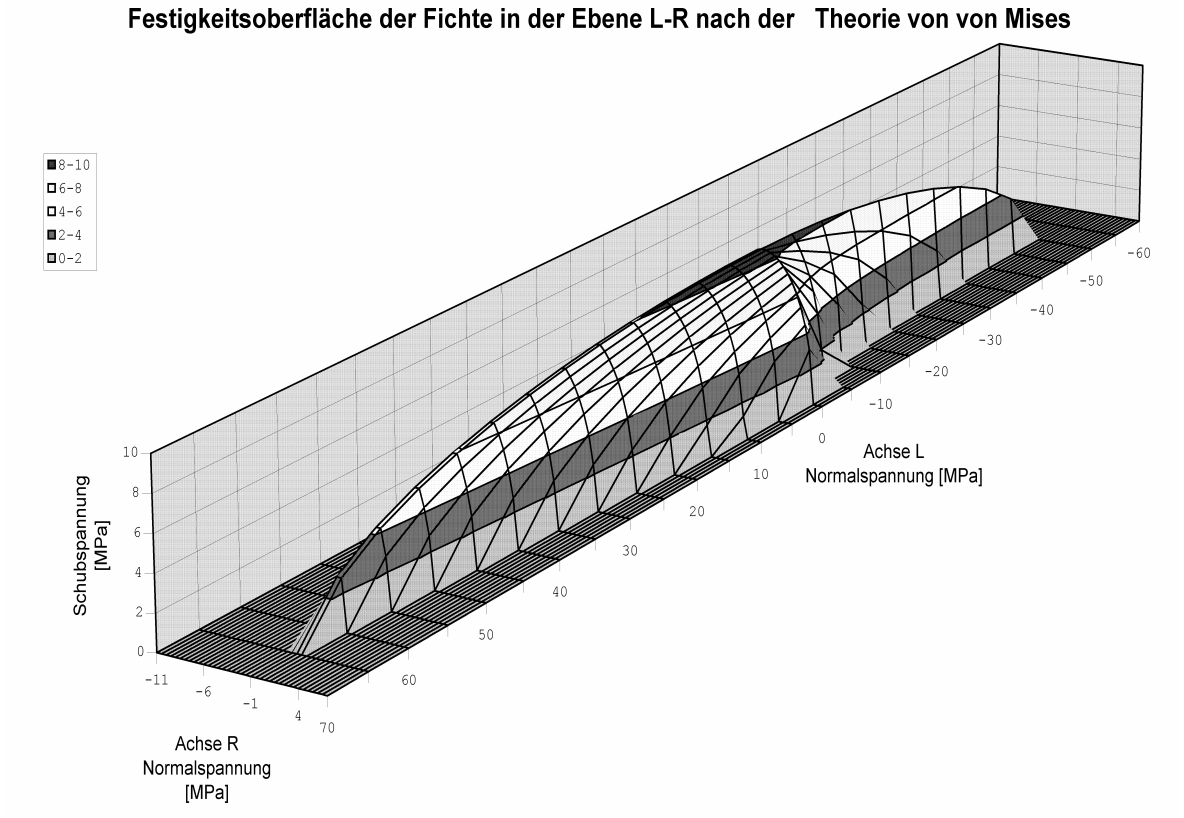

Bild 1. Die von Mises'sche Festigkeitsoberfläche in der Ebene L-R von Fichtenholz
Figure 1. Strength surface of von Mises in the plane L-R of spruce.

2.2 Die Tsai-Wu'sche Festigkeitstheorie

S.W. Tsai und E.M. Wu, (1971) haben das erste und das zweite Glied der Gleichung (2.1) beibehalten. Ihr Festigkeitskriterium hat somit die Form:

$$t_{ij}\sigma^{ij} + t_{ijkl}\sigma^{ij}\sigma^{kl} \le 1, \qquad \text{mit} \quad i,j,k,l = L, R, T. \tag{2.5}$$

Die Komponenten des Tensors zweiten und vierten Ranges sind:

$$t_{ii} = \frac{1}{f_i^+} - \frac{1}{f_i^-}, \qquad \text{mit} \quad i = L \quad \text{oder} \quad R \quad \text{oder} \quad T, \tag{2.6/a}$$

$$t_{iiii} = \frac{1}{f_i^+ f_i^-}, \qquad \text{mit} \quad i = L \quad \text{oder} \quad R \quad \text{oder} \quad T, \tag{2.6/b}$$

$$t_{ij} = \frac{1}{t_{ij}^+} - \frac{1}{t_{ij}^-} = 0, \qquad \text{mit} \quad i,j = L, R \quad \text{oder} \quad L, \text{T} \quad \text{oder} \quad R, T, \tag{2.6/c}$$

$$\left(t_{ijij} + t_{ijji} + t_{jiij} + t_{jiji}\right) = \frac{1}{t_{ij}^+ t_{ij}^-}, \qquad \text{mit} \quad i,j = L, R \quad \text{oder} \quad L, \text{T} \quad \text{oder} \quad R, T. \tag{2.6/d}$$

Eine Möglichkeit für die Bestimmung der interaktiven Komponente:

$$\left.\begin{aligned}
&\left(t_{iijj} + t_{jjii}\right) = \frac{4}{\left(f_{ij}^{k(45)+}\right)^2}\left[1 - \frac{f_{ij}^{k(45)+}}{2}\left(\frac{1}{f_i^+} - \frac{1}{f_i^-} + \frac{1}{f_j^+} - \frac{1}{f_j^-}\right) - \right.\\
&\left. - \frac{\left(f_{ij}^{k(45)+}\right)^2}{4}\left(\frac{1}{f_i^+ f_i^-} + \frac{1}{f_j^+ f_j^-} + \frac{1}{t_{ij}^+ t_{ij}^-}\right)\right],\\
&\text{oder}\\
&\left(t_{iijj} + t_{jjii}\right) = \frac{4}{\left(f_{ij}^{k(45)-}\right)^2}\left[1 + \frac{f_{ij}^{k(45)-}}{2}\left(\frac{1}{f_i^+} - \frac{1}{f_i^-} + \frac{1}{f_j^+} - \frac{1}{f_j^-}\right) - \right.\\
&\left. - \frac{\left(f_{ij}^{k(45)-}\right)^2}{4}\left(\frac{1}{f_i^+ f_i^-} + \frac{1}{f_j^+ f_j^-} + \frac{1}{t_{ij}^+ t_{ij}^-}\right)\right] \quad ,
\end{aligned}\right\} \tag{2.6/e}$$

mit $i,j = L, R$ oder L, T oder R, T.

Auch dieses Kriterium kann durch eine Oberfläche dargestellt werden. Diese hat – im allgemeinen Fall – die Form eines Ellipsoides. Wie *Bild 2* zeigt, sind die Hauptachsen des Tsai-Wu'schen Ellipsoides zu den Spannungskoordinaten nicht parallel.
Der Ausdruck der Oberfläche für einen ebenen Spannungszustand lautet:

$$\sigma^{ij} = \sqrt{\frac{1 - t_{ii}\sigma^{ii} - t_{jj}\sigma^{jj} - t_{iiii}\sigma^{ii}\sigma^{ii} - t_{jjjj}\sigma^{jj}\sigma^{jj} - (t_{iijj} + t_{jjii})\sigma^{ii}\sigma^{jj}}{t_{ijij} + t_{ijji} + t_{jiij} + t_{jiji}}} \tag{2.7}$$

mit $i, j = L, R$ oder L, T oder R, T.

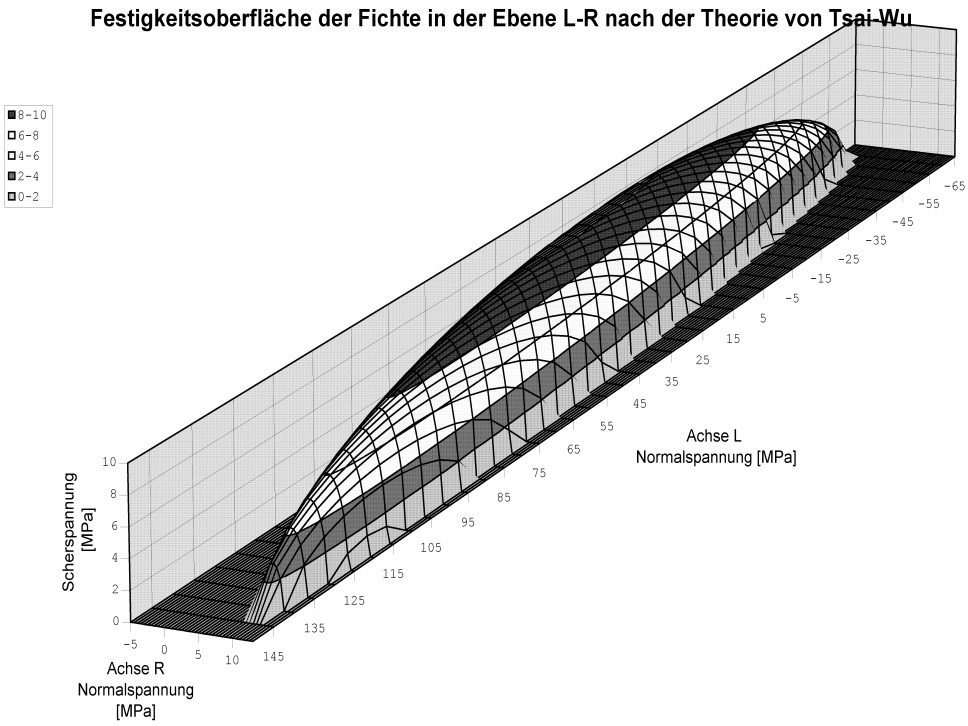

Bild 2. Die Tsai-Wu'sche Festigkeitsoberfläche in der Ebene L-R von Fichtenholz
Figure 2. Strength surface of Tsai-Wu in the plane L-R of spruce

2.3 Die Ashkenasi'sche Festigkeitstheorie

Ashkenasi (1966, 1967, 1976, 1978, Askenasi – Ganov 1972) hat zuerst einen Festigkeitstensor vierten Ranges definiert, dessen Struktur der des Nachgiebigkeitstensors der Elastizität völlig ähnlich ist. Sie hat das zweite und das vierte Glied von Relation (2.1) behalten. Es ist ihr aber gelungen, die Komponenten des Tensors achten Ranges mit den Komponenten des von ihr definierten Festigkeitstensors vierten Ranges auszudrücken. Nach einigen Umformungen (Szalai, J. 1994) ergibt sich die neue Form des Kriteriums zu:

$$\frac{t_{ijkl}\sigma^{ij}\sigma^{kl}}{\left|\sqrt{I_1^2 - I_2}\right|} \le 1 \quad , \tag{2.8}$$

worin I_1 und I_2 – die erste und zweite Invariante des Spannungszustandes ist. Die Komponenten des Festigkeitstensors sind nun:

$$t_{iiii} = \frac{1}{f_i^+} \quad \text{oder} \quad = \frac{1}{f_i^-}, \qquad \text{mit} \quad i = L \quad \text{oder} \quad R \quad \text{oder} \quad T, \tag{2.9/a}$$

$$\left(t_{ijij} + t_{ijji} + t_{jiij} + t_{jiji}\right) = \frac{1}{t_{ij}}, \qquad \text{mit} \quad i, j = L, R \quad \text{oder} \quad L, T \quad \text{oder} \quad R, T, \tag{2.9/b}$$

$$\left.\begin{aligned} &\left(t_{iijj} + t_{jjii}\right) = \frac{4}{f_{ij}^{k(45)+}} - \frac{1}{f_i^+} - \frac{1}{f_j^+} - \frac{1}{t_{ij}}, \\ &\text{oder} \\ &\left(\mathrm{t}_{\mathrm{iijj}} + t_{jjii}\right) = \frac{4}{f_{ij}^{k(45)-}} - \frac{1}{f_i^-} - \frac{1}{f_j^-} - \frac{1}{t_{ij}}, \\ &\qquad\qquad \text{mit} \quad i, j = L, R \quad \text{oder} \, L, T \quad \text{oder} \quad R, T. \end{aligned}\right\} \tag{2.9/c}$$

Gl. (2.8) repräsentiert eine Oberfläche vierten Grades. Für den ebenen Spannungszustand ergibt sich daraus folgender Ausdruck:

$$\sigma^{jj} = \pm\sqrt{\frac{1}{q_{ij}}\left[\frac{1}{2q_{ij}} - t_{iiii}\left(\sigma^{ii}\right)^2 - t_{jjjj}\left(\sigma^{jj}\right)^2 - \left(t_{iijj} + t_{jjii}\right)\sigma^{ii}\sigma^{jj} \pm \right.}$$

$$\left. \pm\sqrt{\frac{1}{4q_{ij}^2} - \left(\frac{t_{iiii}}{q_{ij}} - 1\right)\left(\sigma^{ii}\right)^2 - \left(\frac{t_{jjjj}}{q_{ij}} - 1\right)\left(\sigma^{jj}\right)^2 - \left(\frac{t_{iijj} + t_{jjii}}{q_{ij}} - 1\right)\sigma^{ii}\sigma^{jj}}\right], \qquad (2.10)$$

wobei

$q_{ij} = t_{ijij} + t_{ijji} + t_{jiij} + t_{jiji}$, mit $i, j = L, R$ oder L, T oder R, T ist.

Wie am *Bild 3* zu sehen ist, die Festigkeitsoberfläche von Ashkenasi im allgemeinen Fall kein Ellipsoid, sondern eine allgemeinere Fläche ist. Sie muss natürlich „hügelartig" sein, da die Festigkeit in keiner Richtung unendlich gross sein darf. Sie kann jedoch konkave Flächenteile besitzen, was im Falle der ersten zwei Kriterien nicht vorzustellen ist. Einige Versuchsergebnisse (Ashkenasi 1978) bestätigen tatsächlich das Vorkommen konkaver Flächenteile auch in der Praxis vorkommen können.

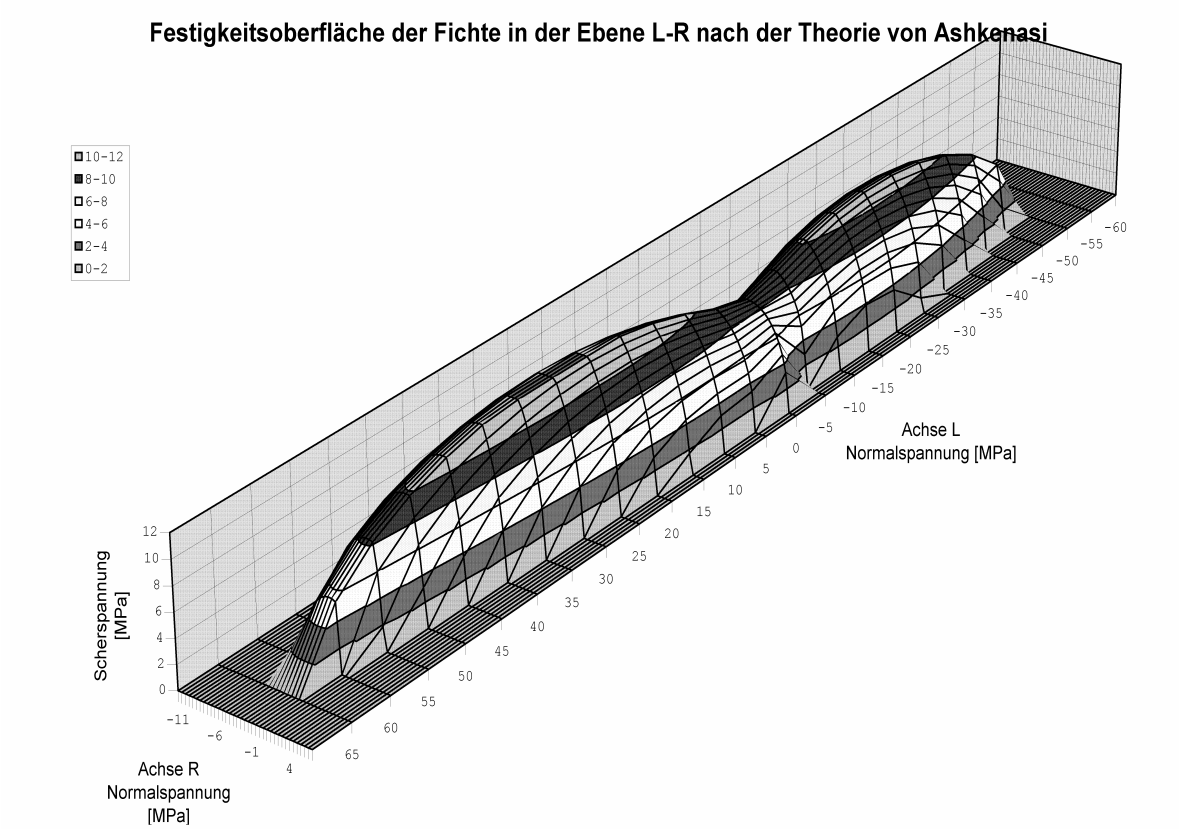

Bild 3. Die Ashkenasi'sche Festigkeitsoberfläche in der Ebene L-R von Fichtenholz
Figure 3. Strength surface of Ashkenasi in the plane L-R of spruce

2.4 Allgemeine Bemerkungen zu den Festigkeitshypotesen

Es ist noch zu bemerken, dass in der Literatur viele Bruchkriterien existieren. Die sind aber meistens nur vereinfachte Formen der ersten beiden Festigkeitskriterien. Die Vereinfachung besteht darin, dass einige Komponenten des Festigkeitstensors a priori als Null betrachtet wurden (zusammenfassende Arbeiten stammen von Covin 1979 und Edlund 1982). In diesem Sinne bedeuten sie keine selbständigen Kriterien und die Aussagen, die später gemacht werden, gelten auch für sie.

Wenn die Relationen. (2.2), (2.5) und (2.8) erfüllt sind, bleibt das Material intakt und zerstörungsfrei. Im ebenen Spannungszustand ist dieses geometrisch sehr gut zu veranschaulichen. Die Gleichheit der linken und rechten Seite von Gl. (2.2), (2.5) und (2.8) bedeutet, dass der Spannungpunkt mit den Koordinaten σ^{LL}, σ^{RR}, $\sigma^{LR} = \sigma^{RL}$ im *Bild 1, 2 oder 3* genau auf der Oberfläche liegt. Der untersuchte Materialpunkt ist gerade im Anfangszustand des Versagens oder im Endzustand der Intaktheit. Beide Zustände haben die gleiche Bedeutung, nämlich den Grenzzustand. Liegt der Spannungspunkt unterhalb der Festigkeitsoberfläche, kann die Belastung noch erhöht werden. Befindet sich der Spannungspunkt ausserhalb der Festigkeitsoberfläche, ist das Versagen bereits erfolgt.

Von Mises hat sein Kriterium eigentlich für plastisches Fliessen von anisotropen Stoffen entwickelt. Nach dem Postulat der Stabilität von D.C. Drucker und dem Normalitätsgesetz muss diese Fliessoberfläche überall konvex sein. Hill (1950) hat das von Mises'sche Fliesskriterium durch ein lineares Glied, den sog. Bauschinger-Tensor (das erste Glied von Gl. (2.1)) ergänzt. Dieser Tensor zweiten Ranges hat die Berücksichtigung unterschiedlicher Zug- und Druckfestigkeit ermöglicht. Mit dem Bauschinger-Tensor können auch die eventuell vorhandenen Eigenspannungen berücksichtigt. Die Fliessoberfläche ist ein – auf der Hauptebene i-j – schief stehendes Ellipsoid, also überall konvex. Tsai und Wu haben zunächst angenommen, dass das Kriterium (2.5) nicht nur für plastisches, sondern auch für sprödes Material gültig und anwendbar ist. Das Ashkenasi'sche Bruchkriterium kann – da Gl. (2.8) eine Gleichung vierten Grades ist – konkave Oberflächenteile aufweisen. Die Frage lautet, wie ein solches Bruchverhalten zu erklären und physikalisch zu begründen ist?

3 BRUCHVERHALTEN VON WERKSTOFFEN

3.1 Bruchverhalten von zähen Werkstoffen

Nach dem Postulat von D.C. Drucker verhält sich das material solange stabil, solange sich die Relation

$$d\varepsilon_{ij} d\sigma^{ij} \rangle\ 0 \tag{3.1}$$

erfüllt. Hier bedeuten

$d\varepsilon_{ij}$ – der elementare Zuwachs des Deformationszustandes (bei Holz $i, j = L, R, T$),

$d\sigma^{ij}$ – der elementare Zuwachs des Spannungszustandes (bei Holz $i, j = L, R, T$).

Relation (3.1) ist physikalisch so zu interpretieren, dass die von der elementaren Zunahme des Spannungszustandes hervorgerufene elementare Zunahme des Deformationszustandes, bzw. die ihnen entsprechenden Vektoren miteinander einen spitzen Winkel einschliessen. Der Zuwachs der Formänderung kann somit den Zuwachs der Spannungen folgen, es verhält sich also stabil. Der entgegengesetzte Fall bedeutet, dass die Vektoren der Spannungs- und Deformationszunahmen miteinander einen stumpfen Winkel einschliessen, die Teilchen des Materials bewegen sich in die entgegensetzte Richtung gegenüber dem Zuwachs der

Spannungen. Das kann nur dann geschehen, wenn die Kontinuität des Materials zu existieren aufhört. Das bedeutet, dass das Material bereits versagt hat.

Bei jedem Spannungszustand, bei dem die elastische, plastische, viskoelastische oder plastisch-verfestigende Deformation beginnt, liegt der Spannungspunk im Spannugsraum auf einer geschlossenen (Hyper)oberfläche. Es ist leicht zu beweisen (Lippmann, 1981), dass die Wirkungslinie des Deformationszuwachses mit der Auswärtsnormalen dieser Oberflächen parallel ist (Normalitätsregel). Aus dem Normalitätsregel und dem Postulat von Drucker folgt das Konvexitätgesetz, das aussagt, dass die (Hyper)oberfläche überall konvex sein muss. Bei jedem Materialverhalten, wo ein kleiner Deformationszuwachs noch zu keiner Zerstörung führt, wie bei elastischen, plastischen, viskoelastischen und plastisch-verfestigenden Stoffen, ist die Oberfläche konvex, unabhängig davon, ob das Material sich isotrop, anisotrop, linear oder nichtlinear verhält.

3.2 Bruchverhalten von spröden Werkstoffen

Das Spannungs-Dehnungs-Verhalten von elastisch-spröden Stoffen ist meistens bis zum Versagen linear oder weicht kaum davon ab. Das Versagen von Bauteilen erfolgt in der Art eines spröden Bruches. Dabei tritt keine verhältnismässig grosse Formänderung entsprechend von zähen Materialien auf. Der Deformationsvorgang ist praktisch bis zum Bruch elastisch (manchmal fast vollkommen linear). Auch Holz und Holzwerkstoffe zeigen solches Verhalten.

Bei linear elastischen Stoffen liegt der zum Bruch führende Spannungspunkt auf einer Oberfläche, das elastische Ergänzungspotential (spezifische potentielle Energie) heisst:

$$\tilde{u} = \int_0^{\sigma^{ij}} \varepsilon_{ij}\, \mathrm{d}\sigma^{ij} = \frac{1}{2}\varepsilon_{ij}\sigma^{ij} = \frac{1}{2} s_{ijkl}\, \sigma^{ij}\sigma^{kl} \quad , \qquad \text{mit} \quad i,j,k,l = L, R, T, \tag{3.2}$$

wobei

s_{ijkl} – der Nachgiebigkeitstensor des anisotropen Stoffes ist.

Gl. (3.2) zeigt, dass das elastische Ergänzungspotential die Quadratische Funktion der Spannungskomponente ist. $\tilde{u}$ kann – infolge seiner Interpretierung – nur positiv sein. Der Spannungspunkt befindet sich bei jedem Spannungszustand – auch noch vor Eintreten des Bruches – auf einem Hyperellipsoid. Die Oberflächen der Unterräume sind Ellipsoide, Ellipsen usw.

Bei einem linear elastischem Werkstoff wird die Deformation von dem Ergänzungspotential gemäss der Gl. (3.2) bestimmt. Wenn die Spannungskomponenten kontinuierlich wachsen, sind die Gesetze der Normalität und der Konvexität bis zum Bruch gültig. Ist das Material isotrop, liegt der Bruchspannungspunkt immer auf demselben Hyperellipsoid, da die Orientierung hier keine Rolle spielt. Bei einem anisotropen Material gehört zu jeder Orientierung ein anderer Wert des Ergänzungspotentials. Die zum Bruch führenden Spannungspunkte liegen auf verschiedenen Hyperellipsoiden. Kommt nach der elastischen Verformung eine plastische, übernimmt die plastische Fliessoberfläche die Rolle der Oberfläche des ergänzenden Potentials und die Gesetze der Normalität und der Konvexität sind weiterhin gültig. Folgt der elastischen Deformation ein spröder Bruch, besteht die Stabilitätsrelation (3.1) nicht mehr. Die Kontinuität des Stoffes hört auf, das Produkt $\mathrm{d}\varepsilon_{ij}\mathrm{d}\sigma^{ij}$ verliert also seinen Sinn. Die Gesetze der Normalität und der Konvexität sind nicht mehr gültig. Die zu den grössten Hyperellipsoiden gehörenden Spannungspunkte sind auch Punkte der Festigkeitsoberfläche. Diese Fläche kann aber – wie es *Bild 4* im Falle eines zwei-dimensionalen Spannungszustandes zeigt – auch konkave Teile aufweisen, die mit praktischen Erfahrungen im Einklang sind und auch theoretisch verständlich und zu beweisen sind.

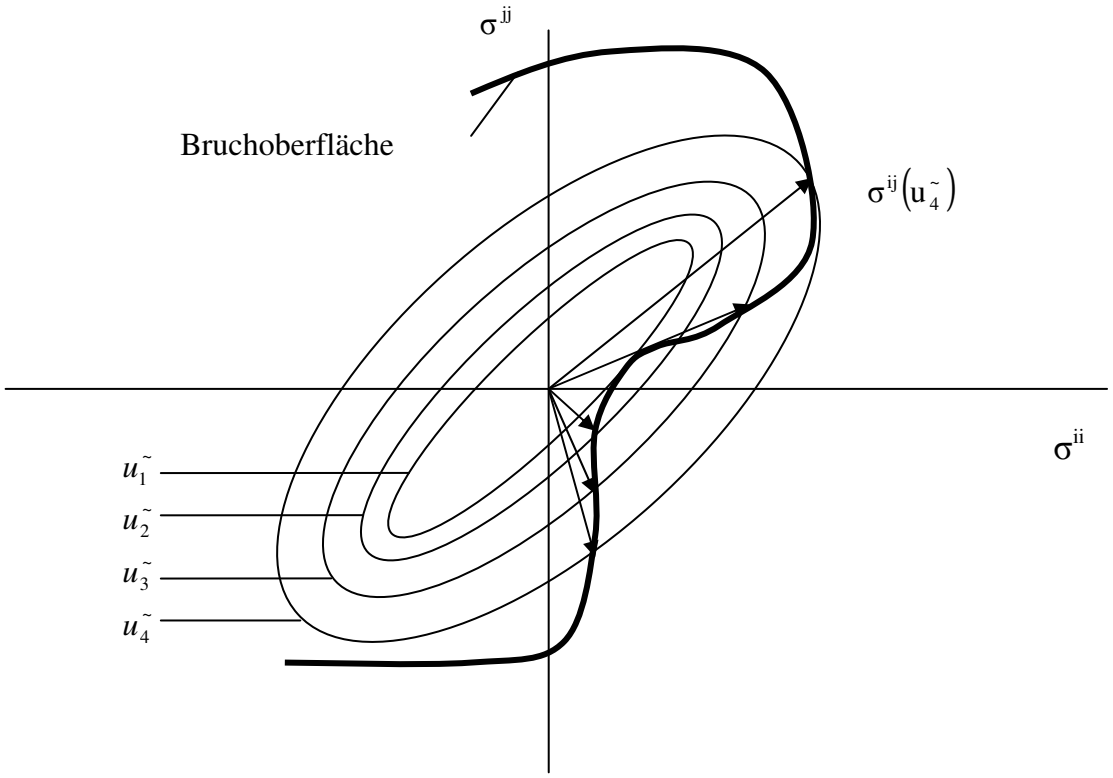

Bild 4. Die Entstehung der Festigkeitsoberfläche eines elastischen Materials mit sprödem Bruch bei zweidimensionalem Spannungszustand
Figure 4. Evolution of strength surface of an elastic material with brittle rupture in plane stress state

4 ENERGIEBILANZ DES BRUCHVORGANGES

Die Relationen (2.2) und (2.5) umgeformt, indem beide Seiten mit f_L^+ multipliziert, ergibt:

$$\tilde{u_M} = f_L^+ t_{ijkl}\sigma^{ij}\sigma^{kl} \le f_L^+ = \text{const}, \qquad \text{mit} \quad i,j,k,l = L, R, T, \tag{3.3}$$

und

$$\tilde{u_{TW}} = f_L^+ \left(t_{ij}\sigma^{ij} + t_{ijkl}\sigma^{ij}\sigma^{kl}\right) \le f_L^+ = \text{const}, \quad \text{mit} \quad i,j,k,l = L, R, T. \tag{3.4}$$

Die Relation (2.8) ist auf die folgende Form zu bringen:

$$\tilde{u_A} = t_{ijkl}\sigma^{ij}\sigma^{kl} \le \left|\sqrt{I_1^2 - I_2}\right|, \qquad \text{mit} \quad i,j,k,l = L, R, T. \tag{3.5}$$

Auf der linken Seite der Relationen (3.3), (3.4) und (3.5) befindet sich ein Grösse, welche – auf Grund der Gl. (3.2) – eine Art Ergänzungspotential ist. Verhält sich das Material bis zum Bruch linear, sind die linken Seiten von Gl. (3.3), (3.4) und (3.5) den wahren Zusammenhang des elastischen Ergänzungspotentials proportional, wie es im Anhang A bewiesen wird. Ist das Material nicht linear, gilt weiterhin, dass die linken Seiten die bis zum Bruch angehäuften Ergänzungspotentiale, bzw. damit proportionale Grössen sind. So betrachtet, dürfen die von Mises'schen und Tsai-Wu'schen Festigkeitskriterien folgendermassen formuliert werden: *Ein*

anisotropes Material versagt, wenn das angehäufte Ergänzungspotential im Körper einen – für das Material charakteristischen - konstanten Wert erreicht. Das bedeutet, dass die angehäuften Ergänzungspotentiale bei jedem Spannungszustand und jeder Orientierung im Grenzzustamd des Versagens gleich gross sind. Das Festigkeitskriterium von E.K. Ashkenasi lautet: *Ein anisotropes Material versagt, wenn das angehäufte Ergänzungspotential im Körper einen bestimmten Wert erreich. der keine Konstante, sondern eine Funktion der ersten und zweiten Invariante des Spannungszustandes ist. Das Ergänzungspotential hängt von den ersten zwei Invarianten des Spannungszustandes und damit indirekt vor der Orientierung ab.*

Dass die erste Definition unseren physikalischen Vorstellungen widerspricht, ist aus einem natürlichen technischen Sinn spürbar. Im Anhang B wird jedoch gezeigt, dass die Gleichheit des Ergänz8ungspotentials vorausgesetzt, zwischen den elastischen Materialkonstanten und den Festigkeiten theoretisch beweisbare Beziehungen bestehen müssen. Diese Zusammenhänge erfüllen sich aber in der Praxis niemals.

Im Anhang C wird gezeigt, dass das den verschiedenen Bruchspannungszuständen entsprechende Potential in Kenntnis der Materialkonstanten (beziehungsweise der Spannungs-Dehnungs-Diagramme) zu bestimmen ist. Hier müssen die elastische Konstanten und die Festigkeiten keinerlei Verbindungen erfüllen.

5 SCHLUSSFOLGERUNGEN

Die Geschichte der Wissenschaft zeigt, dass eine neue Theorie unter den früher angenommenen Theorien sehr schwer Fuss fassen kann und noch schwerer in deren praktischer Anwendung. Es wurde versucht zu berweisen, dass das Ashkenasi'sche Bruchkriterium eine viel allgemeinere Gültigkeit gegenüber den wesentlich bekannteren Kriterien hat. Das Ashkenasi'sche Kriterium kann den Eigenschaften der sprödbrüchigen Stoffe folgen, dass seine Festigkeitsoberfläche auch konkave Teile verfügen darf. Seine Anwendung führt nicht zu Widersprüchen.

Es ist natürlich wichtig neben den theoretischen Feststellungen auch der praktische Beweis der Verwendbarkeit der Festigkeitstheorien. Im Labor der West-Ungarischen Universität sind Untersuchungen begonnen worden, welche die praktische Prüfung der Festigkeitshypothesen nicht nur im ebenen, sondern auch im räumlichen Spannungszustand ermöglichen. Wir haben aber auch die Versuchsergebnisse ähnlicher Art anderer Wissenschaftler verwendet. Dabei wurden Arbeiten von Eberhardsteiner Mitarbeitern verwendet. Die Ergebnisse der im Labor des Institutes für Festigkeitslehre der Technischen Universität Wien durchgeführten Untersuchungen auf dem Gebiet der biaxialen Festigkeit sind in mehreren Artikeln und einem Buch (Eberhardsteiner 1995, 2002; Eberhardsteiner, J. et al. 1991, 1996) publiziert worden. In diesen Versuchen wurde das mechanische Verhalten, vor allem die Festigkeit von Fichtenholz (*Picea abies* Karst.) in der anatomischen Hauptebene *L-R* geprüft. Die Resultate seiner Untersuchungen sind dem Verfasser freundlicherweise zur Verfügung gestellt worden. Im Teil 2 werden die Auswertung und Vergleich der experimentellen Resultate mit denen der verschiedenen Festigkeitshypothesen behandelt.

LITERATUR

ASHKENASI, E.K. (1966): Protschnost' anisotropnüh drevesnüh i sintetitscheskih materialov. [Festigkeit des anisotropen Holzstoffes und von syntetischen Stoffen] 1. kiadás. Moszkva: Isdatelstvo Lesnaja Promüschlennost. (auf Russisch)

ASHKENASI, E.K. (1967): K voprosu o geometrii teorii protschnosti. [Zur Frage der Geometrie der Festigkeitstheorie] Mechanika Polimerov, (4): Riga. 703-707. (auf Russisch)

ASHKENASI, E.K. (1976): Esso ras pro geometriu protschnosti anisotropnüh materialov. [Noch einmal zur Frage der Geometrie der anisotropen Festigkeitstheorie] Mechanika Polimerov, (2): Riga. 269-278. (auf Russisch)

ASHKENASI, E.K. (1978): Anisotropia drevesinü i drevesnüh materialov. [Anisotropie von Holz und Holzwerkstoffen] 1. kiadás. Moszkva: Isdatelstvo Lesnaja Promüschlennost'. (auf Russisch)

ASHKENASI, E.K. – Ganov, E.V. (1972): Anisotropia konstrukzionnüh materialov. [Anisotropie von Baustoffen] Leningrad: Isdatelstvo Maschinostroenie. (auf Russisch)

AZZI. V.D. – TSAI, S.W. (1956): Anisotropic Strength of Composites. Experimental Mechanics, 283-288

COVIN, S.C. 1979: On the Strength Anisotropy of Bone and Wood. Department of Biomedical Engineering, Tulane University, New Orleans, LA. 70118.

DRUCKER, D.C. (1967): Introduction to mechanics of deformable solids. Mc Graw Hill.

EBERHARDSTEINER, J. (2002): Mechanisches Verhalten von Fichtenholz. Experimentelle Bestimmung der biaxialen Festigkeitseigenschaften. Springer-Verlag Wien New York. 174

EBERHARDSTEINER, J. (1995): Biaxial Testing of Orthotropic Materials Using Electronic Speckle Pattern Interferometry. Measurement, (16): 139-148.

EBERHARDSTEINER, J. – GINGERL, M. – ONDRIS, L' (1996): Beurteilung der Messgenauigkeit eines 3D-ESPI-Systems bei der biaxialen Festigkeitsprüfungen von Holz. GESA-Symposium 1996. Experimentelle Beanspruchungsanalyse, neue Entwicklungen und Anwendungen, Schliersee, NSZK.

EBERHARDSTEINER, J. – PULAY, F. – MANG, H. (1991): Zur Frage der Lasteinleitung bei experimentellen Festigkeitsuntersuchungen von zweiaxial beanspruchtem Holz. Österreichesche Ingenieur- und Architekten Zeitschrift (136): 265-272.

EDLUND, B. 1982: Festigkeitshypotesen von orthotropen Werkstoffen. Ingenieurholzbau in Forschung und Praxis. Karlsruhe: Bruderverlag

EHLBECK, J. – HEMMER, K. (1986): Erfassung, systematische Auswertung und Ermittlung von Grundlagen über das zusammenwirken von Längs-, Quer- und Schubspannungen bei fehlerfreiem und fehlerbehaftetem Nadelholz. Technischer Bericht. Stuttgart: IRB Verlag.

FLÜGGE, W. (1972): Tensor Analysis and Continum Mechanics. Berlin-Heidelberg-New York: Springer Verlag.

GOODMAN, J.R. – BODIG, J. (1971): Ortotropic Strength of Wood in Compression. Wood Science, 4 (2): 83-94.

HEMMER, K. (1984): Versagensarten des Holzes der Weisstanne (abies alba) unter mehrachsiger Beanspruchung. Dissertation. Karlsruhe. Selbstverlag.

HILL, R. 1950: The Mathematical Theory of Plasticity. London: Oxford University Press.

KOLLMANN, F. (1982): Technologie des Holzes und der Holzwerkstoffe. 2. Ausgabe. Berlin-Heidelberg-New York: Springer Verlag.

SZALAI, J. (1990): Anizotrop szilárdsági kritériumok összehasonlítása a természetes faanyagra való alkalmazhatóságuk szempontjából. [Vergleich der anisotropen Festigkeitskriterien hinsichtlich ihrer Verwendbarkeit für natürlisches Holz] Építés-, Építészettudomány, XXI. (1-4): 23-57. (auf Ungarisch)

SZALAI, J. (1992): Comparing of failure theories for orthotropic materials on the basis of theoretical criteria of their applicability. Acta Facultatis Ligniensis. (1): 15-31.

SZALAI, J. (1994): A faanyag és faalapú anyagok erőtani méretezése összetett feszültségi állapot esetén. [Bemessung von Konstruktionen aus Holz und Holzwerkstoffen in zusammengesetztem Spannungszustand] Építés-, Építészettudomány. XXVI (3-4): 215-223. (auf Ungarisch)

SZALAI, J. (1996): Az erdei fenyő (Pinus silvestris) technikai szilárdságai. [Technische Festigkeiten von Kieferholz (Pinus silvestris)] Bútor- és Faipar. (6-7) 14-15. (auf Ungarisch)

SZALAI, J. (1997): Technische Festigkeiten des Buchenholzes (Fagus silvatica). Drevársky Vyskum. 42 (3): 1-14.
SZALAI, J. (1998): Technische Festigkeiten der Akazie (Robinia pseudo-Acacia) und der Fichte (Picea excelsa). Drevársky Vyskum. 43 (3-4): 39-51.
SZALAI, J. (1999): A tölgy (Quercus Robur) technikai szilárdságai. [Technische Festigkeiten der Eiche (Quercus Robur)] A Soproni Egyetem Tudományos Közleményei. 1996-1999. 42-45: 189-198. (auf Ungarisch)
SZALAI, J. (1999): A természetes faanyag tönkremeneteli kritériumok által meghatározott szilárdsági felületének általános jellemzői. [Allgemeine Eigenschaften der von den Festigleitskriterien bestimmten Oberflächen des natürlichen Holzes] Faipar. XLVII (2-3): 15-17. (auf Ungarisch)
SZALAI, J. (2001): Faszerkezetek méretezését és gyártását befolyásoló sajátosságok. [Spezifische Eigenschaften, die die Bemessung und Produktion von Holzkonstruktionen beeinflussen] In: WITTMANN, GY. (ed.) Mérnöki faszerkezetek. [Technische Holzkonstruktionen] II. kötet. Mezőgazdasági Szaktudás kiadó. Budapest. 143 - 259. (auf Ungarisch)
SZALAI, J. (2003): A természetes faanyag szilárdsági felületének jellemzői. [Eigenschaften von Festigkeitsoberflächen des natürlichen Holzes] Építés- Építészettudomány XXXI (1-2): 43-59. (auf Ungarisch)
SZALAI, J. (2004): Technische Festigkeiten der Pannonia Pappel (Populus x euramericana cv. Pannonia) und der Zerreiche (Quercus cerris L.). Acta Silv. Lign. Hung. 1 (93-103).
SZALAI, J. – NIEMZ, P. – ANDOR, K. – BARISKA, M – HOWALD, M. (2004): Untersuchungen zum Einfluss der Holzfeuchtigkeit auf das Bruchverhalten von Fichte bei Zugbelastung in Faserrichtung. Schweizerische Zeitschrift für Forstwesen. 155 (1) 1-5.
TSAI, S.W. – WU, E.M. (1971): A general theory of strength for anisotropic material. J. Composite Materials, 5: 58-80.
VOIGT, W. (1928): Lehrbuch der Kristallphysik. Leipzig-Berlin: Teubner Verlag.
VON MISES, R. (1928): Mechanik der plastischen Formänderung von Kristallen. Z. angew. Math. Mech. 8: 161-185.
WU, E.M. (1972): Optimal experimental measurements of anisotropic Failure Tensors. J. Composite Materials, 6: 472-489.

Anhang A

Es soll ein bis zum Bruch annähernd lineares Spannungs-Dehnungs-Verhalten – wie bei vielen spröden Werkstoffen – angenommen werden (*Bild A1*). Es werde ein Holzstab untersucht, dessenLängsachse in Faserrichtung fällt, und auf reinen Zug belastet ist. Die einzige von Null verschiedenen Nomalspannung des Spannungszustandes im Grenzzustand des Bruches sei f_L^+. Das bis zum Bruch angehäufte elastische Ergänzungspotential ist dann:

$$\tilde{u} = \frac{1}{2} s_{ijkl} \sigma^{ij} \sigma^{kl} = \frac{1}{2} s_{LLLL} \sigma^{LL} \sigma^{LL} = \frac{1}{2} s_{LLLL} f_L^+ f_L^+ \quad . \tag{A1}$$

Ddie linke Seite der Gl. (3.3) voll ausgeschrieben, ergibt:

$$\tilde{u}_M = f_L^+ t_{ijkl} \sigma^{ij} \sigma^{kl} = f_L^+ t_{LLLL} \sigma^{LL} \sigma^{LL} = f_L^+ t_{LLLL} f_L^+ f_L^+ \quad . \tag{A2}$$

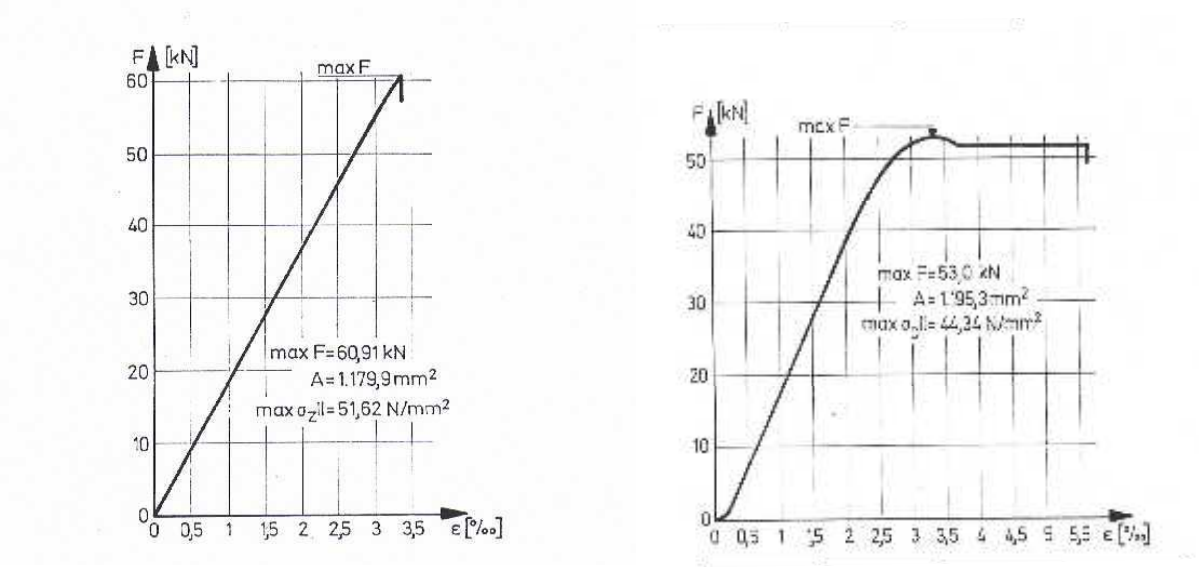

Bild A1. (Ehlbeck, J.-Hemmer, K. 1986)
a) Typische Last-Verformungslinie bei Zugbeanspruchung in Faserrichtung von Holz
b) Typische Last-Verformungslinie bei Druckbeanspruchung in Faserrichtung von Holz

Figure A.1. (Ehlbeck, J.-Hemmer, K. 1986)
a) Typical load-deformation during tensile stress parallel to the grain of wood
b) Load-deformation line during compression stress parallel to the grain of wood

Gl. (A2) durch (A1) dividiert, ergibt weiter:

$$u_M^{\sim} = \lambda_M u^{\sim} \ , \tag{A3}$$

wobei

$$\lambda_M = 2 f_L^+ \frac{t_{LLLL}}{s_{LLLL}} = const. \tag{A4}$$

ist. Gl. (A3) sagt aus, dass die linke Seite des von Mises'schen Kriteriums (3.3) zu dem bis zum Bruch angehäuften elastischen Ergänzungspotential proportional ist und $u_M^{\sim}$ – da λ_M eine dimensionslose Konstante ist –selbst eine Art Ergänzungspotential ist.

Ähnlicherweise kann bewiesen werden, dass die linken Seiten von Gl. (3.4) und (3.5) die bis zum Bruch angehäufte Ergänzungspotentiale sind. Nach kurzer Rechnung ergeben sich die folgenden Konstanten. Für die Tsai-Wu'sche Theorie:

$$\lambda_{TW} = 2 \frac{\left(t_{LL} + t_{LLLL} f_L^+\right)}{s_{LLLL}} = const. \tag{A5}$$

und für das Ashkenasi'sche Kriterium:

$$\lambda_A = 2 \frac{t_{LLLL}}{s_{LLLL}} = const. \tag{A6}$$

Anhang B

Ein Probekörper aus Holz – der parallel zu den anatomischen Hauptrichtungen in der Ebene L-R ausgeschnitten wurde (*Bild B1*) – werde in radialer Richtung mit Normalspannung σ^{RR} bis zum Bruch belastet. Die grösste Normalspannung sei $\sigma^{RR} = f_R^+$. Da es sich um Holz handelt, ist das Deformation- und Spannungsdiagramm bei jeder Holzfeuchte praktisch linear (Szalai, J. et al. 2004), das bis zum Bruch angehäufte Ergänzungspotential lautet:

$$\tilde{u} = \frac{1}{2} s_{ijkl} \sigma^{ij} \sigma^{kl} = \frac{1}{2} s_{RRRR} \sigma^{RR} \sigma^{RR} = \frac{1}{2} s_{RRRR} f_R^+ f_R^+ \qquad \text{(B1)}$$

wobei

s_{ijkl} – der Nachgiebigkeitstenzor, zum Beispiel $s_{1111} = \frac{1}{E_L}$, $s_{2222} = \frac{1}{E_R}$ ist,

wo

E_L und E_R – die Elastizitätsmoduli des Holzes in den anatomischen Hauptrichtungen *L* und *R* sind.

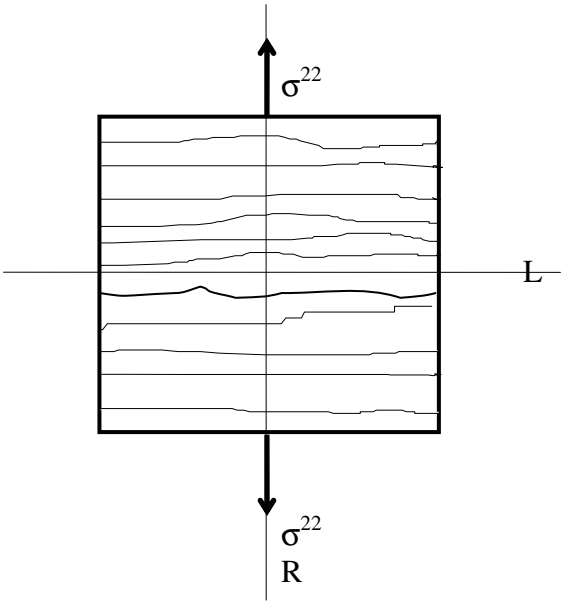

Bild B1. Belastung eines würfelförmigen Probekörpers in radialer Richtung in der Ebene L-R
Figure B1. Loading of a prismatic specimen in the Plane L-R in radial direction

Der Probekörper werde nun in der anatomischen Hauptebene um 90° gedreht. Die einzige Spannung der linearen Spannungszustandes wird dann:

$$\sigma^{LL} = f_R^+ \quad ,$$

wodurch natürlich noch kein Bruch verursacht wird, da beim Holz $f_L^+ \geq f_R^+$ *is,*. f_L^+ und f_R^+ die Zugfestigkeiten in den anatomischen Hauptrichtungen *L* und *R* sind. Es soll die Spannung σ^{LL} solange, bis zum Versagen des Probekörpers gesteigert werden. Die grösste Spannung im Grenzzustand des Bruches ist dann:

$$\sigma^{LL} = k\sigma^{RR} = f_L^+ \quad .$$

Sie ist also das k-Fache der Spannung σ^{RR}. (k – eine beliebige positive Grösse ist).

Im Grenzzustand des Bruches entsteht das folgende elastische Ergänzungspotential:

$$\tilde{u} = \frac{1}{2} s_{ijkl} \sigma^{ij} \sigma^{kl} = \frac{1}{2} s_{LLLL} k^2 \sigma^{RR} \sigma^{RR} = \frac{1}{2} s_{LLLL} k^2 f_R^+ f_R^+ \qquad \text{(B2)}$$

Wird angenommen, dass ein anisotropes Material dann versagt, wenn das elastische Ergänzungspotential einen bestimmten, konstanten Wert erreicht, müssen die Gl. (B1) und (B2) gleich grossen Wert ergeben. (Ist das Material isotrop, kann diese Vermutung angenommen werden, da dort die Orientierung keine Rolle spielt. Bei anisotropen Werkstoffen kann diese Behauptung bezweifelt werden, Betrachtung von Versuchsergebnissen weist darauf hin. Trotzdem verwenden die von Mises'sche Theorie, die Tsai-Wu'sche Theorie und noch viele andere diese Vermutung.) Somit wird:

$$\frac{1}{2} s_{RRRR} \sigma^{RR} \sigma^{RR} = \frac{1}{2} s_{LLLL} k^2 \sigma^{RR} \sigma^{RR} ,$$

woraus sich

$$k = \sqrt{\frac{s_{RRRR}}{s_{LLLL}}} = \sqrt{\frac{E_L}{E_R}} \qquad \text{B3}$$

ergibt.

Zusammenhang (B3) bedeutet im allgemeinen: wird angenommen, dass das zu den verschiedenen Spannungszuständen gehörende Ergänzungspotential eines anisotropen Stoffes gleich gross sind, existiert ein Spannungsfaktor *k*, der zeigt, in welchem Mass die Komponenten des Spannungszustandes bis zum Bruch zu steigern sind. Im mehrachsigen Spannungszustand wird die Funktion des Faktors *k* verwickelter als die von Gl. (B3), ist aber immer irgendeine Funktion der elastischen Konstanten des anisotropen Stoffes.

Es sollen nun die Festigkeitskriterien für beide Spannungszustände angewendet werden.

B1 Schlussfolgerungen aus dem von Mises'schen Festigkeitskriterium

Das Kriterium lautet:

$$t_{ijkl} \sigma^{ij} \sigma^{kl} = 1 \quad ,$$

wo die Komponenten t_{ijkl} durch Gl. (2.3) bestimmt werden.

In unserem Falle:

$$t_{RRRR} \sigma^{RR} \sigma^{RR} = 1 \quad , \qquad t_{LLLL} k^2 \sigma^{RR} \sigma^{RR} = 1 \quad .$$

Aus dem Vergleich der beiden Zusammenhänge ergibt sich:

$$k = \sqrt{\frac{t_{RRRR}}{t_{LLLL1}}} = \frac{f_L}{f_R} \quad ,$$

bzw. bei Verwendung der Gl. (B3):

$$\frac{f_L}{f_R} = \sqrt{\frac{E_L}{E_R}} \quad . \qquad \text{B4}$$

B2 Schlussfolgerungen aus dem Tsai-Wu'schen Festigkeitskriterium

Aus der Gleichung

$$t_{ij}\sigma^{ij} + t_{ijkl}\sigma^{ij}\sigma^{ki} = 1 \quad ,$$

in der die Komponenten t_{ij} und t_{ijkl} durch Gl. (2.6) bestimmt werden, ergibt die gleiche Untersuchung entsprechend den zwei Belastungsfällen:

$$t_{22}\sigma^{RR} + t_{2222}\sigma^{RR}\sigma^{RR} = 1 \quad , \qquad t_{11}k\sigma^{RR} + t_{1111}k^2\sigma^{RR}\sigma^{RR} = 1 \quad .$$

Mit Gl. (B3) bekommt man den folgenden Ausdruck:

$$\frac{E_L}{E_R}\frac{f_R^+}{f_L^+ f_L^-} + \sqrt{\frac{E_L}{E_R}}\left(\frac{1}{f_L^+} - \frac{1}{f_L^-}\right) = \frac{1}{f_R^+} \quad . \qquad \text{B5}$$

Die Gl. (B4) und (B5) weisen darauf hin, dass ein gewisser Zusammenhang zwischen den elastischen Konstanten und technischen Festigkeiten bestehen soll, wenn das bis zum Bruch angehäufte ergänzende Potential im Körper unabhängig von der Orientierung einen konstanten Wert hat. Diese Verhältnisse treffen aber für die in der Praxis gemessenen Materialkennwerte nie zu. Für übliche Holzmaterialkonstanten, ergibt sich mindestens ein Unterschied in Grössenordnung der linken und rechten Seiten der Gl. (B5). Auch Gl. (B4) wird niemals erfüllt. Bei unseren Ableitungen wurde angenommen, dass sich das Material bis zum Bruch linear verhält. Dadurch werden die Berechnungen erleichtert, lineares Materialverhalten ist aber nicht notwendig. Die Feststellungen sind allgemein gültig. Es soll hingewiesen werden, dass sich die Gl. (B4) und (B5) für isotrope Werkstoffe erfüllt werden.

Anhang C

Wird die Gleichheit des Ergänzungspotentials aufgegeben – entsprechen der Theorie von Ashkensi – kann folgendes festgestellt werden. Nach Quadrieren der Gl. (3.5), dessen Koeffizienten durch die Gl. (2.9) gegeben werden (I_1 und I_2 – die erste und zweite Invariante des Spannungszustandes sind) ergibt:

$$\left[t_{ijkl}\sigma^{ij}\sigma^{kl}\right]^2 = I_1^2 - I_2 \quad . \qquad \text{C1}$$

Zu den beiden Belastungsfällen zurückgekehrt, bekommt man:

$$\left(t_{RRRR}\sigma^{RR}\sigma^{RR}\right)^2 = \left(\sigma^{RR}\right)^2 = \frac{2u^{\sim R}}{s_{RRRR}} \quad , \qquad \left(t_{LLLL}k^2\sigma^{RR}\sigma^{RR}\right)^2 = k^2\left(\sigma^{RR}\right)^2 = \frac{2u^{\sim L}}{s_{LLLL}} \quad ,$$

wobei (A1) und (A2) verwendet wurde. Daraus ergibt sich weiter:

$$u^{\sim R} = \frac{1}{2}\frac{f_R^2}{E_R} \quad , \qquad \text{bzw.} \qquad u^{\sim L} = \frac{1}{2}\frac{f_L^2}{E_L} \quad ,$$

Der Quotient der beiden Ausdrücke:

$$\frac{u^{\sim L}}{u^{\sim R}} = \frac{E_R}{E_L}\left(\frac{f_L}{f_R}\right)^2 \quad . \qquad \text{C2}$$

Den Quotient für ein fiktives Nadelholz mit den folgenden Materialkennwerten (E_L = 10000 MPa, E_R = 1000 MPa, f_L = 100 MPa, f_R = 5 MPa)berechnet, ergibt:

$$\frac{u^{\sim L}}{u^{\sim R}} = \frac{1000}{10000}\left(\frac{100}{5}\right)^2 = 40 \quad .$$

Das Ergänzungspotential im Falle einer Belastung bis zum Bruch beträgt in Faserrichtung das 40-Fache gegenüber der radialen Richtung.

Auf Grund der Ashkenasi'schen Festigkeitstheorie sind die zum Bruch führenden Spannungszustände zu ermitteln und ermöglichen in Kenntnis der Materialkonstanten die Bestimmung das den verschiedenen Bruchspannungszuständen entsprechende Potential oder deren Verhältnis. In der gezeigten Ableitung ist linear-elastisches Verhalten vorausgesetzt worden. Diese Annahme vereinfacht die Berechnungen, es ist aber nicht unbedingt notwendig. In Kenntnis des Spannungs-Dehnungs-Diagramms kann das Ergänzungspotential theoretisch bestimmt werden.

Acta Silv. Lign. Hung., Vol. 4 (2008) 81-93

General Regularities of Wood Surface Roughness

Endre MAGOSS*

Department of Wood Engineering, University of West Hungary, Sopron, Hungary

Abstract – The surface roughness of wood products is depending on many factors related both to wood properties and wood working operational parameters. Probably this is the reason why there are no generally valid correlation determining surface roughness parameters as a function of influencing factors. In particular, the account of wood structure in the surface roughness interpretation proved to be difficult.

In the last years an important progress was made in recognizing the role of the anatomical structure of wood species in the attainable surface roughness. The introduction of a structure number made it possible to express and characterize the different wood species numerically.

The aim of these studies was the separation of roughness components due to the anatomical structure and the woodworking operation. Using a special finishing technique, the roughness component due to woodworking operations was not significant and could be separated. The same specimens were also subjected to different woodworking operations using cutting velocities between 10 and 50 m/s. The processing of experimental data resulted in a chart showing the minimum roughness component due to different woodworking operations. Special experimental investigation was conducted to clear the influence of edge dullness on the surface roughness, especially on its Abbott-parameters. The measurements showed that the R_k-parameter is a good indicator to predict edge dullness.

structure number/ anatomical structure / woodworking / edge dullness / cutting speed / Abbott-parameters

Kivonat – Természetes faanyag felületi érdességének alapvető összefüggései. A faanyagok érdessége igen sok tényező együttes hatásaként jön létre, ezért az általános törvényszerűségek megtalálása sokáig váratott magára. Az utóbbi évtized új elgondolásai és a modern méréstechnika lehetővé tette az alapvető törvényszerűségek felismerését. A struktúra szám bevezetése lehetővé tette, hogy segítségével a fafajok számszerűsíthetők a felületi érdesség szempontjából, és lehetővé teszik általánosabb érvényű összefüggések felállítását.

A megmunkálás után kialakuló érdesség két fő összetevőre bontható: a megmunkálás okozta érdesség és a belső struktúra okozta érdesség. Speciális felületi megmunkálás alkalmazásával a megmunkálási érdesség részaránya minimalizálható és szétválasztható a belső struktúra okozta érdességtől. Megállapításra került továbbá a forgácsolási sebesség (10 m/s-50 m/s) és a szerszám él kopottságának hatása a felületi érdességre. Az R_k-paraméter változása jól mutatja szerszámkopás folyamatát.

* magoss@fmk.nyme.hu; H-9400 SOPRON, Bajcsy-Zs. u. 4.

1 INTRODUCTION

Roughness characterises the fine irregularities on a machined surface. These irregularities can be determined by measuring the height, width and shape of the peaks and valleys produced by woodworking operations or by anatomical structural properties. The surface quality is a complex definition and it is characterised today by different parameters such as the more common Ra, Rz and Rmax parameters. Further details can be established using the Abbott-curve and its related parameters Rpk, Rk and Rvk. These parameters are standardised (EN ISO 4287 and 13565-2) and for their determination modern measuring units are commercially available.

The surface quality is depending on many influencing factors and can be related both to wood properties and machining conditions. Among the wood properties the wood species, density, moisture content, the structural properties are to be mentioned. The structural properties include the specific number and distribution of inside diameter of tracheids and vessels.

The machining process has also a significant influence on the surface roughness. The most important factors are the cutting velocity and the dullness of knives, but the knife cutting angle, the cutting angle to the grains and the vibration amplitude of machine table and workpiece have also proved to be an influence on the surface roughness (Sitkei et al. 1990)

One of the main difficulties is the fact that the wood is not a true solid material having caves inside (vessels, cell lumens) and, furthermore, the wood as a brittle material is inclined to brittle fracture. As a consequence, the cutting mechanism is always associated with local fracture of the material giving uneven surface. The caves cut during the machining give also uneven surface. In this latter case, the surface irregularities depend on the local position of the cavities relatively to the surface. Wood species with large vessels in the early wood (ring porous wood) may locally cause large surface irregularities which have nothing to do with the machining process.

In the last decade an important progress was made recognizing the role of anatomical structure of wood species in the attainable surface roughness. The diameter of vessels, tracheids and other cell lumens cut during the machining process fundamentally determine the depth of irregularities in the surface. In order to characterize the effect of the anatomical structure on the surface roughness, a structure number is established and introduced (Magoss-Sitkei 2001) Another possible method is the removal of deep valleys (vessels) from the surface profile. Thus the surface roughness parameters will be more sensitive to the change of a given influencing factor (Fujiwara et al. 2003).

A further important progress could have been the separation of roughness components due to the anatomical structure and woodworking operations. Some researchers assumed that the parameters of Abbott-curve are suitable for separating the above components. In fact, these efforts were not fully successful and, therefore, further research works are still needed.

2 THEORETICAL CONSIDERATIONS

The diameter of vessels, tracheids and other cell lumens cut during the machining process fundamentally determine the depth of irregularities. The specific number of vessels related to the unit length in cutting direction is also an important factor. The diameter of vessels and tracheids always show a given distribution. However, if the distribution is generally normal, the use of the mean diameter will cause no greater errors.

The local position of vessels to the cutting plane is always random therefore, it may be treated as a probability variable. This means that the resultant effect of the vessels on the surface roughness will be given as a mean value with standard deviation.

It is assumed that in the cutting plane different vessels and tracheids will be cut (*Figure 1*) and these valleys contribute to the resultant roughness. The cross-section of valleys related to the unit length can be given as

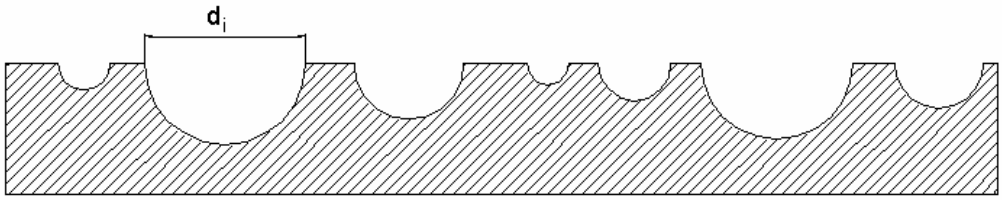

Figure 1. Definition of structure number

$$\Delta F = \frac{\Pi}{8}\left[a \cdot \left(\sqrt{n_1} \cdot d_1^2 + \sqrt{n_2} \cdot d_2^2\right) + b \cdot \left(\sqrt{n_3} \cdot d_3^2 + \sqrt{n_4} \cdot d_4^2\right)\right] \quad [\mathrm{cm^2/cm}] \qquad (1)$$

where

n_1, n_2 – are the number of vessels and tracheids in the early wood, in the unit cross-section,

n_3, n_4 – are the number of vessels and tracheids in the late wood, in the unit cross-section,

d_1-d_4 – are the mean diameter of vessels and tracheids in the early and late wood, respectively,

a, b – are the portions of early and late wood.

The use of structure number makes it unnecessary to use the wood species as a variable, which can not be quantified. If the surface irregularities due to machining are small, then the surface roughness will mainly be determined by the anatomical structural properties and it can be regarded as the attainable optimum surface roughness.

The main problem of the roughness component separation is the overlapping of component sizes and, therefore, the filtering method can not give accurate results. One possible way to separate the above components seems to be the following method. Using a special finishing technique, the irregularities due to woodworking operation can be kept minimal and these irregularities are rising from an apparently flat surface (*Figure 2*). In this case, these irregularities are not higher than 10-15 μm and can be measured and evaluated.

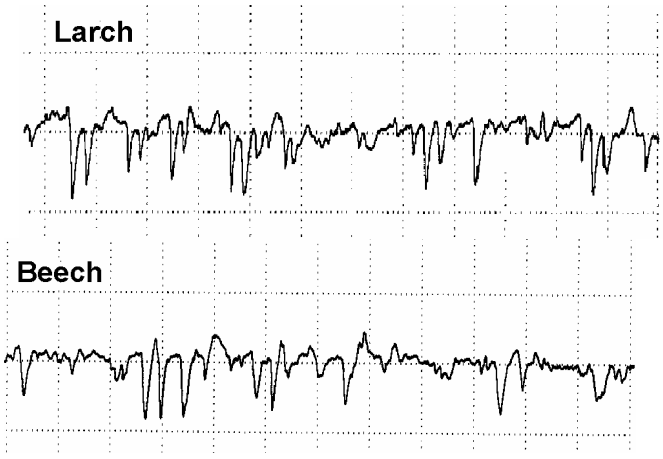

Figure 2. Roughness profiles for finished surfaces.

3 MATERIALS AND METHODS

In order to verify the usability of the new structure number, a wide variety of wood species were selected having different density and inside structure. Five broad leaved (cottonwood, ash, beech, black locust, oak) and five conifers (scotch pine, larch, fir, spruce, eastern white cedar) were selected and air dried at 50-60 % relative humidity.

Three 20- by 5-cm samples were tangentially cut from each wood species and were equally machined using sharp milling head on a CNC-controlled milling machine. On each specimen four measuring surfaces were machined and displaced by 0.3 mm to each other. This method should take into account the fact that the relative placing of cutting plane and vessels to each other is random. The cutting speed was generally 50 m/s, but special measurements were conducted to clear the effect of cutting speed on the different roughness parameters, especially on the Abbott-parameters. The cutting speed varied between 10 and 50 m/s.

The Mahr Company stylus unit (Model S3P MFW 250) was used in this study. The pick-up has a skid type diamond stylus with a tip radius of 5 µm. The active tracing length is 12.5 mm. Each measurement was represented by the surface profile, the Abbott-curve and by the calculated roughness parameters R_a, R_z, R_{max}, R_{pk}, R_k, R_{vk}, M_{r1} and M_{r2}. On each measuring surface a minimum of three tracing were made.

In order to calculate the structure number, the size and specific number of vessels and tracheids are needed. From each specimen used to roughness measurements additional small specimens were cut to determine the structural properties. While the structure number is sensitive to the accuracy of experimental data, a combined image processing method and light microscope method was used. The image processing method alone generally gave insufficiently accurate results. The measured data are summarized in Table1 (Magoss – Sitkei 1990).

Table1. Structural properties of specimens

wood species	early wood			late wood		
	$\overline{d_i}$ [µm]	$\overline{n_i}$ [piece/cm^2]	$\bar{a}$	$\overline{d_i}$ [µm]	$\overline{n_i}$ [piece/cm^2]	$\bar{b}$
thuja	26.5	142 800	0.8482	14.0	316 600	0.1518
spruce	30.0	111 335	0.8478	19.0	160 400	0.1522
pine	28.0	125 100	0.6694	20.0	135 840	0.3306
larch	38.0	65 490	0.6310	17.5	145 000	0.3690
beech (vessel)	66.0	15 740	0.7000	48.0	14 020	0.3000
beech (tracheid)	8.2	342 890		6.4	490 290	
oak (vessel)	260.0	400	0.5900	35.7	12 000	0.4100
oak (tracheid)	22.5	120 000		19.6	85 000	
b. locust (vessel)	230.0	546	0.5800	120.4	1 500	0.4200
b. locust (tracheid)	15.0	270 000		9.6	280 000	
cottonwood (vessel)	69.7	9 500	0.6666	44.0	12 700	0.3333
cottonwood (tracheid)	12.7	309 500		11.0	300 892	
ash (vessel)	177.0	670	0.6100	52.0	750	0.3900
ash (tracheid)	19.0	190 000		14.0	230 000	

In order to separate the roughness components three 20 by 5 cm samples were tangentially cut from each wood species and after machining they were subjected to finishing using a special finishing machine. The finishing was repeated until the measured profile was flat and thus suitable for evaluation.

Establishing the finished surfaces, the same samples were subjected to milling operation using various cutting speeds between 10 and 50 m/s. These surfaces were evaluated with the common surface measuring methods.

On the finished surfaces a hypothetical base line was first established and, taking only the positive amplitudes into consideration, the corresponding R_z'-value was calculated (*Figure 3*). This is the roughness component due to woodworking operation. Knowing the overall R_z-value and the latter subtracted from it, we get to an R_z-value due to the anatomical structure of wood.

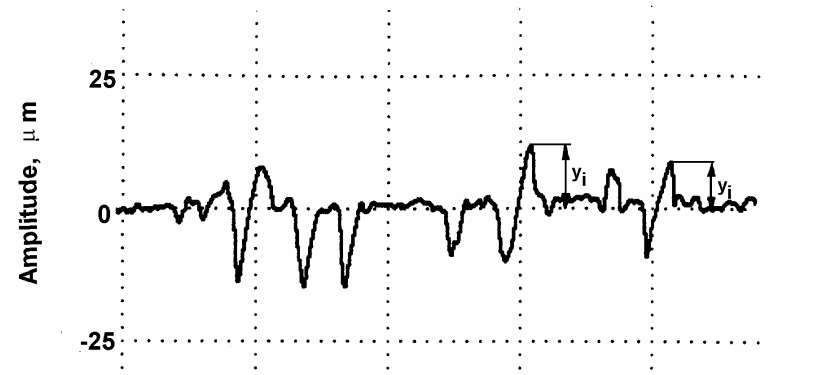

Figure 3. To the calculation of roughness component due to woodworking operation

For the evaluation of standard deviations large number of measurements was needed, approx. 60-100.

4 EXPERIMENTAL RESULTS

4.1 The effect of cutting speed

It is generally well-known that increasing cutting velocities will give better surface quality, using the common roughness parameters such as the average roughness R_a or mean peak-to-valley height R_z. At the same time, no experimental results were presented to clear the relationship between the overall roughness parameters (R_a and R_z) and their components in the Abbott distribution.

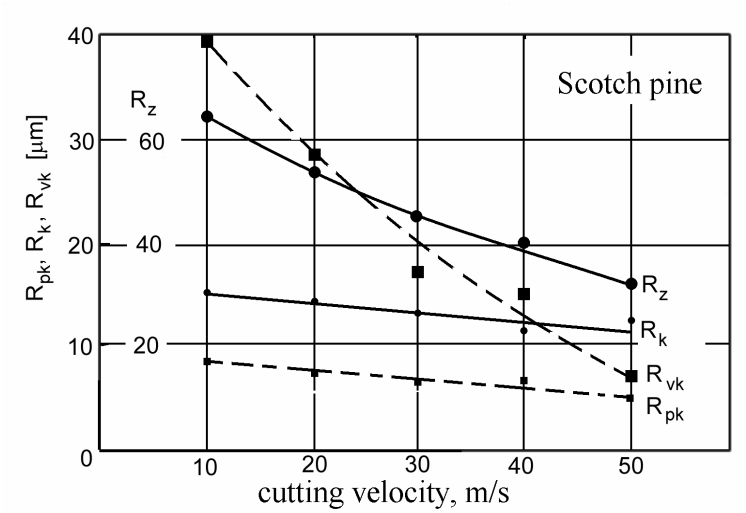

Figure 4. Surface roughness parameters as a function of cutting speed. Scotch pine.

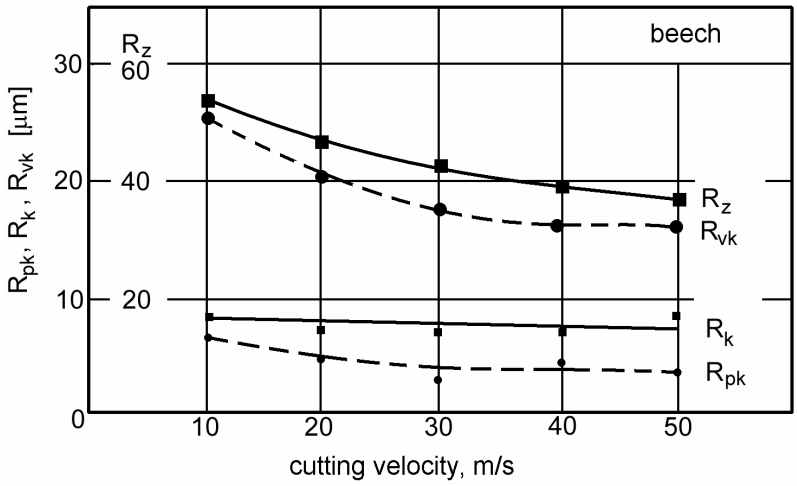

Figure 5. Surface roughness parameters as a function of cutting speed. Beech.

Figures 4 and *5* depict R_z-values and their components as a function of cutting speed using sharp knives. The beech had an average vessel diameter of 60 µm and the thick-walled fibres among the vessels had cavities of 10-15 µm diameters. The scotch pine in the early wood showed tracheid diameters of 25-30 µm and in the late wood 13-18 µm.

From *Figure 4* and *5* it can be concluded that in both cases the R_{pk} and R_k values remain nearly constant or slightly decrease as a function of cutting speed. On the other hand, R_{vk}-values fundamentally depend on cutting speed. It may also be seen that, in the case of pine, this dependence is stronger, especially at low cutting velocities. This result may be explained by the fact that the pine wood had smaller local stiffness around the cutting edge, therefore, inertia forces play a more important role to ensure a clear cutting surface. At the same time, beech had larger structural cavities giving greater R_{vk}-values even at high cutting velocities.

Further measurements were carried out at a cutting velocity of 50 m/s and the angle of tracing to grains was 90º. Observations have shown that this cutting speed can minimise the roughness component due to machining (see the upper curve in *Figure 14*).

4.2 The use of structure number

As outlined earlier, all wood species can be characterized by the structure number given by Eq.(1). Using the data summarized in Table1, the structure number can be calculated for each specimen used in these investigations and it can be interrelated to the measured roughness parameters.

The obtained results are depicted in *Figure 8* as a function of structure number. The smallest structure numbers are of the conifers and the biggest of the oak species. Some results obtained on African ebony specimens are also included. Curve No. 3 shows the roughness of specimens due to the anatomical structure and this is the ultimately attainable minimum surface roughness for a given anatomical structure.

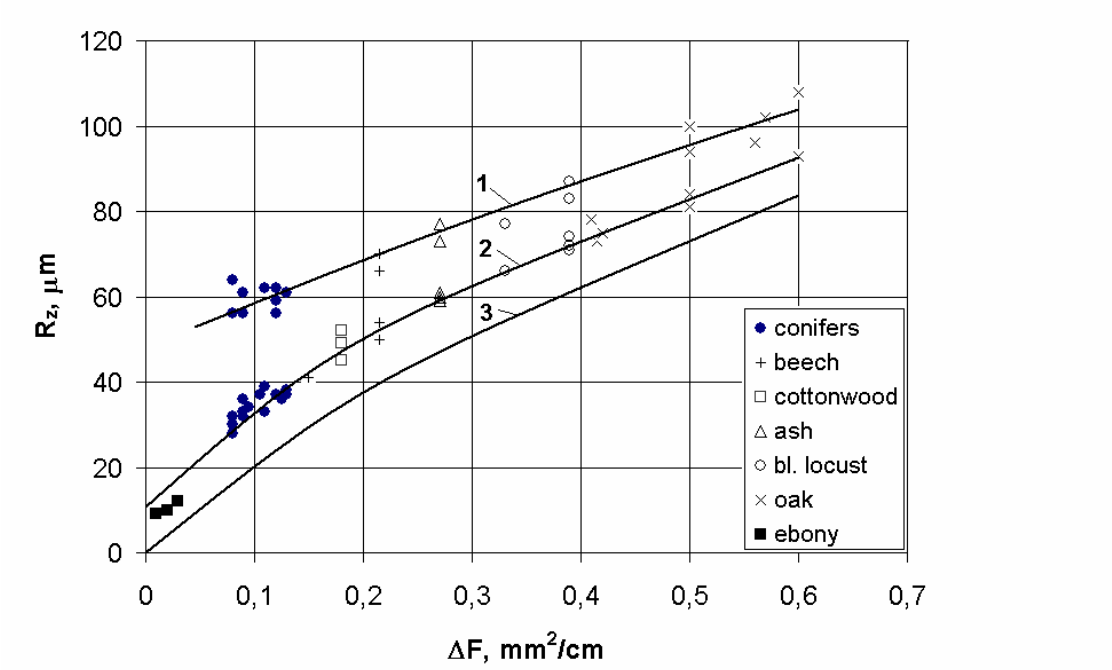

Figure 6. Peak-to-valley height as a function of structure number
1. - cutting velocity is 10 m/s,
2. - cutting velocity is 50 m/s,
3. - roughness component due to anatomical structure.

The effect of cutting speed on the surface roughness is given by the curves 1 and 2. It is noticable that the differences between curves 1 and 2 are higher for conifers in comparison to hard woods. This finding may explained by the higher rigidity (E modulus) of hard woods allowing smaller local deformations during the cutting process. It may generally be stated that conifers have higher roughness component due to woodworking operations in comparison to hard woods. It appeared that the surface roughness will probably be determined by the anatomical structure of wood, especially for hard woods with big vessels. The effect of main influencing factors on the surface roughness was also determined and the following general relationship was obtained (Magoss –Sitkei 2000):

$$R_z = \left(123\Delta F^{0,75} + 35e_z{}^{0,6}\right)\cdot\left(1+\frac{50-v_x}{50}\frac{0,1183}{\Delta F^{0,83}}\right) \qquad 10m/s \le v_x \le 50m/s \qquad (2)$$

Where
ΔF is the structure number, mm^2/cm
ez is the tooth feed, mm
vx is the cutting velocity, m/s

The use of the structure number allows finding further noteworthy relationships among the different surface roughness parameters.

Choosing the R_a/R_k ratio, a strong variation is obtained as a function of structure number (*Figure 7*). This means that different wood species can not be compared to one another using simply a given roughness parameter.

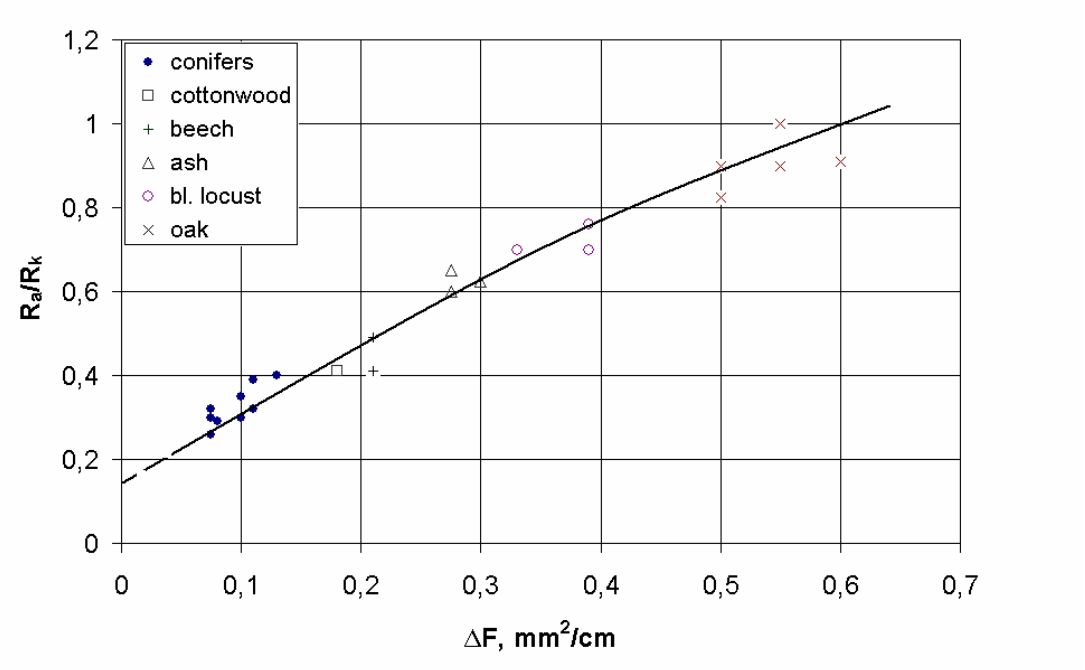

Figure 7. Variation of the R_a/R_k ratio as a function of structure number

The reduced valley height related to the peak-to-valley height (R_{vk}/R_z) shows also definite correlation with the structure number, which is given in *Figure 8*. The height ratio for hard woods means that most of the roughness is given by deep valleys due to the anatomical structure of wood.

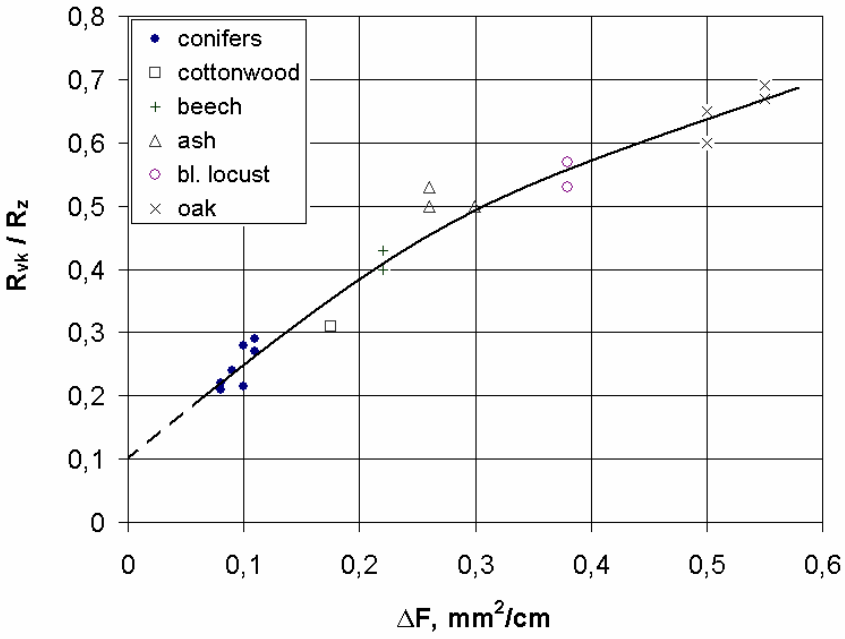

Figure 8. Variation of the R_{vk}/R_z ratio as a function of structure number

The R_k/R_z ratio versus structure number is shown in *Figure 9*. This relationship is also uniquely defined and shows that the reduced mid part of Abbott-curve plays an important role in the development of the resultant roughness in soft wood surfaces.

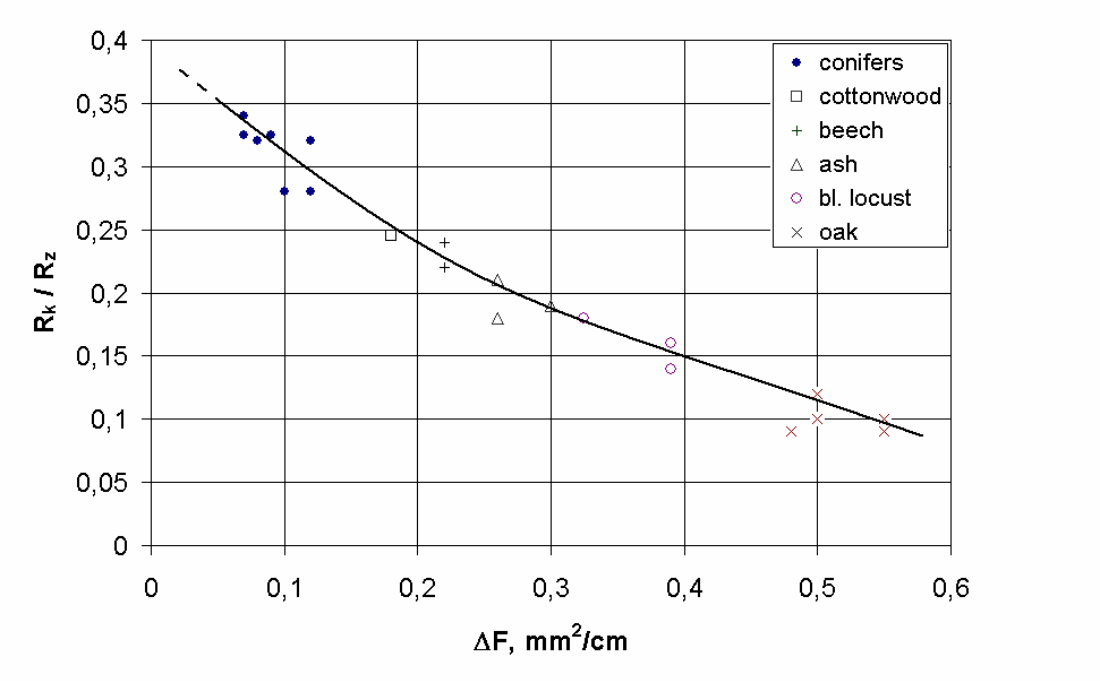

Figure 9. R_k/R_z ratio versus structure number

4.3 Interrelations among the roughness parameters

In the following the interrelation between the common roughness parameters (R_a and R_z) and Abbott-parameters was investigated. Strong relationship was observed between the average roughness and the sum of Abbott-parameters. Its graphical representation is given in *Figure 10*.

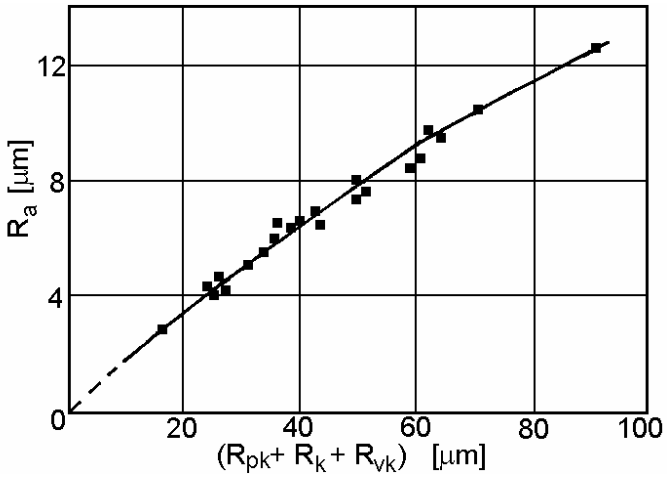

Figure 10. Relationship between average roughness and Abbott-parameters

It is well-known that between R_a and R_z only an insignificant interrelation exists (Sander 1993). As a consequence, no uniquely defined relationship between R_z and the sum of Abbott-parameters can be expected. Nevertheless, the experimental results depicted in *Figure 11* show an interesting picture.

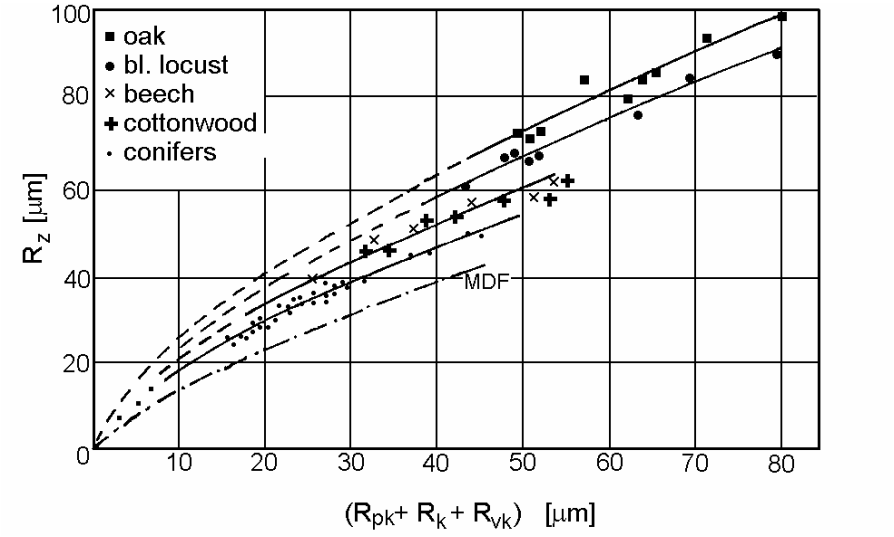

Figure 11. Peak-to-valley height versus Abbott-parameters

A large number of curves are obtained and, as an addition for a more accurate explanation, the measurement results on MDF-boards of different volume density are included (Devantier 1997). MDF has the most uniform anatomical structure which gives the lowest curve. The oak possesses large vessels and hereby a much less uniform structure and, therefore, gives the uppermost curve. The curves for other species are lying between the two extremes according to their inhomogeneities. The curves obeys the following general form

$$R_z = A \cdot \left(R_{pk} + R_k + R_{vk}\right)^{0.65} \tag{3}$$

The constant can be expressed as

$$A = 7.45 \cdot \left(R_k + R_{vk}\right) / R_z \tag{4}$$

Using the Abbott-curve, the lack of material in the uneven surface can be determined. An equivalent layer thickness may be calculated as follows

$$\Delta h_e = R_{pk} \cdot \left(1 - \frac{M_{r1}}{2}\right) + \frac{R_k}{2} + \frac{R_{vk} \cdot \left(1 - M_{r2}\right)}{2} \tag{5}$$

Where: M_{r1} and M_{r2} should be substituted as decimal values. The following rough estimation shows the weight of the parts in Eq. (5):

$$\Delta h_e = 0.95 \cdot R_{pk} + 0.5 \cdot R_k + 0.08 \cdot R_{vk} \tag{6}$$

In practical cases the R_{pk}-layer can eventually be neglected due to the fact that the few peaks rising out from the surface can easily be crushed by pressing.

The graphical representation of the lack of materials related to the unit surface is seen in *Figure 12*. The upper curve refers to the case including also the R_{pk}-layer. The deviation of measurement data is somewhat higher than in other cases.

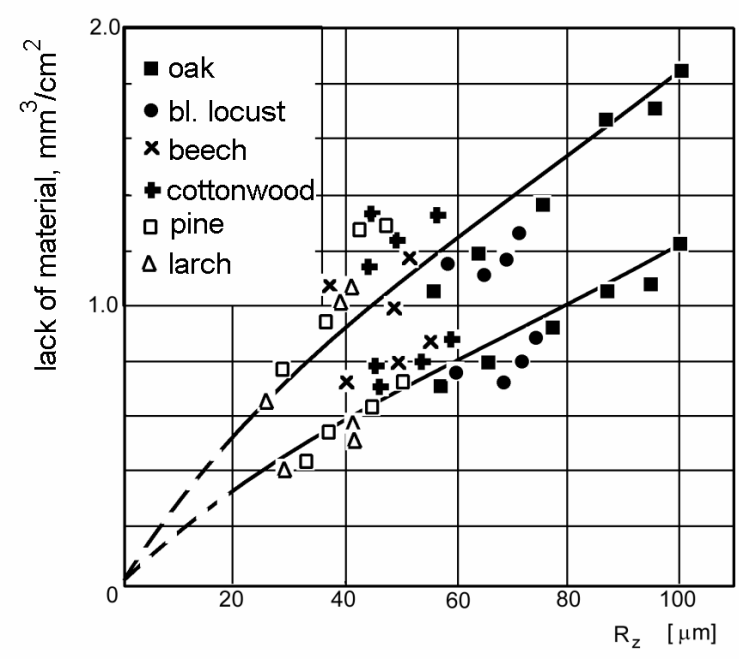

Figure 12. Lack of material as a function of surface roughness

4.4 Effect of blunt cutting edges

It is well-known that the use of blunt knives fundamentally increases the surface roughness. Our measurements have also shown that, in the case of pine and beech and using edge radius between 10 and 53 μm, the roughness with increasing dullness nearly linearly increased. A more detailed processing of experimental results showed that the R_k-value may be an important indicator characterising edge dullness. *Figure 13* shows experimental results for four wood species using sharp and blunt edges.

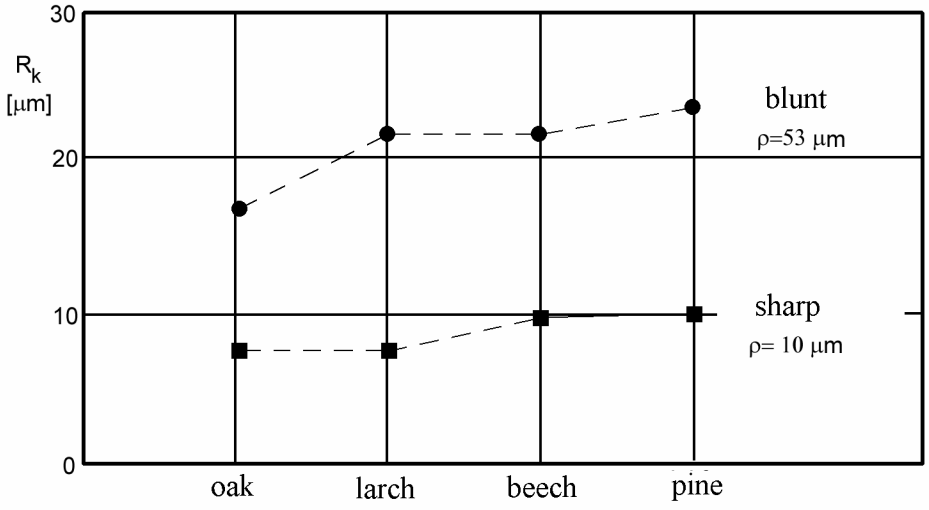

Figure 13. R_k-values for four wood species using sharp and blunt cutting edges

In this study, the oak has shown an unusual behaviour. Using increasingly blunt edges, the overall roughness R_z only slightly increased or remained constant. At the same time, the R_k-value doubled quite similarly to the other species. The surface machined with blunt edges showed a wavy character which did not correlate to the large vessels (*Figure 14*).

Furthermore, most of the vessels cut during the machining disappeared in the surface due to the deformation of upper layers (Magoss - Sitkei 2001). It may also be assumed that even the deep cavities in the surface contribute to the deforming action of the blunt edge.

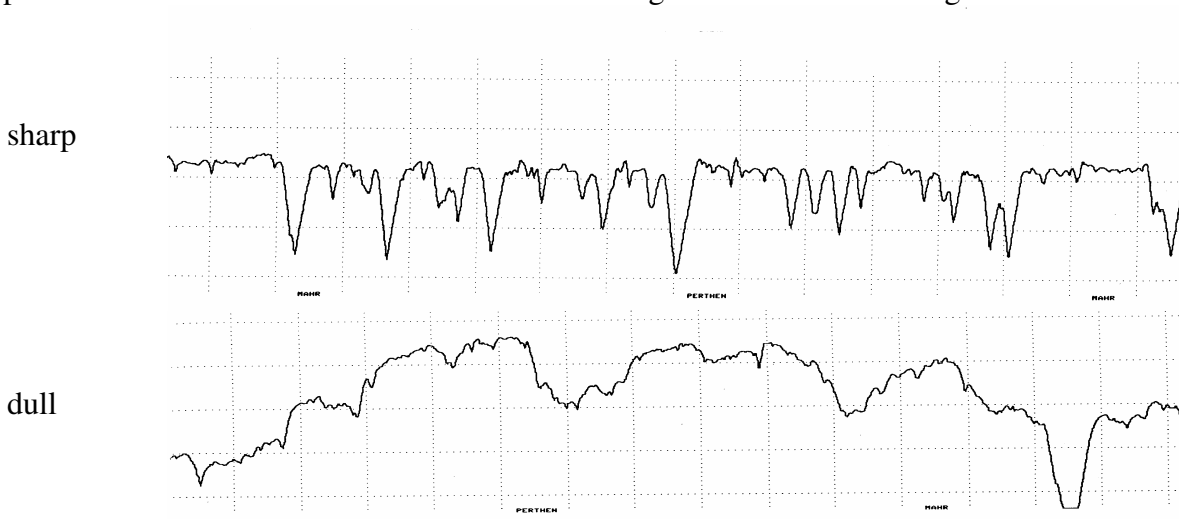

Figure 14. Surface profiles of oak wood using sharp and blunt cutting edges

The deformed and fractured layers make surfaces less stable and a subsequent surface treating may cause further waviness and local deformations. Consequently, the surface roughness alone is not always sufficient to characterise surface quality in every respect.

5 CONCLUSIONS

Based on theoretical considerations and experimental results, the following conclusions may be drawn:

- an increasing cutting speed reduces the surface roughness, primarily by diminishing the R_{vk}-values,
- the soft wood species are more sensitive to the change of cutting velocity concerning surface roughness,
- the proposed structure number shows strong correlation with the attainable surface roughness,
- different roughness parameter ratios show definite correlation with the structure number. This finding further stresses the beneficial use of the structure number uniquely characterizing the different wood species.
- among the different roughness parameters interrelations are found,
- the lack of material in the rough surface can be expressed as a function of surface roughness,
- the mid component of the total roughness R_k is a good indicator to predict edge dullness.
- using a special surface finishing technique, the separation of roughness components due to anatomical structure and woodworking operations has been carried out with reasonable accuracy.

REFERENCES

DEVANTIER, B. (1997): Prüfmethode zur objektiven Bewertung der Rauhigkeit und Welligkeit von Holzwerkstoffen. Abschlußbericht IHD Dresden. 79 p.

FISCHER, R. – SCHUSTER, C. (1993): Zur Qualitätsentstehung spanend erzeugter Holzoberflächen. Mitteilung aus dem Institut für Holztechnik der TU Dresden.

FUJIWARA, Y. – FUJII, Y – OKUMURA, S. (2003): Effect of Removal of Deep Valleys on the Evalution of Machined Surfaces of Wood. Forest Products Journal,.58-62.

MAGOSS, E. – SITKEI, G. (2001): Fundamental Relationships of the Wood Surface Roughness at Milling Operations. Proc. of the 15th IWMS Conf. Los Angeles. 437-446.

MAGOSS, E.– SITKEI, G. – LANG, M. (2004): Allgemeine Zusammenhänge für die Rauheit von mechanisch bearbeiteten Oberflächen für Möbel, Tagungsband, Möbeltage 2004 Dresden, S. 273-279

MAGOSS, E. – SITKEI, G. (2000): Strukturbedingte Rauheit von mechanisch bearbeiteten Holzoberflächen. Möbeltage in Dresden, Tagungsbericht S. 231-239.

MAGOSS, E. – SITKEI, G. – LANG, M. (2005): New Approaches in the Wood Surface Roughness Evaluation. Proc. Of the 17th IWMS Conf. Rosenheim. 251-257.

MAGOSS, E. – SITKEI, G. (1999): Influence of Wood Structure on the Surface Roughness at Milling Operations, Proceedings of the 4th ICWSF. 1999. 290-296

MCKENZIE, W.M. (1960): Fundamental aspects of the wood cutting process. Forest Products Journal. 10(9):447-457.

MITCHELL, P. – LEMASTER, R. (2002): Investigation of machine parameters on the surface quality in routing soft maple. Forest Product Journal. 52(6):85-90.

OSTMAN,B. A.L. (1983): Surface roughness of wood-based panels after aging. Forest Products Journal. 33(7/8):35-42.

SANDER, M. (1993): Oberflächenmeβtechnik für den Praktiker. Feinprüf Perthen GmbH, Göttingen. 48 p.

SINN, G., MAYER, H., STANZL-TSCHEGG, S. (2005): Surface properties of wood and MDF after ultrasonic-assisted cutting. Journal of Materials Science. 4325-4332

SITKEI, G. et al. (1990): Theorie des Spanens von Holz. Fortschrittbericht No.1. Acta Fac. Ligniensis, Sopron. 33 p.

SITKEI, G. – MAGOSS, E. (2003): Optimum Surface Roughness of Solid Woods affected by Internal Structure and Woodworking Operations. Proc. of the 16th IWMS Conf. Matsue. 366-371.

TAYLOR, J.B. – CARRANO, A. L. – LEMASTER, R.L. (1999): Quantification of process parameters in a wood sanding operations. Forest Products Journal. 49 (5): 56-60.

Acta Silv. Lign. Hung., Vol. 4 (2008) 95-106

Evapotranspiration Calculation on the Basis of the Riparian Zone Water Balance

Zoltán GRIBOVSZKI[a,b*] – Péter KALICZ[a] – Mihály KUCSARA[a] – József SZILÁGYI[b] – Péter VIG[c]

[a] Institute of Geomatics and Civil Engineering, University of West Hungary, Sopron, Hungary
[b] Department of Hydraulic and Water Resources Engineering, Budapest University of Technology and Economics, Budapest, Hungary
[c] Institute of Earth and Environmental Sciences, University of West Hungary, Sopron, Hungary

Abstract – Riparian forests have a strong influence on groundwater levels and groundwater sustained stream baseflow. An empirical and a hydraulic version of a new method were developed to calculate evapotranspiration values from riparian zone groundwater levels. The new technique was tested on the hydrometeorological data set of the Hidegvíz Valley (located in Sopron Hills at the eastern foothills of the Alps) experimental catchment. Evapotranspiration values of this new method were compared to the Penman-Monteith evapotranspiration values on a half hourly scale and to the White method evapotranspiration values on a daily scale. Sensitivity analysis showed that the more reliable hydraulic version of our ET estimation technique is most sensitive (i.e., linearly) to the values of the saturated hydraulic conductivity and specific yield taken from the riparian zone.

evapotranspiration / riparian zone / water resources / alder forest

Kivonat – Evapotranszspiráció számítása a vízfolyásmenti zóna talajvízmérlegéből. A ligeterdő társulások hatása jelentős a vízfolyásmenti zóna talajvízmérlegére és így a vízfolyások talajvízutánpótlásból származó alapvízhozamára is. A vízfolyás menti zóna talajvízszint változásának vizsgálata alapján egy hidraulikus és egy empirikus almódszerekből álló új eljárást fejlesztettünk ki az ottani vegetáció csapadékmentes időszakokban jellemző, elsősorban a talajvízből táplálkozó evapotranszspirációjának számítására. Az új módszert a Sopron melletti Hidegvíz-völgy kísérleti vízgyűjtőjének adatain teszteltük. A módszer által szolgáltatott evapotranszspirációs értékeket összehasonlítottuk a Penman-Monteith-féle egyenlettel számolt adatokkal félórás időfelbontásban, és a White módszer által szolgáltatott adatokkal napi időfelbontásban. A módszerre készített érzékenységvizsgálat szerint a talaj telített hidraulikus vezetőképességnek és fajlagos hozamának a pontos ismerete nagyon fontos a modell megfelelő működéséhez.

evapotranszspiráció / vízfolyásmenti zóna / vízkészletek / égerliget

1 INTRODUCTION

Riparian vegetation (especially riparian forest ecosystems) typically has a great influence on groundwater levels and groundwater-sustained stream baseflow, therefore calculation of

* Corresponding author: zgribo@emk.nyme.hu; H-9400 SOPRON, Bajcsy-Zs. u. 4.

correct evapotranspiration values is very important from the point of view of nature protection and utilization of water resources. Numerical hydrodynamic models demand exact groundwater evapotranspiration data also to calculate regional or local water balances. Therefore vegetation influence on the riparian groundwater resources and on the baseflow regime has been intensively investigated in almost all parts of the world in the last decades (e.g. Federer 1973, Goodrich et al. 2000 etc.). In Hungary at the Komlósi telep experimental station of VITUKI, the evapotranspiration impact onto the groundwater investigated, and a method developed to estimate groundwater evapotranspiration based on the daily groundwater level readings of piesometer nests (Major 1974).

In the summer season, there is a strong diurnal fluctuation of groundwater levels (*Figure 1 upper*) and stream base flow (*Figure 1 lower*) exists. As a rule, in the case of base flow, the maximum discharge occurs around seven o'clock in the morning and the minimum about in the middle of the afternoon. A detailed description of this characteristic signal and vegetation impact on riparian groundwater balance in case of our experimental catchment (Hidegvíz Valley) can be found in Gribovszki et al. (2006) and Kalicz et al. (2005).

In early investigations the main driving force of the diurnal signal was thought to be the diurnal temperature change-induced succession of evaporation and condensation processes in a shallow groundwater environment (Ubell 1961). Later it was confirmed that this fluctuation is mainly caused by the evapotranspiration of riparian zone vegetation (Pörtge 1996).

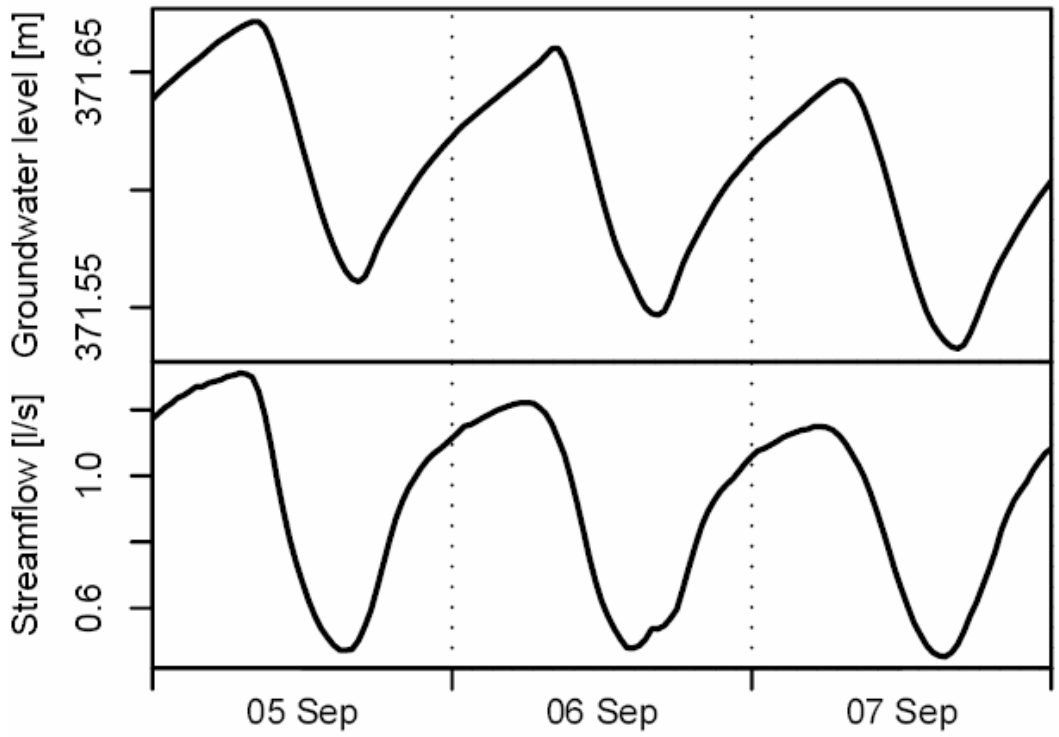

Figure 1. Diurnal fluctuation of riparian groundwater levels and stream base flow in 2005 in the Hidegvíz Valley

Several authors have investigated the linkage between riparian transpiration and streamflow rates (Troxell 1936, Croft 1948, Tschinkel 1963, Reigner 1966, Pörtge 1996, Lundquist and Cayan 2002) but only a few attempted to estimate the evapotranspiration (ET) rate of the riparian zone (White 1932, Bond et al. 2002) by using the observed streamflow and groundwater fluctuations, or to provide an analytical description of these signals (Czikowsky 2003, Czikowsky - Fitzjarrald 2004).

It can readily be established that the diurnal fluctuation of the riparian zone groundwater table and stream base flow (*Figure 1 and Figure 2*) are due to the transpiration needs of the plant life (because evaporation is negligible in the riparian forest in dry periods). The water to supply these needs can be drawn from the inflow to the area or from groundwater storage, or from both. For example, during highest groundwater levels, the water table remains constant for a short period. This means that during this period the inflow to the groundwater table is sufficient to supply all the transpiration demands. At sinking part of the groundwater levels transpiration not only uses all the inflow but also heavily utilizes the groundwater supply. At the minimum point the transpiration losses have decreased to a level where the inflow is again sufficient to supply these needs. At the rising part of the curve the transpiration needs are much less than the inflow, and surplus water is stored, causing a rise in the groundwater table. It is thus apparent that the groundwater record is merely an accumulative curve of the rates of inflow and the transpiration-use (Troxell 1936).

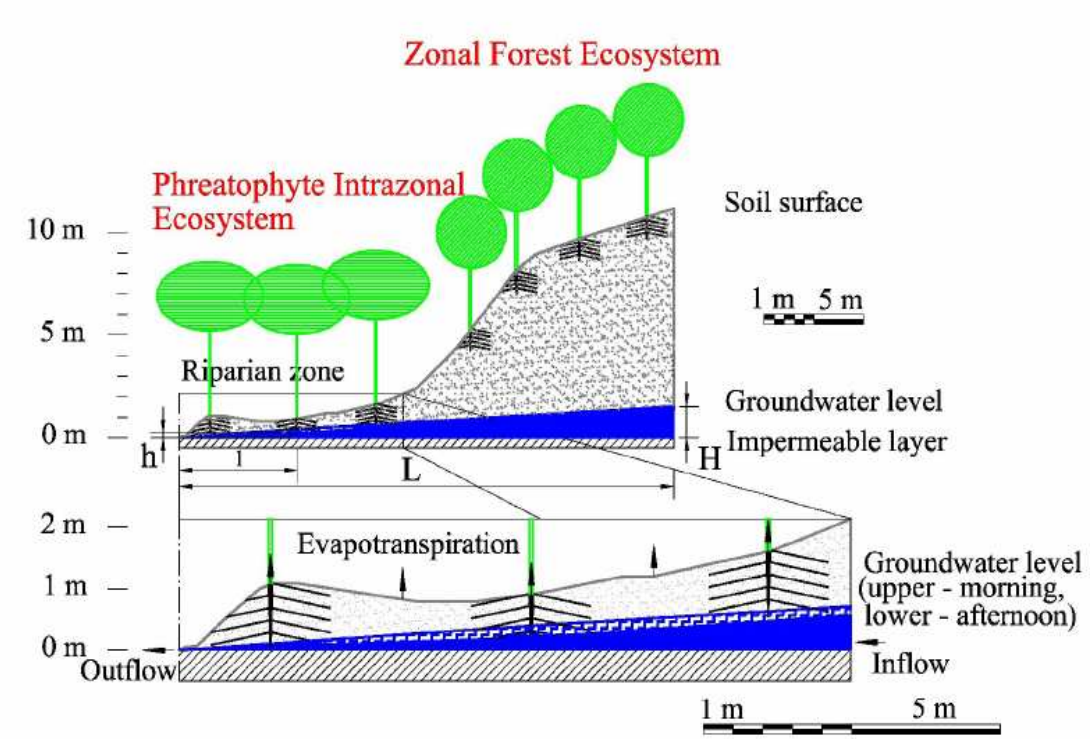

Figure 2. Schematic model of riparian zone

The maximum transpiration will occur at the point showing the maximum rate of decrease in the groundwater table. This point of maximum use occurs at or near the time of maximum temperature. Likewise the period of minimum transpiration begins when there is the point showing the maximum rate of rise in the groundwater table. This point agrees fairly well with the beginning of the night, and therefore lower temperature period, without significant net radiation (*Figure 1*).

Walter N. White (1932) suggested that it was possible to determine the daily transpiration by means of groundwater records diurnal fluctuation (*Figure 3*). If the transpiration is assumed to be practically zero during the early hours of the morning, about 2:00 to 4:00 a.m., then the rate of rise in the groundwater table during that period would be the rate of recharge. A tangent was then drawn to the curve at this point marked *r* [L]. This represents the rate of recharge of the groundwater table. If this rate was to continue throughout the 24 hours and there were no transpiration or other losses, the water table would rise an amount equivalent to the distance marked *24r*. Transpiration occurred, of course, and instead of rising, the

groundwater table dropped the distance *s* [L] during the day. Consequently, the transpiration-loss would be the following equation (1).

$$ET = S_y(24r \pm s) \tag{1}$$

Where S_y is the readily available specific yield of a soil in which the fluctuation takes place. The readily available specific yield is taken as 50% of its specific yield (Meyboom 1964). A reduction is certainly justified since it takes some time for the drainage to adjust to any new conditions introduced.

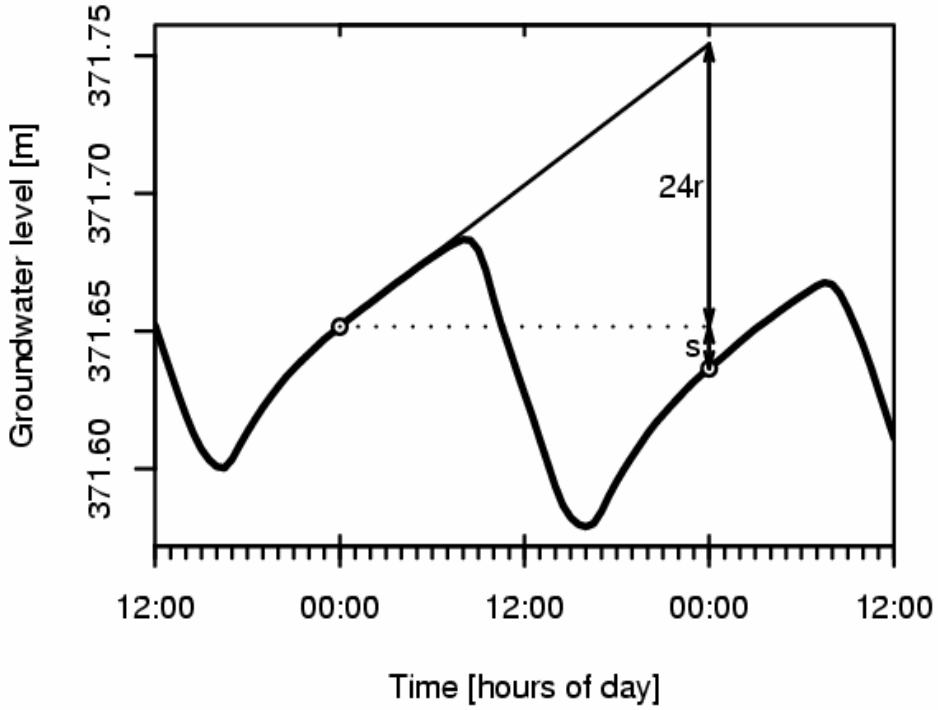

Figure 3. Basic principle of White method

2 MATERIAL AND METHODS

Although White method might provide a fairly good estimate, they are subject to a certain error. This error is based on the assumption that the rate of recharge continues as a straight line throughout the 24 hours (Troxell 1936). *Figure 4* shows a typical daily fluctuation of the riparian zone groundwater table. Late at night or early in the morning, when transpiration is practically nothing, the height of the groundwater table and the static head are nearly the same and the processes are similar to those in the dormant season. In early morning, when the groundwater table in the riparian zone is the highest, the difference between the static head and the ground water level the smallest, so the rate of recharge will be the minimum at this time. The increase of the transpiration drain on the groundwater supply causes a depression in the riparian zone. As the water table drops, the distance between the static head and the ground water increases. This increase in difference of height causes an increase in the rate of recharge *r*, so that in the afternoon the rate of recharge will be the maximum.

Thus it is evident that the rate of recharge *r* is not a straight line but a curve which ranges from zero at the height of the static head to a maximum some distance below that point. In

view of *Figure 4*. it is not unreasonable to expect that at the point of maximum groundwater levels, the rate of recharge will be a minimum and at the point of minimum groundwater levels, the rate will be a maximum.

Evapotranspiration rates were calculated from the diurnal cycle of groundwater levels. A simplified water balance equation (2) and Dupuit's theory equation (3) (Kovács 1972) were used for the evapotranspiration calculation.

$$\mathrm{d}S/dt = Q_{net} - ET \tag{2}$$

$$Q_{net} = Q_{inflow} - Q_{outflow} = \frac{k}{2(L-l)}\left(H^2 - h^2\right) - \frac{k}{2l}\left(h^2 - h_0^2\right) \tag{3}$$

Where S [L^3] is the stored volume of a unit area of the riparian zone, ET [L^3T^{-1}] is the evapotranspiration rate and Q_{net} [L^3T^{-1}] is the net inflow rate (which represents the recharge rate and is defined as the difference between in- (Q_{inflow}) and outflows (Q_{out}) to the unit area of the riparian zone), k [LT^{-1}] is the average saturated hydraulic conductivity of the riparian zone aquifer, H [L] is the groundwater levels far enough (L [L]) from the riparian zone where diurnal fluctuation or its impact is close to zero, l [L] is the position (distance from the stream) and h [L] is the water levels of the riparian zone groundwater well, h_0 [L] is the water levels in a stream (*Figure 2*). *dS/dt* calculated from *dh Sy /dt*. H, h and h_0 are taken relative to an assumed horizontal impervious layer (*Figure 2*), not necessarily at the stream-bed elevation. The method is moderately sensitive to the elevation of this impervious layer as datum. With every 0.1 m lowering of the datum (within the 0–0.5 m interval, which seems realistic in our geomorphological situation), the daily *ET* estimates increased by only 3–5%.

We assumed that in a small scale catchment the drought streamwater levels (only a few cm) compared to riparian zone groundwater levels is negligible ($h_0 \approx 0$). Therefore equation (3) can be simplified to equation (3a).

$$Q_{netinflow} = k\left(\frac{(H^2 - h^2)}{2(L-l)} - \frac{h^2}{2l}\right) \tag{3a}$$

The method of *ET* calculation has the following steps (*Figure 4*):

First derivatives of groundwater levels were made (half hourly interval). This curve represents the rate of change in the riparian groundwater table, or the rate of Q_{net} minus the rate of *ET* are divided by S_y.

Q_{net} values were calculated with two different methods (empirical and hydraulic).

In the empirical method the maximum of Q_{net} for each day was calculated by selecting the largest positive time rate of change value in the groundwater level readings such as $Q_{net} \approx S_y\, dh/dt$, while the minimum was obtained by calculating the mean of the smallest time rate of change in h taken in the predawn hours. The resulting values of the Q_{net} maximum and minimum in *Figure 4* then were assigned to those temporal locations where the groundwater level minimum and maximum took place. It was followed by a spline interpolation of the Q_{net} values to derive intermediate values between the specified extrema. Most probably the resulting empirical maxima are somewhat smaller than the corresponding actual maximum supply rates by virtue of the *ET* term being unaccounted for in Eq. 6 in this empirical method. At the same time, the estimated minima are somewhat larger than the actual minimum supply rates, due to the necessary averaging and due to observational evidence that groundwater levels reach their maxima somewhat later, i.e., between 6 and 8 a.m. in the summer. However,

the *dh / dt* values of this period (i.e., between 6 and 8 a.m.) should not be used because by that time *ET* may have already become significant, thus leading to increased *dh / dt* rates.

In the *hydraulic method* we use Dupuit's assumption (3) to calculate Q_{net} (*Figure 4*). The values of *k*, *h*, *l*, *H*, and *L* are required for calculating of $Q_{net.}$ The values of *k, h* and *l* are known from local measurements, but *H* and *L* must be estimated. *H* values can be determined from the assumption, that in the late night hours when *ET* is around zero, $dS/dt = Q_{net}$ (4).

$$H = \sqrt{\left(\frac{dS}{dt}\frac{1}{k} + \frac{h^2}{2l}\right)2(L-l) + h^2} \tag{4}$$

Only one *H* value (between 2 and 4 am) can be calculated for each day. We must interpolate between these *H* values so as to get as much *H* data as we need. (Spline interpolation was used.)

If we have information about the exact direction of the groundwater flow in the riparian zone at the baseflow period, we can better describe the real situation if we lay down the cross section in the main direction of the groundwater flow. This is important when the groundwater streamlines become parallel to stream near the steam channel.

Half hourly *ET* values were computed from the difference between Q_{net} values and the stored volume change (*dS*) of the riparian zone (*Figure 4*) as rearranging Eq. 2. $ET = Q_{net} - dS/dt$.

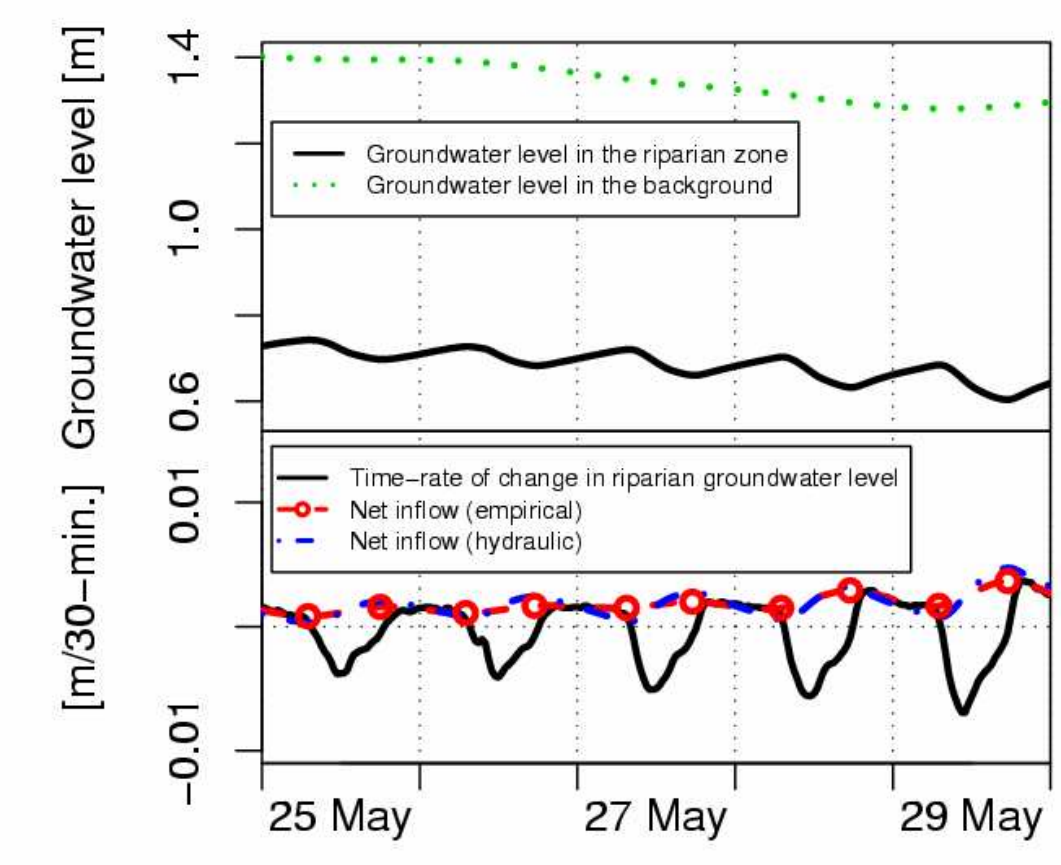

Figure 4. Groundwater levels, their derivative and the transformed Q_{net} (recharge)

Before the application of the hydraulic theory, one has to decide about the location at which the groundwater levels must be observed, and its temporal derivatives must be computed. As Bauer et al. (2004) and Loheide et al. (2005) demonstrated, the middle part of the riparian zone expresses the least spatial variations and represents average conditions as long as the riparian-zone vegetation is fairly homogeneous. They also note that boundary condition effects (such as a heavily damped signal of diurnal groundwater level fluctuations near the channel) typically die out within a few meters from the stream.

It is important to note, that the exactness and undisturbed state of the basic groundwater level data set is very important, because differentiation of the groundwater level record may invoke large errors in the resulting ET estimation whenever the original groundwater level measurements are inaccurate. Therefore in most cases it is necessary to smooth data with a low pass filter. But you must care about the width of the filter window and the type of the filter, so not to loose too much information. One of the solutions to get a better data set is to collect as frequent data as possible, and afterward a stronger filter can be used (e.g. if you need hourly *ET* data, you must sample groundwater data at least every ten minutes).

3 RESULTS

We compared diurnal patterns of vegetation transpiration with riparian groundwater levels in our study site (6 km^2 the Hidegvíz Valley watershed in Sopron Hills) in Western Hungary (*Figure 5*). A detailed description of the study catchment characteristics can be found in Gribovszki et al. (2006).

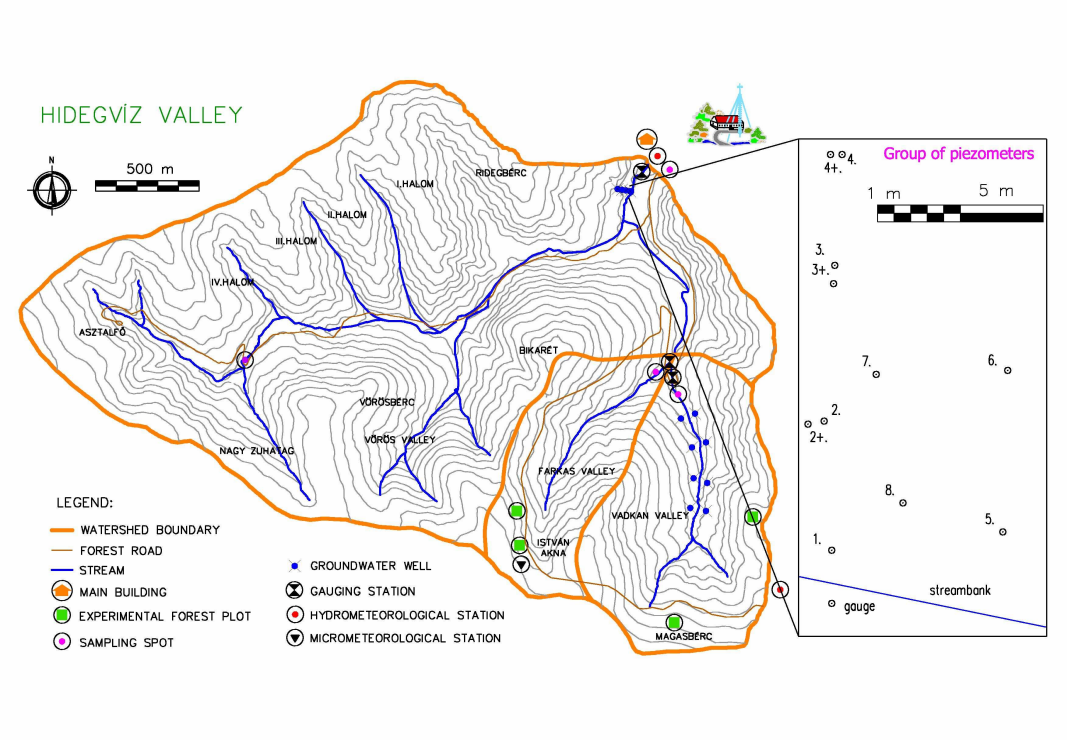

Figure 5. The study catchment and the location of the group of groundwater wells

The geology of the catchment is crystalline bedrock deposited in the tertiary (Miocene) period, and fluvial sediment, which is strongly unclassified. The fluvial sediment was deposited in five layers.

Only the two upper layers appear on the surface. On the hilltop and hill slope a Felstödl Gravel Formation is found. It is 10 – 50 meters thick. This contains coarser gravels and finest loam, and is therefore strongly unclassified. On the valley bottom, the finer material of the Magasbérc Sand Formation appears everywhere. These layers are a good aquifer, so the valleys have a perennial streamflow (Kisházi-Ivancsics 1981-85).

The riparian zone vegetation is an alder [Alnus glutinosa (L.) Gaertn.] dominated forest ecosystem. The mean height of the young to middle aged riparian forest stand is 15 m and the mean diameter of the trees is 13 cm.

The groundwater levels distance form the soil surface changes between 0.6-0.9 m in the riparian zone in dry periods. Therefore the root zone of the trees can reach groundwater levels (or at least the zone of capillarity) every day of the year.

Groundwater levels were measured close to the outlet point of the main study catchment (where a group of wells were bored some years ago) by sensors functioning on the principle of water pressure (*Figure 5*). We used the data of one groundwater well (denoted by 2+ in *Figure 5*), which is situated in the middle of an approximately 20-m wide riparian zone of the west bank of the stream.

The above mentioned parameters of our site, which are necessary for the *ET* calculation can be found in *Table 1*. *H* values come from the computation. The *h* values were measured in the groundwater well of the riparian zone.

Table 1. Parameters for ET calculation

	k (m/s)	S_y	l (m)	L (m)
Used values	$1.8\ 10^{-5}$	0.05	9.4	30
Range	$1.1\ 10^{-6}$ - $2.9\ 10^{-4}$	0.01 - 0.1	-	20 - 110

k saturated hydraulic conductivity, determined from several (16) slug tests (Thyll et al. 1983, Schwartz-Zhang 2003).
S_y, readily available specific yield, computed from $n_0/2$, where n_0 is the drainable porosity (we assumed that in case of shallow groundwater table the drainable porosity and specific yield is nearly the same).
l, the position (distance from the stream) of the riparian zone groundwater well
L, the distance from the stream, where diurnal fluctuation probably has no impact on the water table

Representative rainless periods in the year 2005 have been chosen from hydro-meteorological data sets for analysis. Some micro-meteorological models (Monin-Obukhov, Svedrup, Thornthwaite-Holzmann, Penman-Monteith) were used to calculate the riparian evapotranspiration and results were compared with each other. The Penman-Monteith model (Allen et al., 1998) was the best correlation with evapotranspiration values which were determined from groundwater levels. Therefore it was used in the further analyses. Parameters (which were used for the Penman-Montieth method) were measured some hundred meters from the group of groundwater wells.

Firstly three dry periods (a spring, a summer and an autumn) was chosen for the analysis of the new method. Half hourly *ET* values were computed and these values were compared with the Penman-Monteith *ET* values (*Figure 6*). This comparison showed that the Penman-Monteith *ET* values are similar in daytime but lower at night than empirical and hydraulic diurnal method *ET* values.

A problem can be seen around the time of the maximal change of groundwater levels. *ET* values of the new method go to zero or below zero at this time. This mistake was caused because the calculated Q_{net} rate is not able to follow the strong change of the real recharge rate. The problem is most obvious on hot days and almost negligible in the first part of the recession periods.

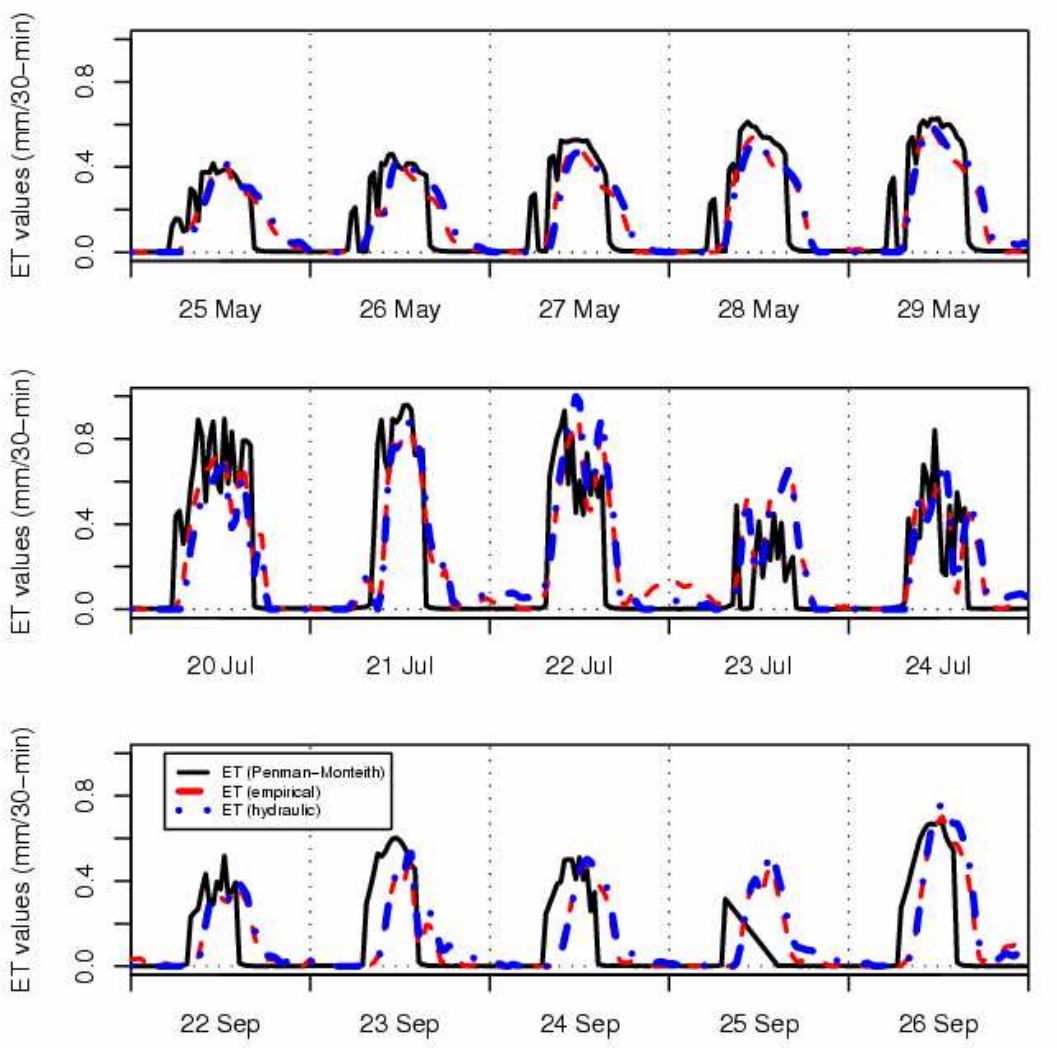

Figure 6. Half hourly ET values for three characteristic periods

The White method was used for calculation of comparable daily *ET* values (Eq. 4). Daily *ET* values of new methods were computed from summing up half hourly *ET* data and compared with the White *ET* values (*Figure 7*). Both empirical and hydraulic diurnal methods give higher daily *ET* values than the White method. These differences come from the basis of the methods. The White method takes a constant recharge rate into consideration for the whole day, and this recharge rate comes from the minimum recharge period (in the late night), when groundwater level differences between the riparian zone and the background is minimal. Empirical and hydraulic methods calculate a periodical changing recharge rate, which is maximal in the afternoon and minimal in the late night or early morning. Therefore they give higher daily *ET* rates (*Figure 6*). Making a comparison between the hydraulic and empirical methods, we found that different methods give different values in different seasons. Generally we can say that mistakes in water table records influence empirical method values more. Therefore the hydraulic method values are more reliable.

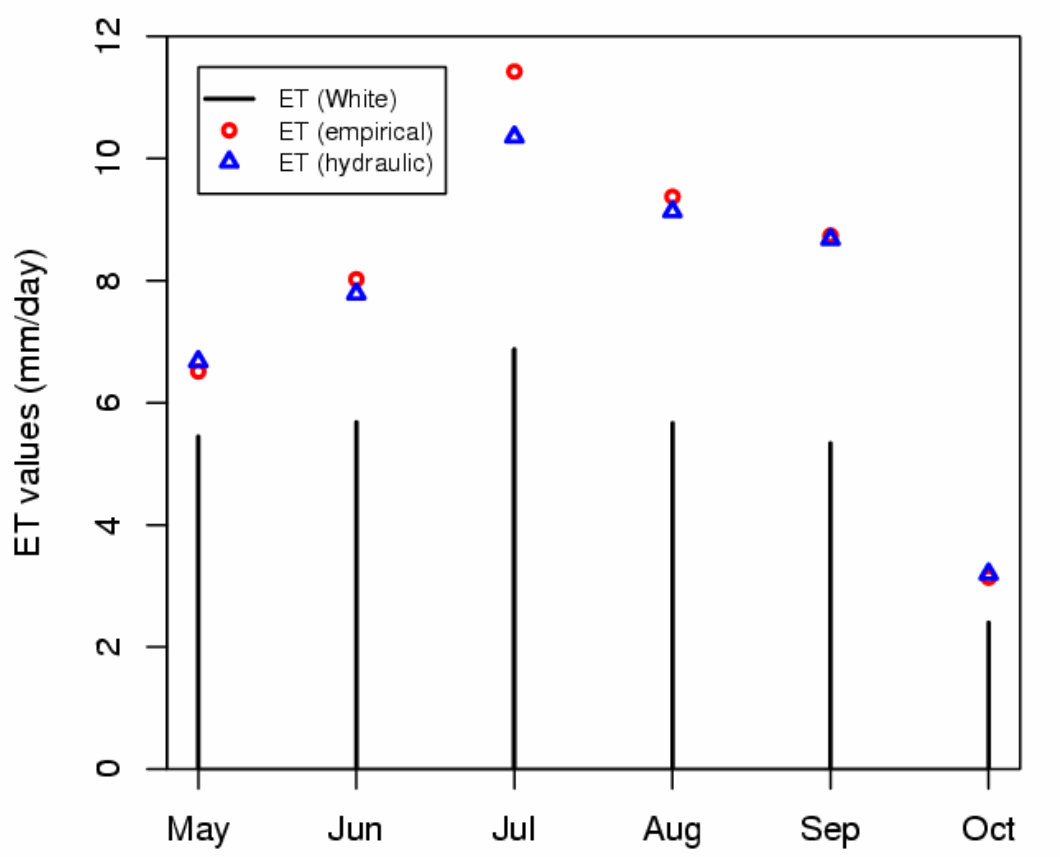

Figure 7. Daily ET values of White, empirical and hydraulic method

Sensitivity analysis (*Table2*) of the above mentioned hydraulic method showed that changing of the hydraulic conductivity (k) values has a strong influence on *ET* values. Changing of *L* cause only a slight modification of *ET* values.

Table 2. Sensitivity analysis of the method for k and L (test period 29.08 to 09.09)

	k (m/s)	S_y	*ET* value (mm/day)
k minimum	1.1×10^{-6}	0.01	1.32
k median	1.8×10^{-5}	0.05	8.51
k maximum	2.9×10^{-4}	0.1	55.10
	L (m)		*ET* value (mm/day)
L (side of the riparian zone)	20		9.43
L (proper distance)	40		8.51
L (a magnitude further)	110		7.93

Sy is also changed, because it is strongly related to k.

L (side of the riparian zone) means that distance of *H* from the stream is exactly the same as the width of the riparian zone.

L (proper distance) means the distance, where the riparian diurnal fluctuation has no significant impact on groundwater levels any more.

L (a magnitude further) means that *L* - *l* distance is one magnitude longer than *L* (side of the riparian zone)

4 CONCLUSIONS

The new *ET* estimation method is a modified version of the original White method (1932). This new method is based on the diurnal fluctuation of groundwater and can give daily or more frequent *ET* values. These *ET* values can be estimated from the record (in a rainless period) of one correctly situated groundwater well. Two sub methods were developed (called an empirical and a hydraulic method). For *ET* determination using the hydraulic method we need only high frequent groundwater levels data and a reasonable value of riparian zone saturated hydraulic conductivity. If you had no reasonable value of hydraulic conductivity, you should use the empirical method for *ET* calculation.

The new hydraulic method is sensitive to the exact determination of k (hydraulic conductivity) and S_y (specific yield) values. If we want to use this method for hourly or more frequent *ET* determination, we must note that the method (which comes from the main principle of the assumption) always gives *ET* values around zero at late night.

Acknowledgements: This research was partly funded by the Forest- and Wood Utilisation Regional University Knowledge Centre (ERFARET) research grant and by the Hungarian Scientific Research Fund (OTKA) research grant (registry numbers: T 030632 and F 046720).

REFERENCES

ALLEN R. G. – PEREIRA, L. S. – RAES, D. – SMITH, M. (1998): Crop evapotranspiration - Guidelines for computing crop water requirements - FAO Irrigation and Drainage, paper #56, Rome (http://www.fao.org/docrep/X0490E/x0490e06.htm).

BAUER, P. – THABENG, G. – STAUFFER, F. – KINZELBACH W. (2004): Estimation of the evapotranspiration rate from diurnal groundwater level fluctuations in the Okavango Delta, Botswana. J. Hydrol. 288, 344–355.

BOND, B. J. – JONES, J. A. – MOORE, G. – PHILLIPS, N. – POST, D. – MCDONNELL, J. J. (2002): The zone of vegetation influence on baseflow revealed by diel patterns of streamflow and vegetation water use in a headwater basin. Hydrol. Process. 16 (8): 1671-1677.

CROFT, A. R. (1948): Water loss by stream surface evaporation and transpiration by riparian vegetation, Transactions, American Geophysical Union. 29 (2): 235-239.

CZIKOWSKY, J. (2003): Seasonal and successional effects on evapotranspiration and streamflow. M.S. thesis, Dept. of Earth and Atmospheric Sciences, The University at Albany, State University of New York, 105 p.

CZIKOWSKY, J. M. – FITZJARRALD, D. R. (2004): Evidence of seasonal changes in evapotranspiration in eastern U. S. hydrological records. J. Hydrometeor. 5: 974-988.

FEDERER, C. A. (1973): Forest Transpiration Greatly Speeds Streamflow Recession. Water Resources Research, 9 (6): 1599-1604.

GOODRICH, D. C. – SCOTT, R. – QI, J. – GOFF, B. – UNKRICH, C. L. – MORAN, M. S. – WILLIAMS, D. – SCHAEFFER, S. – SNYDER, K. – MACNISH, R. – MADDOCK, T. – POOLE, D. – CHEHBOUNIF, A. – COOPERG, D. I. – EICHINGERH, W. E. – SHUTTLEWORTH, W. J. – KERRI, Y. – MARSETTA, – NI W. (2000): Seasonal estimates of riparian evapotranspiration using remote R. and in situ measurements. Agricultural and Forest Meteorology. 105 (1-3): 281-309.

GRIBOVSZKI, Z. – KALICZ, P. – KUCSARA, M. (2006): Streamflow characteristics of two forested catchments in Sopron Hills. Acta Silvatica et Lignaria Hungarica. 2: 81–92. URL http://aslh.nyme.hu/

KALICZ, P. – GRIBOVSZKI, Z. – KUCSARA, M. – VIG, P. (2005): A vegetáció hatása a felső vízgyűjtők patakjainak alapvízhozam mintázatára [Vegetation impact on base flow pattern of upper watershed streams] Hidrológiai Közlöny, 85. évf. 6. szám, 2005. November-December., XLVI. Hidrobiológus Napok Kiadványa, Tihany, 2004 október 6-8.: 50-52. (in Hungarian)

KISHÁZI, P. – IVANCSICS, J. (1981-85): Sopron környéki üledékek összefoglaló földtani értékelése. [Geological assessment of sediments in the neighbourhood Sopron] Sopron. Kézirat, 48 p. (in Hungarian)

KOVÁCS, GY. (1972): A szivárgás hidraulikája. [Seepage Hydraulic] Budapest, Akadémiai Kiadó, 536 p. (in Hungarian)

LOHEIDE, S. P. II. – BUTLER, JR. J. J. – GORELICK, S. M. (2005): Use of diurnal water table fluctuations to estimate groundwater consumption by phreatophytes A saturated-unsaturated flow assessment, Water Resour. Res., 41, W07030, doi:10.1029/2005WR003942.

LUNDQUIST, J. D. – CAYAN, D. R. (2002): Seasonal and spatial patterns in diurnal cycles in streamflow int he western United States. J. Hydrometeor. 3: 591-603.

MAJOR, P. (1974): A síkvidéki erdő hatásának vizsgálata a talajvízpárolgás és tényleges beszivárgás folyamataira. [Examination of lowland forest impact on soil evaporation and infiltration processes] Hidrológiai közlöny, 1974. 6: 281-287.

MEYBOOM, P. (1964): Three observations on streamflow depletion by phreatohytes. Journal of Hydrology. 2: 248-261.

PÖRTGE, K.H. (1996): Tagesperiodische Schwankungen des Abflusses in kleinen Einzugsgebieten als Ausdruck komplexer Wasser- und Stoffflüsse,Verlag Erich Goltze GmbH KG, Göttingen.

REIGNER, I. C. (1966): A method for estimating streamflow loss by evapotranspiration from the riparian zone, Forest Science. 12: 130-139.

SCHWARTZ, W. F. – ZHANG, H. (2003): Fundamentals of Groundwater, John Wiley & Sons, Ltd., New York,

THYLL, SZ. – FEHER, F. – MADARASSY, L. (1983): Mezőgazdasági talajcsövezés. [Agricultural drainage] Mezőgazdasági Kiadó, Budapest, 322 p. (in. Hungarian)

TROXELL, H. C. (1936): The diural fluctuation in the ground-water and flow of the Santa Ana river and its meaning. Transactions, American Geophysical Union. 17 (4): 496-504.

TSCHINKEL, H. M. (1963): Short-term fluctuation in streamflow as related to evaporation and transpiration, Journal of Geophysical Research. 68 (24): 6459-6469.

UBELL, K. (1961): Über die Gesetzmassigkeiten des Grundwassergangs and des Grundwasserhaushalts in Flachlandgebieten. Wasserwirtschaft und Wassertechnik. 11: 366-372.

WHITE, W. N. (1932): Method of Estimating groundwater supplies based on discharge by plants and evaporation from soil – results of investigation in Escalante Valley, Utah – U.S. Geological Survey. Water Supply Paper 659-A., 1-105 p.

Acta Silv. Lign. Hung., Vol. 4 (2008) 107-123

Profile Tests to Optimize the Utilization of Wind Energy

Andrea KIRCSI* – Károly TAR

Department of Meteorology, University of Debrecen, Debrecen, Hungary

Abstract – We have to know the property of air movement in hub height of wind turbine on understanding that we want to utilize of wind power economically. We can calculate wind speed from near ground measurement to hub height but always have mistake in results depend on applied method. In Hungary the Hungarian Meteorological Service carried out expedition wind measurements with SODAR equipment to study wind potential of the country within a frame of a scientific competition. We analysed SODAR data from Budapest, Paks and Szeged with statistical method looking for answer to our following question: How can frequency distributions of wind speed and wind direction in different height change? Are there any differences in form of wind profiles and in wind power in different wind direction sector? How can daily course of wind speed and potential of wind energy in different height change? At the same time, we suppose that there is a so-called "inflection altitude," where the daily course of the wind speed and wind energy is random. We try to determine this altitude on the basis of tower measurements in Paks. Finally we get an example to the distribution of specific wind power according to parts of the day

power law exponent / daily course of wind speed / SODAR and tower measurements

Kivonat – Profilvizsgálatok a szél energetikai hasznosításának optimalizálásához. Ismernünk kell a légmozgás tulajdonságait a szélerőmű tengelymagasságában, amennyiben gazdaságosan szeretnénk hasznosítani a szél energiáját. Talaj közelében végzett mérésekből számítható a tengely magasságában a szél sebessége, azonban eredményeink az alkalmazott módszertől függően mindig hibával terheltek. Magyarországon az Országos Meteorológiai Szolgálat SODAR berendezéssel végzett expedíciós szélméréseket az ország szélpotenciálját felmérő kutatás keretében. Ebben a tanulmányban Budapesten, Pakson és Szegeden végzett SODAR mérések adatait statisztikai módszerekkel elemeztük a következő kérdésekre keresve a választ: Hogyan változik a szélsebesség és a szélirány gyakorisági eloszlása különböző magasságban? Van-e különbség a szélprofil alakjában különböző irányszektorokban? Hogyan változik a szélsebesség és a fajlagos szélteljesítmény napi menete különböző magasságban? Ugyanakkor feltételezzük, hogy létezik egy ún. „inflexiós magasság", ahol a szélsebesség és szélenergia napi menete véletlenszerű. A paksi toronymérések segítségével próbáltuk meghatározni ezt a magasságot. Végül bemutatunk egy példát a fajlagos szélteljesítmény napszakok szerinti eloszlásáról.

szélerő függvény kitevő / szélsebesség napi menete / SODAR és torony mérések

* Corresponding author: kircsia@delfin.unideb.hu; H-4010 DEBRECEN, Pf. 13.

1 INTRODUCTION

The National Meteorological Service has bought a SODAR (Sonic Detection and Ranging) appliance, which measures the horizontal components of wind with sound waves, to prepare a detailed study of changes in wind power vs altitude in a research aimed at measuring the solar and wind energy potential of Hungary. It is corroborated by international tests and experiences gained in Hungary that measurements by SODAR are very precise (Vogt – Thomas 1995; Seibert 1998; Baumann-Piringer 2001; Dobi et al. 2006). Several studies have been written on testing the properties of the Hellman-exponent used for a simple description of the wind-profile (Tar 2007a; Dobi et al. 2006).

By analysing the expeditionary measurements made with SODAR in Budapest, Paks and Szeged between 2003 and 2004. We were trying to find the answer to the question of how wind properties change at varying heights and which well—known wind-profile context approaches it more precisely. The properties of wind-speed and specific wind power were studied at several heights during the day on the basis of data of tower measurements in Paks, during the years 2000 and 2001 (Tar 2004, Tar 2007b).

The new measuring device can measure the properties of motion even at 20 different heights, between 30 m and 315 m with a resolution of 15 metres. One part of analyses was carried out between height of 30 metres and 120 metres in accordance with onshore wind energy utilization on the basis of data of 7 altitudes. The number of data that can be evaluated above 120 metres, as is shown by experience in Hungary, can be decreased even below 60%, which means significant statistical uncertainty. On the other hand, the full height of onshore wind turbines with rotor blades included cannot exceed 150 metres by European law, so the wind-data measured at an altitude of 120 metres provided information about wind motion characteristic of the hub height of the highest possible wind turbines which can be deployed.

The distribution of wind direction frequency was calculated on the basis of 12 30° intervals. A specific feature of the representation in *Figure*s *1*, *2*, and *3* is that it shows the distribution of wind speed with 1 m/s precision. Thus, not only the more frequent, dominant wind directions can be seen, but other ones too that is important in terms of strength and is characterized by a higher average speed. In addition, the frequency of wind direction as well as the resulting wind direction calculated by means of the average wind speeds measured by directions as show in the *figures 1-3* too.

The observations were of expeditionary nature, so the data of Budapest extends from 1st April of 2003 to 30th June, the beginning of summer. The observations in Paks were made from 1st November of 2003 to 29th February of 2004, mostly in winter, whereas the data from Szeged processed are available for 4 months from 1st June to 30th September of 2004. Wind measurements carried out between 30 m and 315 m with 1 minute frequency. The averaging period was 10 minutes.

Parts of the analyses were made with software developed by Mistaya Engineering Inc., called *Windographer 1.04,* while the others with that of Lakes Environmental *WRPLOT View 5.2.1* representing a wind rose.

2 RESULTS

2.1 Changes in wind direction and wind speed at different altitudes

Measurements made in Budapest (*Figure 1*) show that in the spring and early summer period North-Westerly winds were the most common at all altitudes in 2003. At higher and higher altitudes, the dominance of North-Western wind direction was even more pronounced marked, while closer to the ground Northern wind frequency is significant. If we account for

the distribution of wind speed by direction, it can be seen that the generally dominant North-Westerly wind has the highest average speed, and through its volume, the biggest potential energy content. Detailed tests showed that wind speed is lowest at early dawn, or sunrise at all heights. During a day the highest average-speed period at height of 120 metres was typical between 5 and 10 p.m.

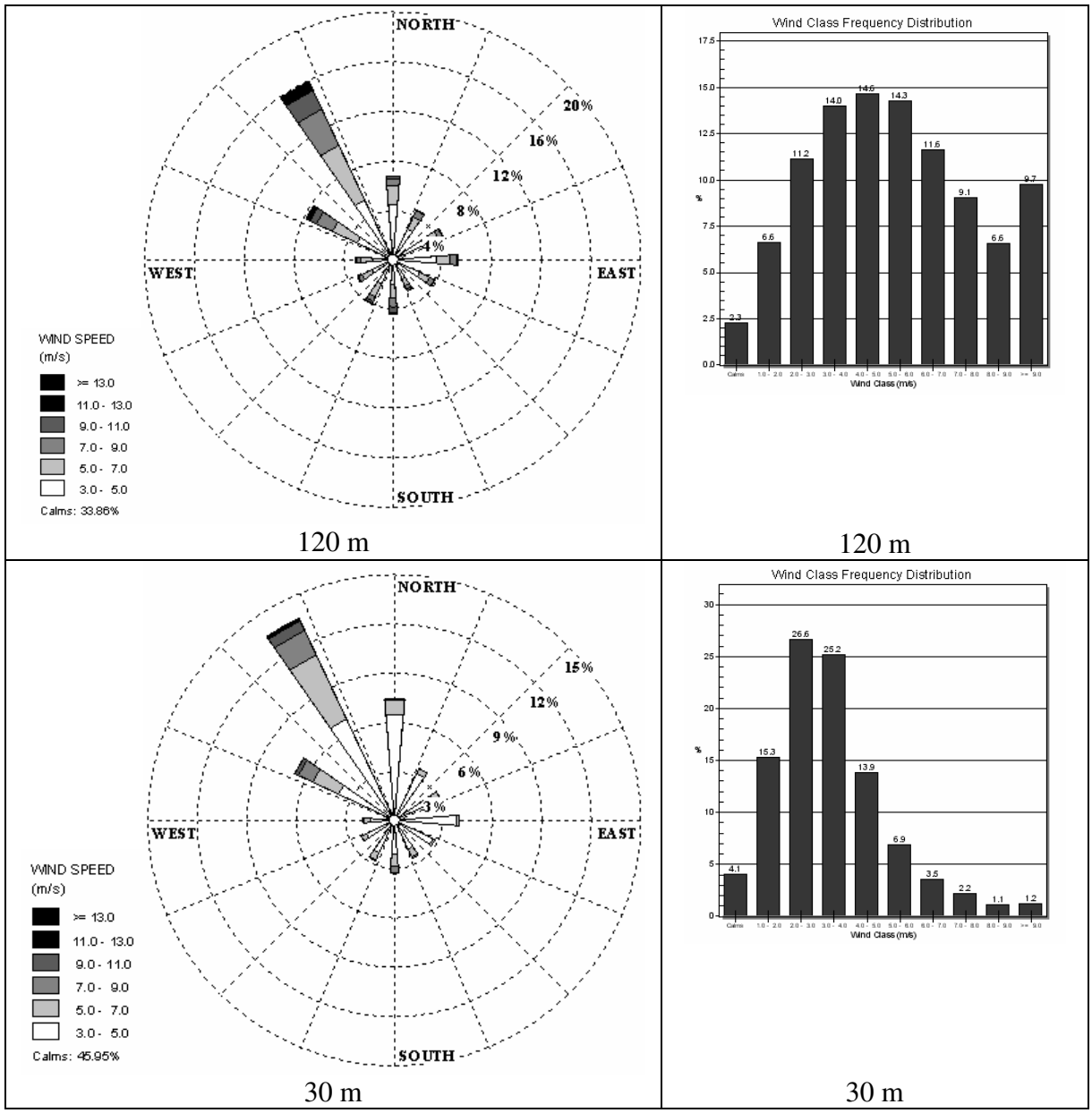

Figure 1 Relative frequency distribution of wind direction and wind speed by wind direction categories 30 m and 120 m above the surface from SODAR measurements in Budapest

The average wind speed increased at higher levels, which also leads to a change in the shape of distribution. In *Figure 1* the relative frequency distribution is shown in two heights. In Budapest, the frequency of the calm period (<3 m/s wind speed) is more than 20% even at a height of 120 m, which may reach 45% near ground level (30 m). The commonly used Weibull distribution is applied. Its scalar (c) and shape (k) parameters can be calculated in different ways at all heights. Our study shows that the shape parameter of the Weibull distribution applied for the measured data is $k=2$ and it only changes to a hundredth value up to 120 m. At the same time, scale parameter c has a speed dimension (m/s), which changes

within a wide range depending on the average speed and the height (in a range of 3.9-5.96 m/s at a height of 30-120 m). As a result, the potential specific wind power of the air is almost tripled between 30-120 m (30 m: 47 W/m^2 and 120 m: 162 W/m^2).

With fluctuating wind, a wind turbine produces electricity in a well-definable wind-speed range. It reaches its nominal power at a given wind speed. It is determined by the distribution of wind speed and the technical properties of the wind turbine as a function of the time available for the wind turbine to produce electricity for a network. With the distribution of wind speed known, the value of utilized capacity factor (%) is a crucial parameter in assessing how economical a wind turbine will be and as well as in testing the feasibility of an investment. In Europe, it is 23-25%, which does not even rise above 40-45% in excellent offshore seats (IEA 2005). If there had been a VESTAS V90 1.8MW nominal capacity wind turbine with an axis height of 105 m in the examined period near the measuring site in Budapest, its capacity factor would have remained below 20% (19.2%) based on local wind measurements at an altitude of 105 m. Of course, this factor does not only depend on the technical parameters of the wind turbine, but on the wind conditions of the given year too.

The place of setting up SODAR in Budapest cannot be regarded as most optimal for a wind turbine from the aspect of energy. Although the rate of utilization is below the European average, it is not the worst in Hungary. Anyway, if we know exactly the distribution of wind-speed, we can find a type of wind turbine, optimal axis height, which exploits the local conditions best.

In *Figure* 2 it can be observed that near ground level in Paks, between 1st November of 2003 and 29th February of 2004, both North-Western-Northern and Southern-South-Eastern winds were very frequent.

This local element of the terrain is of key-importance from the aspects of wind-motion, and it can be explained with the location of the Danube Valley. The North-Western wind is dominant at an altitude of 120 m, but Southern winds, so much common elsewhere, are less frequent here.

However, the dominant character of North-Western winds is obvious based on the energy content of fair motion. Southern air motions are of primary importance mainly in the morning period, while in the afternoon and in the evening, North, North-Western winds of considerable specific wind-power are common.

Average wind-speed at an altitude of 120 m approaches 6 m/s though near ground level, the average values are around 3 m/s similarly to the one measured in Budapest.

According to measurements made mainly in the winter period, wind speed changed less during the day than in Budapest. The shape parameter of Weibull distribution (k) hardly changed ($k=2$), whereas the speed-dependent scale parameter (c) doubled (3.09 m/s 30 m, while 6.66 m/s at an altitude of 120 m). Accordingly, specific wind power at 30 m above ground level increased from 24 W/m^2 to ten times higher at 120 m, to 224 W/m^2.

The place of measurement in Paks seems a more favourable location in terms of available wind force compared to the one in Budapest, as the energy content of the wind exceeded 220 W/m^2 at an altitude of 120 m. Vestas V90 wind turbine with an axis height of 105 m, and with nominal power of 1,8 MW would have reached 25% capacity factor under similar wind condition. North of Paks, in Kulcs is an operating Enercon E-40 wind turbine with nominal power of 600 kW since 2001. According to experiences between 2002 and 2006 the yearly capacity factor has not reach higher than 25%, but the axis level is only 67 m (Stelczer, 2007).

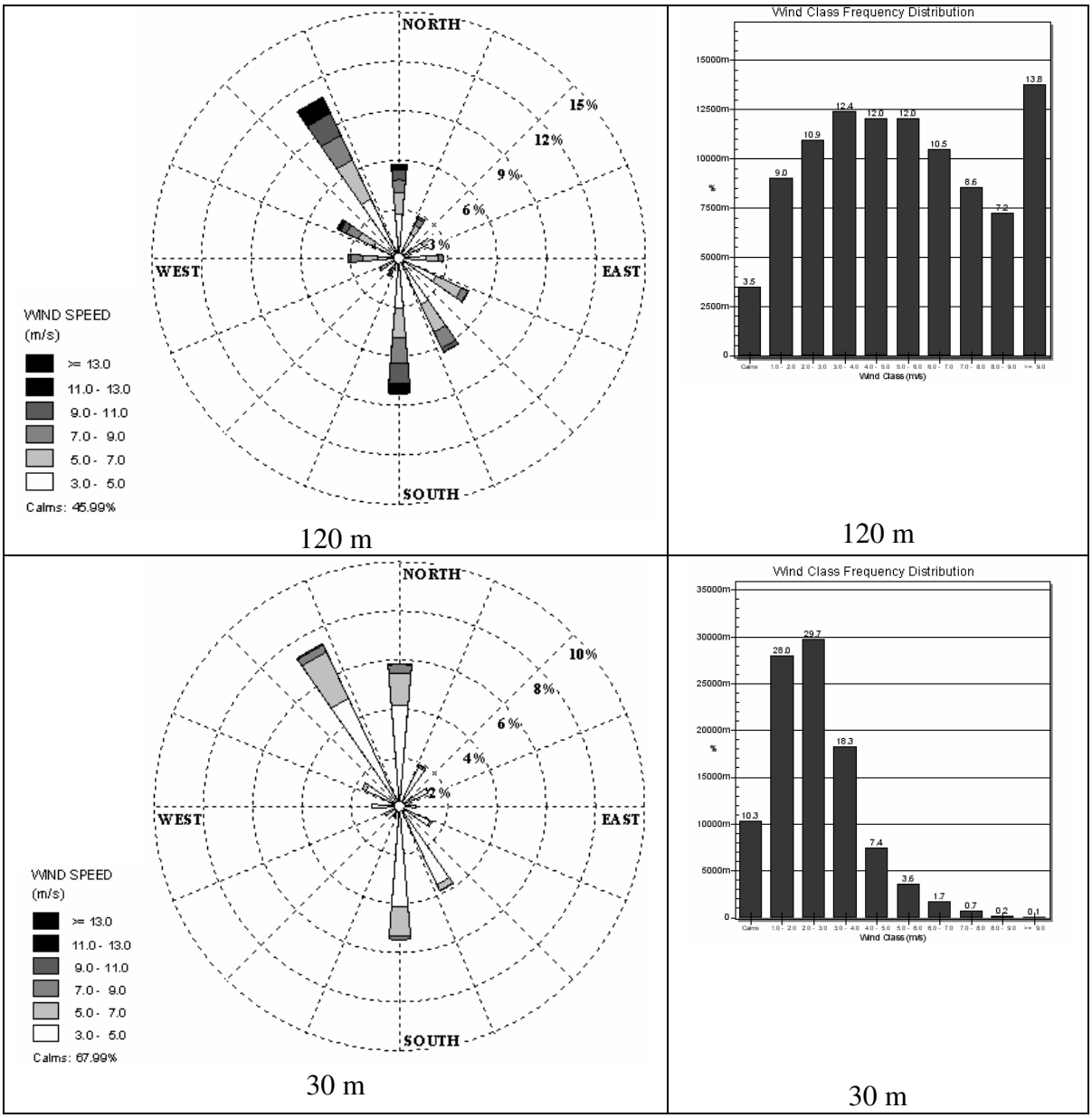

Figure 2. Relative frequency distribution of wind direction and wind speed by wind direction categories between 30 m and 120 m above the surface from SODAR measurements in Paks

The data measured between 1st June and 30th September of 2004 with SODAR at the airport of Szeged is available to analyse. The North-western winds seem to be dominant on the basis of wind direction frequency as is shown in *Figure 3*. As the height increases the number of southern directions decrease, while Northern, North-Eastern winds are more frequent, though Southern directions have strong wind speed at an altitude of 120 m. The parameters of Weibull distribution in Szeged between 30 - 120 meters are between 2.1 - 2.2, while the scale parameter (*c*) 30 m - 3.77, at 120 m – 6.09.

The average wind speed in Szeged at 120 m hardly exceeds 5 m/s, which means that the energy content of the summer months in 2004 at this altitude was lower than the values measured in Paks (140-160 W/m^2 at altitudes 105 and 120 m, though they did not differ significantly from the data measured in Budapest. It is common knowledge that the summer period is less windy in Hungary than winter or spring, which explains why Szeged seems unfavourable place in terms of a wind supply in the examined period for industrial-size wind turbines producing electricity for the energy network.

Taking into account the data of the measurements in the 4 month period, a Vestas V90 with 105 m hub heights with 90 m of rotor diameter and 1.8 MW nominal power could have reached around 20% utility rate in Szeged.

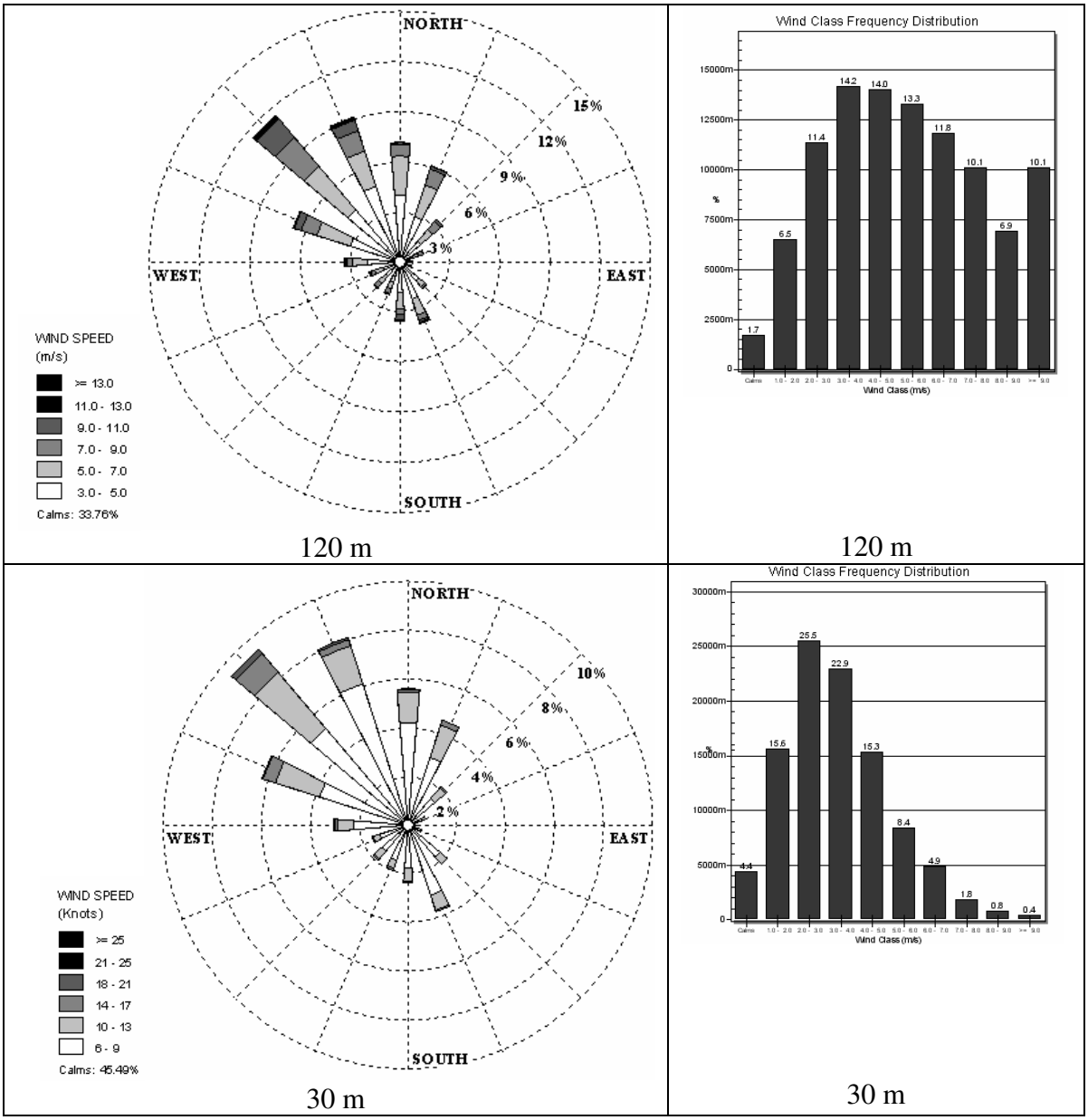

Figure 3 Relative frequency distribution of wind direction and wind speed by wind direction categories between 30 m and 120 m above the surface from SODAR measurements in Szeged

2.2 Average and normalized wind profiles

Changes in wind speed at different altitudes can be described with well-known wind-profile contexts: with logarithmic relation used in meteorology,

$$u(z) = \frac{u_*}{\kappa} \ln \frac{z}{z_0} \tag{1}$$

(where u_* is friction velocity, κ=*0.4* is Karman's constant, z_0 is roughness height) or in engineers' work with a simpler exponent variant,

$$\frac{u_2}{u_1} = \left(\frac{z_2}{z_1}\right)^{\alpha} \tag{2}$$

(where u_1 is wind speed (m/s) in z_1 reference height, u_2 is wind speed in sought z_2 height, and α is Hellmann's exponent).

Theoretical logarithmic wind profile (1) context can be easily used according to tests of planetary border-layers above 100 m near the ground, and at higher altitudes at 925-850 hPa altitude in almost neutral unstable balance situations, that is mainly found during the day. The fault-rate of assessment is highest near ground level, in the case of inversion, rather unstable conditions, especially at night.

Owing to the simplicity of the context (2) it is also used in the case of wind measurements aimed wind energy for the extrapolation of wind speeds for the height of the wind turbine. However, based on data from meteorological towers and wind measurements of wind energy, the value α can be made more precise according to surface friction. Radics (2004) says that the values of the exponent are 0.14 over a flat water surface, 0.2 over rough, hilly surface, and 0.28 over settlements. Though she emphasizes that the exponent α depends on wind speed (at higher wind speed its value decreases) beside the roughness of the surface and from temperature layers of the air too.

The value of the exponent has a wide range not only depending on the roughness of the surface but also as the resultant of several atmospheric factors (Tar 2007a; Dobi et al. 2006). All scenes of measurements found determinate daily course of a power law exponent, which reflects seasonal differences.

The shape of average wind profiles at the three locations is the resultant of local effects. We examined with which theoretical relationships the wind profiles defined from the SODAR measurements can be approached more precisely. *Figure 4* shows how the average wind speed calculated for the complete period of measurement depends on a height between 30 and 120 m. Quite strangely, the values of Szeged and Budapest parallel each other up to 60 m, while from this height those of Paks and Szeged, and between 55 and 60 m the averages are almost equal, about 4.2 m/s.

According to correlation indices it is the logarithmic function in Budapest, while in the other two stations the exponent one that suit the best in this layer.

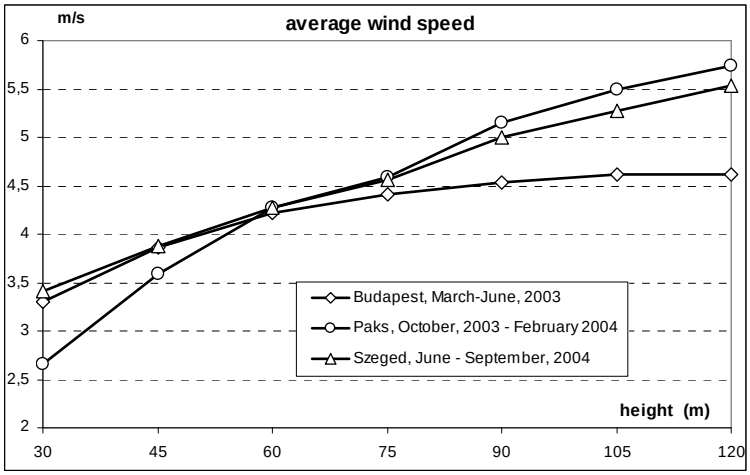

Figure 4. Average wind speeds at different heights for the whole measurement periods

When accounting for all the data available for up to 315 m, it can be pointed out that over 60 m the logarithmic context is excellent in Budapest, while in Paks was unfavourable in

concept (*Figure 5*). Changes in wind speed are best described by the exponent context basically at all heights, but especially above 120 m in Paks. We found a marked breakage point in the shape of the wind profile in Szeged. There we judged the exponent formula more precise up to 75 m near the ground, while between 90-315 m the logarithmic description with a 15 m range.

From another point of view we produced normalized profiles in the most frequent dominant wind-directions (Mellinghoff et al. 2000). When normalizing, we accounted for wind motion stronger than 4 m/s, which is of key importance in terms of energy production.

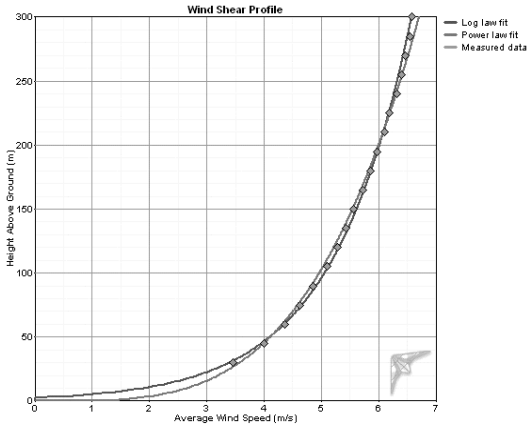

Budapest

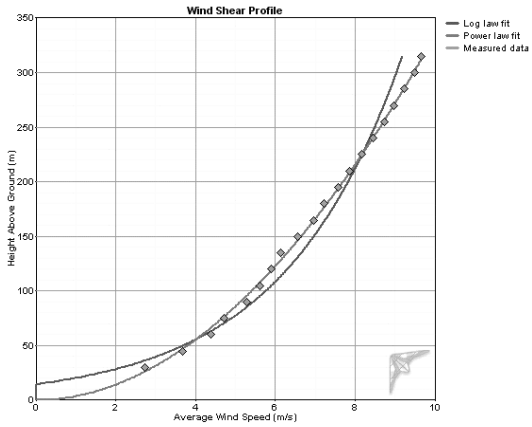

Paks

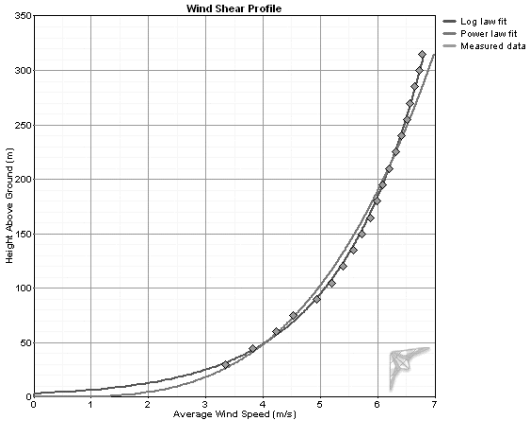

Szeged

Figure 5 Average wind profile in Budapest, Paks and in Szeged and its fit with log law and power law function

Through this condition we managed to decrease the range of our data, whereby smoother profiles could be produced. Normalization was carried out with the wind speed of the 75 m height, so the relative profile (*Figure 6*) depending on wind direction was defined from this base point.

Introducing the wind speed value virtually emphasized the defining character of north-western 315-345° wind direction sector in all locations. This means that we can compare different locations with identical wind directions. The typical wind direction in Paks is (180°) Southern, while in Szeged sector 275-315°.

It can be seen in *Figure 6* that the speed of north-western wind is 25% lower at 30 m above ground level than at 75, but it is only 10% higher at 120 m. There is an inflection

point in the relative profile at about 60 m, and the wind speed per unit height above it hardly changes.

The gradient of wind speed was the highest in Paks, as near-surface wind was even 40% weaker, while at the seventh level it was more than 20% bigger. The speed difference of the two levels was almost twice as high as in Budapest.

On the whole, the experience gained in Szeged was positive compared to Budapest, though as effective as that obtained in Paks. The difference in speed between 30-120 m was almost 40%. The decrease in wind speed near ground level was more moderate, which may be related to the kind of terrain found on the plain.

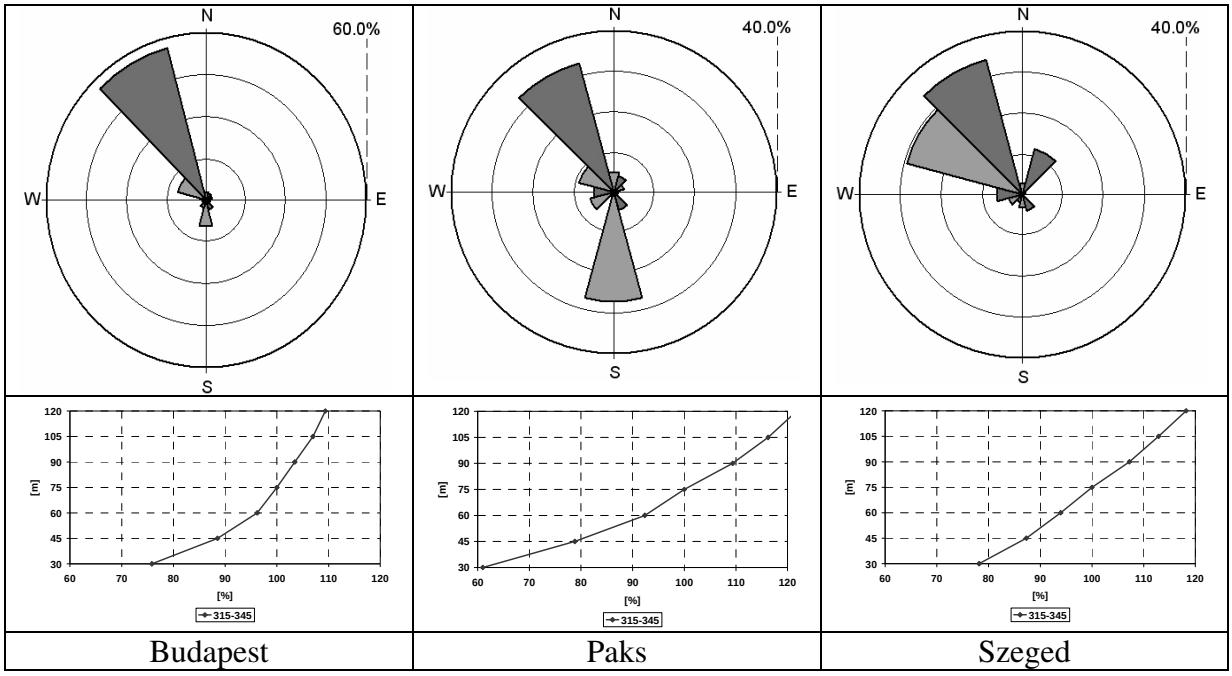

Figure 6. Frequency distribution of wind direction, and normalised wind profile in prevailing wind direction, where average wind speed is higher than 4 m/s, in Budapest, Paks, and in Szeged

Szeged can owe its more favourable evaluation in terms of commercial utilization of wind energy to the fact that the dominant wind direction is westerly, and that winds higher than 4 m/s arrive frequently from sector 285-315°. This local characteristic feature would moderate energy quantity, which would be exhausted by the wind turbine when turning into the direction of the wind.

2.3 Factors influencing the shape of the wind profile

There is general agreement in the literature that apart from the characteristics of the surface (the relief, the cover of the surface, roughness and artificial obstacle) the shape of the wind profile above ground level is regulated by atmospheric factors too. So, it is affected by large area weather phenomena, stability of the atmosphere, its temperature structure as well as the distribution of humidity. During the research, SODAR was only set up on a plain, whereby we could disregard the complex effect of the relief. This made the roughness of the surface a significant factor.

The roughness height z_0 in the logarithmic wind profile means the theoretical height where, wind speed becomes zero. If we know the typical roughness height value of an area, the speed of wind can be defined for other heights with a certain wind profile.

If the wind profile is well-known, roughness height z_0 can even be calculated for wind direction sectors, or in the Hellman context (2) the value of the exponent. This means that SODAR measurements provide detailed information on the close vicinity of the measuring place. Ideally, wind measurements of energetic nature should take place in an environment complying with the practice of synoptic stations, in a completely open flat, short-grassed area with a roughness height area of z_0=0.03 m. Very low z_0 value should be calculated in all directions. On Figure 7 shows calculated z_0 value from SODAR measured wind profile in synoptical station of Hungarian Meteorological Service in Budapest, Paks and Szeged. It can be seen in *Figure 7* that none of the locations seem ideal from all points of view.

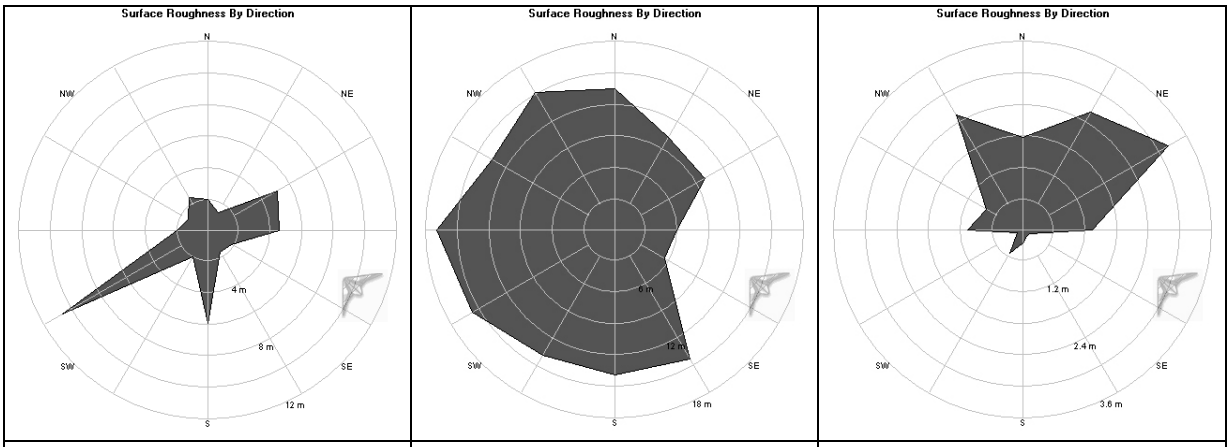

Budapest	Paks	Szeged

Figure 7. Effect of roughness by wind directions in Budapest, Paks and in Szeged

In the surroundings of the Budapest (Pestszentlőrinc) measuring station we found effects of buildings, or a higher roughness element in north-eastern north-western direction (Figure 7). The main observatory of Hungarian Meteorological Service is suburb surroundings of SE part of Budapest. The location is mostly flat, but observatory is on a small hill, so higher than surroundings area. In Paks, the effects of local elements of roughness could be measured virtually from all directions in the period of data collection. This location proved very rough by all categorizations of roughness. This meteorological station locates close to forest belt of the nuclear power plant in Paks, so this forest has an influence on wind measurements. In Szeged the meteorological station located in western side of city nears the airport. We can observe clearly that the north-north eastern sector is characterized by high roughness, while from southern directions the measuring point is completely open. In the north-eastern direction we detected the effects of the industrial and suburban area of Szeged approx. 500m from measuring station.

Our former statements were also corroborated by the values of α exponent in the exponent context defined by wind direction sectors (2), which is shown numerically by *Table 1.*

By this table in the case of Szeged the average is α=0.2, in Budapest it is nearly 0.3, while in Paks it is α=0.4-0.5. If we consider that wind from the north-western (330°) is dominant, then Budapest and Szeged are very similar, α=0.26 , while in Paks it is α=0.52. The latter values reveal good correlation with our results calculated from tower measurements in Paks (Tar 2004, Tar 2007b).

From the aspect of practical use it is worth considering that if the wind reaches our wind turbine from a surface of low roughness in the dominant wind direction, we can produce electricity with a smaller turbine as wind speed is stronger near the surface. In an area of higher roughness, however, we had better choose a bigger wind turbine.

Table 1. Average power law exponent by wind directions in Budapest, Paks and in Szeged

Medium value of wind direction sector (°)	Budapest	Paks	Szeged
0	0.260	0.504	0.244
30	0.235	0.447	0.268
60	0.324	0.427	0.287
90	0.321	0.355	0.238
120	0.252	0.339	0.159
150	0.245	0.501	0.152
180	0.342	0.495	0.168
210	0.256	0.513	0.193
240	0.434	0.539	0.155
270	0.256	0.561	0.222
300	0.239	0.512	0.204
330	0.267	0.526	0.269
α exponent value average	0.29	0.48	0.21

2.4 Determining the „inflection altitude”

It is interesting both from an energy and a practical perspective that the wind speed changes in various layers of the atmosphere according to a different daily course. Over ragged surfaces, up to a supposed altitude of 60-80 m (Radics 2004), wind speed increases at around sunrise, and reaches its maximum by early afternoon. By contrast, at higher altitudes, it shows the opposite course, i.e. it reaches its minimum level around noon. Naturally, the same daily courses can also be observed in both the potential wind energy and in terms of energy utilised as electricity. According to our preliminary studies (Tar in press), the full-day and half-day periods of the daily courses were only realistic in the two layers in a negligible percentage of the cases. At the same time, we suppose that at the boundary of the two layers there is a so-called “inflection height,” where the daily course of the wind speed and wind energy is random. At this height, wind energy may be considered as constant over the entire day, meaning that the operation of a wind power plant would require fewer tasks from the perspective of the electric control systems. The amount of wind energy that can be produced here, is likely to be less than at higher heights.

The basis for the elaboration of the method used for determining the inflection height and the average energy content of the wind was the wind speed data measured every ten minutes at height of 20 m, 50 m and 120 m on the meteorological tower of Paks in 2001. *Figure 8* shows the average daily course, calculated for the entire year, at the three heights.

The average speeds for the entire year were 2.8, 4.0 and 5.9 m/s, while the standard deviation was a 0.47, 0.25 and 0.49 m/s, respectively. The fluctuation of the average annual course at 50 m, therefore, is half of the value measured at the other two heights, which suggests that the inflection height should be sought around here. Further reinforcing this hypothesis are the values of the variance ratio (standard deviation / average), which are 0.169, 0.063 and 0.082, respectively.

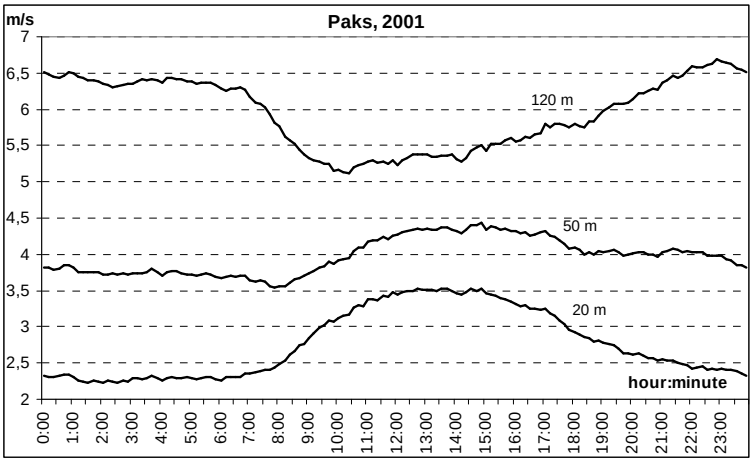

Figure 8. The daily course of the annual average of wind speed data measured every 10 minutes at heights of 20, 50 and 120 m at Paks

The wind speeds measured at every 10 minutes at the three altitudes can be used to determine the current values of the α index of (2), the so-called Hellmann's law, taking various altitudes as the starting level. The average of these will yield the daily average course of the power law exponents, which is shown in *Figure 9*. It is α(h1, h2) on the figure that means the annual average of the current values of the power law exponent calculated from height h1 to height h2 (where h1<h2). The daily averages are, in all three cases, 0.45, the standard deviations are 0.17, while the variance ratios are 0.37. The average values are higher than the values found in the relevant literature. It can also be seen in the figure (*Figure 9*) that the values of α(20,120) can be regarded as the average of the other two. Therefore, this power law exponent will be calculated with first.

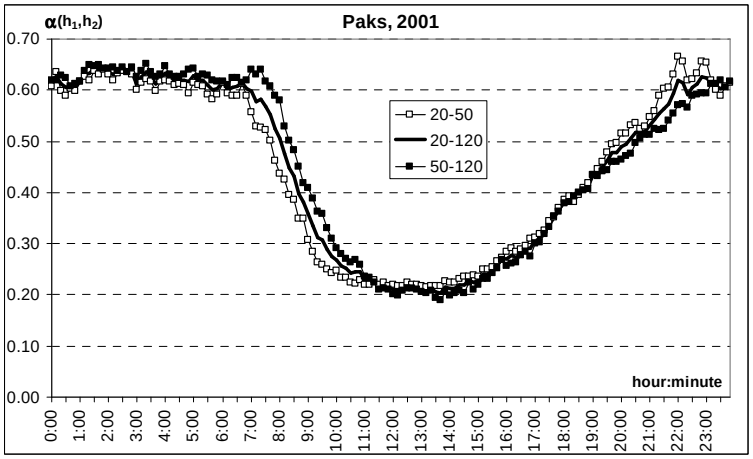

Figure 9. The daily course of the annual average of the Hellman indexes calculated every 10 minutes at Paks

First of all, the error in the estimate with the values of the average daily course of α(20,120) were determined. From the current wind speeds at 20 m, we calculated the speeds at 50 m and 120 m, and with the measured values in hand, we determined the relative error of the estimates in%, and then took the average of these values. The daily course of the average values is shown in *Figure 10*. It can be seen that, as expected, the error of the estimate is generally higher in case of speeds at 120 m altitude, especially in the daytime period. The value of the daily average relative error was 4.8% at 50 m and 5.7% at 120 m.

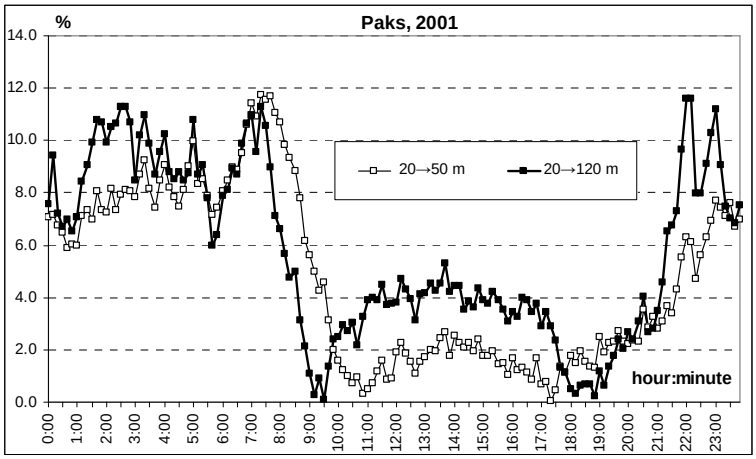

Figure 10. The daily course of the relative error of the estimate with α(20,120) the average power law exponent (20 m → 50m ; 20 m →120 m)

Next, using the 10-minute average values of α(20,120), we calculated the estimated values of the wind speeds and wind speeds raised to the third power for every 10 minutes from the wind speed data measured at 20 m.

The average value of the latter for each point in time is proportionate to the value of the wind power, which means we thus also received the daily course of the average wind power.

Figure 11 shows the annual average wind speed calculated from the estimated values of the wind speed, as well as the standard deviation and the variance ratio. The power law function laid on the average values shows a fairly good correspondence (the correlation index is 0.9952) with a power law exponent (which is also the value of the Hellmann index in this case) of 0.34. The values of the standard deviation and the variance ratio take their minimum values at 50 m, which suggests that the inflection height should also be around this point.

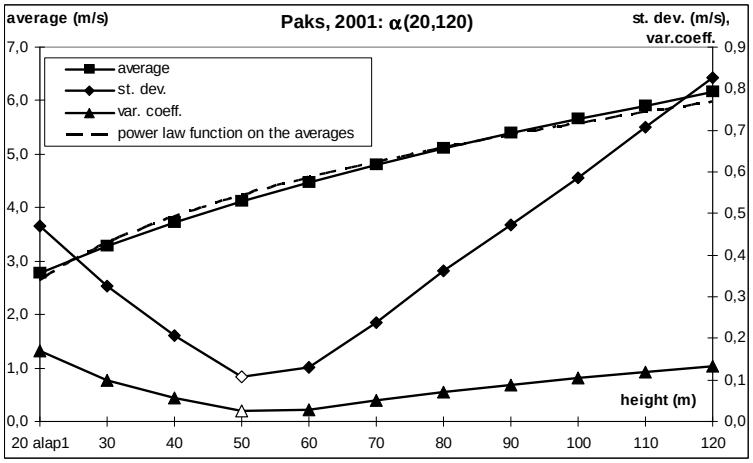

Figure 11. The annual average wind speed and the variance ratio at different altitudes, calculated from 20 m with the α(20,120) average power law exponent

Figure 12 provides further basic statistics on the estimated values. The fact that these are fairly close at a height of 50-60 m also reinforces our earlier hypothesis.

In order to confirm this we carried out a time-series analysis of the average daily courses of the wind speed values raised to the third power at various altitudes: we set a trigonometric polynomial consisting of two waves, and examined the reality of the amplitudes of these.

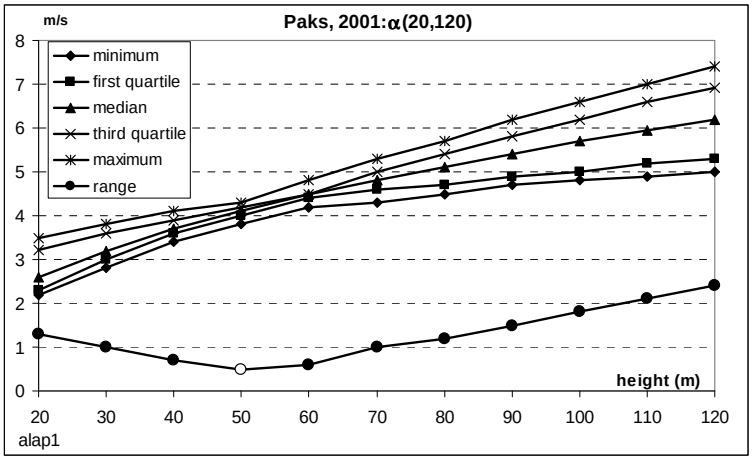

Figure 12. Further basic statistics at various altitudes, calculated from 20 m with the α(20,120) average power law exponent

That level was considered as the inflection height, where the period of either wave (24 or 12 hours) was random, and therefore, its amplitude not significantly different from 0. This can be determined with the A_m/E ratio of the individual amplitudes (A_m, m=1,2) and the expectancy (E, the expected value of the amplitudes) defined by the formula

$$E = s_n \sqrt{\frac{\pi}{N}} \tag{3}$$

If the A_m/E ratio is big enough, then there is a low probability (p) for the period to be a result of the random arrangement of the data, which means that it can be regarded as realistic from a statistical point of view. Generally a value of $A_m/E>2$ can be regarded as acceptable (p=0.05), but in case of the period analysis of weather data, a given wave is also regarded as realistic in case of $A_m/E>1.5$ (p=0.17) values (Koppány 1978). In *Figure 13*, the dependence of the A_1/E and A_2/E ratios on height was depicted. It is seen that the first, 24-hour wave can be regarded as realistic at all altitudes on a 0.05 significance level; however, at 40 m, the A_1/E proportion is 3, decreasing to the critical value belonging to the 0.01 significance level. At 50 m, the second wave of 12-hour period becomes random. This means that the 12-hour period from this point on will not characterise the daily course of the average wind speed values raised to the third power. We therefore believe that the inflection height is around 40 m.

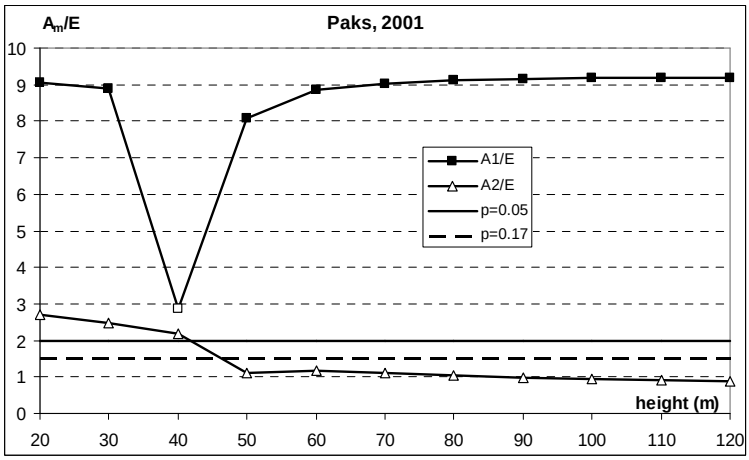

Figure 13. Dependence of the A_1/E and A_2/E ratios on height in Paks

This is also reinforced by *Figure 14*, where the averages calculated from the measured (20 m) or estimated (30, 40 and 50 m) values, as well as their approximations by 1 or 2 waves were plotted at the 20, 30, 40 and 50 m altitudes. It can be seen that at 50 m, the two approximation curves run together, which means that taking the second wave into consideration does not alter the correctness of the approximation. The same can also be experienced at greater heights.

From the comparison of *Figure*s *8* and *14* we can see that the daily course of the estimated values of the measured wind speed values and the wind speeds raised to the third power are different, which partly results from the raising to the third power, but primarily from the error of the estimation. We can conclude, therefore, that the inflection height in the period, year 2001, was around 40 to 50 m, and that the daily course has its maximum value below and its minimum value above this height at around 1 p.m.

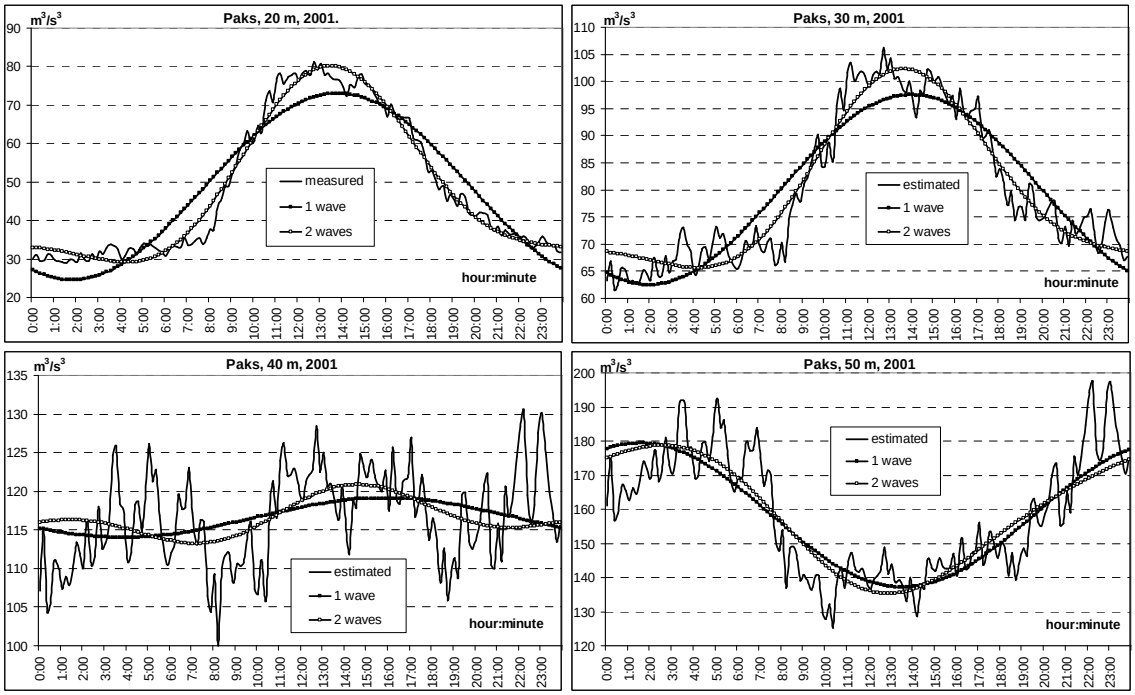

Figure 14. The daily course of the measured or estimated average wind speeds raised to the third power, and their approximation by a trigonometric polynomial consisting of one and two waves

2.5 The distribution of specific wind power according to parts of the day

The specific wind power falling on a single day of a longer time period can be defined as follows: the area under the curve of the approximating function laid on the daily average course of wind speed values raised to the third power. In our case, this function is a trigonometric polynomial consisting of two waves, which has a primitive function, and so the area under the curve can be determined by a definite integral.

In *Table 2* we provide the average specific wind power calculated for the daytime (9 a.m. to 7 p.m.) and the night-time (7 p.m. to 9 a.m.) periods, expressed as a percentage of the total daily average specific wind power.

According to the table, the potential daytime wind power is only higher or equal with the night-time values up to an height of 30 m. The latter is already twice of the former at an height of 60-70 m, and more than 3.5 times the former at 120 m.

Table 2. The average specific wind power calculated for daytime and night-time periods in percentage of the total daily average specific wind power in 2001 in Paks

	Daytime	Night-time
	(%)	
20 m	58.2	41.8
30 m	49.1	50.9
40 m	42.7	57.3
50 m	37.9	62.1
60 m	34.1	65.9
70 m	31.0	69.0
80 m	28.5	71.5
90 m	26.5	73.5
100 m	24.7	75.3
110 m	23.1	76.9
120 m	21.8	78.2

3 CONCLUSION

From the analysis of the research data by SODAR carried out in Budapest, Paks and Szeged, we can make the following statements:

- From the point of view of energy utilisation, it is the north-western winds that have more significant energy content. In case of Paks and Szeged, southern winds are also favourable.
- The wind speed shows characteristic daily courses at different heights. The minimum levels are measured at sunrise and early morning at all height levels. The maximum daytime wind-speed is measured near ground level. The maximum of the daily course above 60-90 m was typical in the late afternoon and in the evening hours. This indicates that even though the construction of increasingly higher hub height wind turbines is believed necessary in Hungary, these wind turbines will generate most electricity not in the period of highest energy demand, this will constitute a system control problem.
- In the measuring points without effects of the terrain, the logarithmic relationship for the description of the average wind profile proved to be better in Budapest and Szeged. The high-gradient wind profile in Paks could be better described with the use of the power law exponent formula. We examined the daily course of the average power law exponent in this formula, and found that in Paks and Szeged, a fairly definite daily course, depending on the stability of the atmosphere, could be observed, which also reflects the seasonal differences. With the average wind profile known, we determined the z_0 roughness altitude, as well as the α exponent of the power law exponent relationship, which proved the direct effect of the roughness elements in the vicinity on the shape of the wind profile.

From the data of the tower measurements in Paks, the following could be determined:

- In Paks, on the basis of the average of 2001, the inflection height, i.e. the height where the wind speed has no daily course, is located around 40-50 m. The daily course around 1 p.m. has its maximum below this altitude and its minimum above it.
- The potential daytime wind power is only higher or equal with the night-time values up to an altitude of 30 m. The potential wind power is already twice as high at night at an altitude of 60-70 m, and more than 3.5 times at 120 m than the corresponding daytime values.

We also intend to carry out further measurements aimed at determining the inflection height and the daily courses of wind energy at other locations, with the use of the SODAR equipment. According to *Figure 4*, the average speeds between 50 and 60 m are more or less the same at all three locations studied; therefore, we expect results similar to that published here. For this reason, the authors propose the reconsideration the concepts of utilisation of wind energy in Hungary.

Acknowledgements: The research project was carried out in the framework of grant programme NKTH 3a/0038/2002 "Investigation of the renewable atmospheric energy resources in Hungary, mapping existing potentials and supporting their use with the help of meteorological measurements and forecasts".

REFERENCES

BAUMANN, K. – PIRINGER, M. (2001): Two-years of Boundary Layer Measurements with a Sodar - Statistics and Application. Phys. Chem Earth (B) 26: 205-211.

DOBI, I. – VARGA, B. - TAR, K. – TÓTH, L. – GERGEN, I. – CSENTERICS, D. (2006): Summary of Hungarian wind and solar energy. In: Proceedings of International Conference on Climate Change: Impact and Responses in Central and Eastern European Countries. 2006. 289-293.

IEA (2005): Variability of wind power and other renewables - Management options and strategies. IEA/OECD, Paris, France. Online: www.iea.org/textbase/papers/2005/variability.pdf.

KOPPÁNY, Gy.1978: Hosszútávú előrejelzés. [Long-range forecast.] Tankönyvkiadó, Budapest (in Hungarian)

MELLINGHOFF, H. – ALBERS, A. – KLUG, H. (2000): SODAR Measurements in Complex Terrain. In: DEWEK 2000 Tagungsband. pp. 116-119. Online: www.dewi.de/dewi/themen/bibli/pdf/mellinghoff_SODAR_DEWEK2000.pdf.

RADICS, K. (2004): A szélenergia hasznosításának lehetőségei Magyarországon: hazánk szélklímája, a rendelkezésre álló szélenergia becslése és modellezése. [The possibilities of wind energy utilization in Hungary] PhD thesis University of L. Eötvös, Budapest (in Hungarian).

SEIBERT, P. (1998): Long-time comparison of Remtech PA2 sodar wind and turbulence measurements with Cabauw tower data. In: Proc. 9th Int. Symp. on Acoustic Remote Sensing and Assoc. Techniques of the Atmosphere and Oceans. Vienna, Austria August 1998.

STELCZER, B. (2007): A kulcsi szélerőmű működési tapasztalatai. [Experience Report from Hungary's First Wind Power Station] RENEXPO Central and South-East Europe 2007 International Trade Fair and Congress for renewable energy and energy efficient construction and renovation. Budapest, Hungary 20 April 2007 (in Hungarian) Online: http://www.mszet.hu/index.php?p=downloads&parent=24&did=24

TAR, K. (2004): Estimation methods to determine the wind energy potential in Hungary. *Magyar Energetika* 2004: XII. 4: 37-48 (in Hungarian).

TAR, K. (2007a): Some statistical characteristics of monthly average wind speed at various heights. Renewable and Sustainable Energy Reviews. Online: DOI: 10.1016/j.rser.2007.01.14

TAR, K. (2007b): Methods for estimation of wind energy potential in Hungary. *Dissertationes Savarienses 44,* Societas Scentiarium Savariensis, Savaria University Press, Szombathely 2007 (in Hungarian).

TAR, K. (in press): Diurnal course of potential wind power with respect to the synoptic situation. Időjárás.

VOGT, S. – THOMAS, P. (1995): SODAR - A useful remote sounder to measure wind and turbulence. Journal of Wind Engineering and Industrial Aerodynamics 54/55: 163-172.

WINDOGRAPHER 1.04 Mistaya Engineering Inc. Calgary, Alberta, Canada. Online: http://www.mistaya.ca/index.htm

WRPLOT VIEW 5.2.1 Lakes Environmental Softwer. Waterloo, Ontario, Canada. Online: http://www.weblakes.com/lakewrpl.html#About

Acta Silv. Lign. Hung., Vol. 4 (2008) 127-132

Black Locust *(Robinia pseudoacacia* L.*)* Improvement in Hungary: a Review

Károly RÉDEI * – Zoltán OSVÁTH-BUJTÁS – Irina VEPERDI

Hungarian Forest Research Institute, Budapest, Hungary

Abstract – Black locust (*Robinia pseudoacacia* L.) was the first forest tree species introduced and acclimated from North America to Europe at the beginning of the 17th century. It is a fast growing, nitrogen fixing, site tolerant, excellent coppicing species with frequent and abundant seed production and relatively high yielding potential. It has a durable and high quality wood, which is used for many purposes. Although native of North America, black locust is now naturalized and widely planted throughout the world from temperate to subtropical areas. In Hungary, this species has played a role of great importance in the forest management, covering approximately 23% of the forested area and providing about 19% of the annual timber output of the country. Due to the increasing interest in black locust growing in many countries, this study has been compiled with the aim of giving a summary on the basis of research and improvement connected with the species over the past decades.

Black locust *(Robinia pseudoacaia* L.) / clone selection / silviculture / yield / energy plantations

Kivonat – Áttekintés a magyarországi akácnemesítésről. A fehér akác (*Robinia pseudoacacia* L.) az első észak-amerikai erdei fafaj volt, amely, alkalmazkodva a klimatikus feltételekhez, a XVII. század elején meghonosodott Európában. Gyorsan növő, nitrogén-megkötő, termőhelytűrő, könnyen sarjadó fafaj, gyakori és bőséges magterméssel és viszonylag jó fatermőképességgel. Tartós, jó minőségű fája számos célra felhasználható. Bár Észak-Amerikában őshonos, mára elterjedt és széleskörűen telepíthető az egész világon a mérsékelt éghajlatútól a szubtropikus területekig. Magyarországon fontos szerepet játszik az erdőgazdálkodásban, az erdősült terület mintegy 23%-át borítja, és az ország éves fakitermelésének 19%-át teszi ki. Tanulmányunkat a fafaj termesztése iránti megnövekedett érdeklődés kapcsán, összefoglalás céljából állítottuk össze az elmúlt évtizedek kutatási eredményei alapján.

Fehér akác (*Robinia pseudoacacia* L.) / klónszelekció / erdőművelés / fatermés / energetikai faültetvények

1 INTRODUCTION

Black locust was introduced in Hungary between 1710 and 1720. The first large black locust forests were established at the beginning of the 19th century on the Great Hungarian Plain stabilizing the wind-blown sandy soil. In the country, black locust occupied 37.000 ha in

* Corresponding author: fuhrere@erti.hu; H-1023 BUDAPEST, Frankel Leó u. 42–44.

1885, 109.000 ha in 1911, 186.000 ha in 1938 and 4.000.000 ha in 2005. At present, it is the most widely planted species in Hungary, covering 23% of the country's total forest area. One-third of these stands are high forests and two-third of them are of coppice origin. In the 1960s, Hungary had more black locust forests than the rest of European countries together.

Black locust forests in Hungary have been established on good as well as on medium and poor quality sites. Establishment of black locust stands producing timber of good quality is possible only on sites with adequate moisture and well-aerated and preferably light soils, rich in nutrients and humus. Black locust forests on medium and poor quality sites are utilized for the production of fuel wood, fodder, poles and props, as well as for honey production, soil protection and environmental improvement.

The most important black locust growing regions in Hungary are located in the south and south-west Transdanubia (hill-ridges of Vas-Zala county, hill-ridges Somogy county), the plain between the rivers Danube and Tisza (Central Hungary) and north-east Hungary (Nyírség region).

2 IMPROVEMENT OF BLACK LOCUST STANDS IN HUNGARY

2.1 Clone and cultivar selection

In Hungary, the main goals of the first black locust breeding programme (in the 1960's) were to select new clones and cultivars providing good quality and volume of industrial wood. Superior tree groups have been identified in some seed grown stands. Graft material was taken from the plus trees and planted in test plots at Gödöllő (experimental station of FRI). *Mono- and multiclonal cultivars* were developed and a seed orchard was established from the selections. The Hungarian Forest Research Institute coordinated this research programme. With respect to the volume expected at felling age, the *'Jászkiséri', 'Kiscsalai', 'Nyírségi', 'Üllői'* and *'Szajki'* cultivars proved to be the best (Keresztesi 1988)

In Hungary, the range of sites optimal for black locust growing is rather limited. Therefore, black locust growing is often exercised on sub-optimal sites. Possibilities for black locust growing are highly influenced by climatic conditions and extremes (temperature and precipitation, water supply and unfavourable soil conditions). In the lowlands, which are the most suitable regions for black locust growing, the annual precipitation is not more than 500-550 mm, most of which is outside the growing season. Thus drought is a frequent phenomenon in the summer period coupled with very high atmospheric temperatures (30-35 ^{o}C). Relative air humidity in July is usually between 20–50%. Due to the filling up of basin-like lowlands in Hungary, site conditions show a mosaic pattern, which changes even over small distances causing widely differentiated growth potential for black locust plantations. For this reason, there are no large, contiguous lands of homogenous site quality for black locust, and their growth and productivity may be very different across a large field. Therefore, the main aim of our new selection work is to find and improve black locust clones and cultivars, which perform good shape, provide good-quality wood material for industrial purposes, and which are able to tolerate the changing ecological conditions as well. As a result of our new selection programme 12 black locust clones ('KH 56A 2/5', 'KH 56A 2/6', 'MB 12D', 'MB 17D 4/1', 'CST 61A 3/1', 'MB 15A 2/3', 'MB 17D 3/10', 'PV 201E 2/1','PV 201E 2/3', 'PV 201E 2/4', 'PV 35 B/2',and 'PV 233 A/2') have been recommended (Rédei et al. 2002, Rédei 2003).

2.2 Propagation

In Hungary, black locust plants are commonly multiplied by two methods: by seed and by root cuttings. Growing trees from *seed* is a relatively simple method for reliably producing seedlings on a large scale under a variety of circumstances. There are two state approved seed production stand-regions meeting the requirements for black locust seeds (one in the plain between the rivers Danube and Tisza and the other in the Nyírség region). Seeds are collected by sieving the top 20 cm of soil beneath the selected seed-producing stands. As the seeds of black locust used to remain dormant in the soil for several years, the age of seeds within the lots collected in this way is very variable. This is the reason of viability and germination are so variable. Therefore, before sowing, an accurate seed test is necessary. Seed production for sowing and scarification is carried out by the agency responsible for collecting the seed. It is advisable to treat the seeds against fungi, and this is done in a small concrete mixer. 200-250 thousand seedlings of 40-90 cm high and 5-12 mm in base diameter are raised on one hectare. Mechanization of the method is easy and the production costs are relatively low.

Propagation from root cuttings is suitable for reproduction of superior individuals or varieties (cultivars). By applying this method, superior traits of the selected trees can be preserved in the clones. Production of plants in this way demands more care than raising seedlings from seeds. For this propagation method, root pieces cut into 8–10 cm or chopped to 3-5 cm in length are used. Plant spacing in the rows should be 5-8 cm.

Almost 25 new cultivars or selected clones were micro-propagated during the last few years in the Micro-propagation Laboratory of Research Institute for Fruit growing and Ornamentals, Érd in collaboration with the Hungarian Forest Research Institute. Plant tissue culture methods provide us with new means to speed up vegetative propagation of recently selected clones and give us the opportunity to establish new clone trials and a seed orchard with them.

2.3 Stand establishment, forest tending and yield

Climate, hydrology and genetic soil types are the factors that determine the site type, and this in turn determines the choice of tree species. The water regime of the soil is also highly influenced by the texture of the soil, whether it is humus, coarse sand, loam or clay. Black locust – because of its high requirement for both water and aeration in the soil – cannot be grown even on any soil composed of humus, coarse sand or clay if the rooting depth is very shallow.

Black locust requires well-drained soils with adequate moisture until the associated nitrogen-fixing *Rhizobium* bacteria are able to thrive. That is why soil preparation (total or partial) to improve aeration and the water regime of the soil and tilling of the inter-row space may become necessary.

Black locust afforestation and artificial regeneration may utilise seedlings. The most popular spacing for black locust in Hungary is 2.4 m by 0.7 to 1.0 m, requiring at least 4000 seedlings/ha. Black locust stands are often regenerated by coppice (from root suckers) as well. In young stands of coppice origin, a cleaning operation should be carried out to adjust spacing when the stands are 3-6 years old and should reduce stocking to less than 5000 stems/ha.

The black locust is a fast-growing tree species, which, up to the age of 10-15 years, is able to close canopy openings caused by tending operations quickly, but the closure is much slower in later years. Height growth peaks within the first five years, while diameter growth culminates in the first decade. The peak of current annual increment is at about the age of 20, whereas that of the mean annual increment is at about the age of 35-40 years.

To find the right cleaning and thinning intensity, the so-called growing space index is a good method. This index expresses the mean distance between trees (in a triangular pattern)

as a percentage of mean height after cleaning and thinning. The mean value of the index for black locust stands should be 23-24%. Pruning of crop trees should also be carried out. After finishing selective thinning, stems must be free of branches up to a height of 4-6 m.

The objective of tending is to produce a high proportion of good quality saw-logs from stands of yield class I and II; some saw-logs and a high proportion of poles and props from stands of yield class III and IV; and poles, props and other small-dimension industrial wood from other yield stands.

According to our yield table (Rédei 1984) the volume of main crop varies between 80 and 280 m^3/ha in function of yield classes at the age of 30 years, which is the average rotation age for black locust stands in Hungary. The black locust stands of Yield Class I–II have a rotation of 35-40 years and an annual increment of total volume of 12-14 m^3/ha/yr. The stands of Yield Class III–IV have a rotation of 30 years and an annual increment of 8-9 m^3/ha/yr. Finally, the poorest stands (Yield Class V–VI) have a rotation of 20-25 years and an annual increment of 4-6 m^3/ha/yr. In first generation coppice stands, growing stock, increment and health are similar to those in high forests.

2.4 Black locust energy plantations

More and more agricultural land is being taken out of use for food crops, some of which can be used for wood energy production plantations. Black locust is the very best tree species for this purpose, since it has excellent energy production properties, such as:

- vigorous growing potential in juvenile phase,
- excellent coppicing ability,
- high density of the wood,
- high dry matter production,
- favourable combustibility of the wood,
- relatively fast drying,
- easy harvesting and wood processing.

In the last decade several energy producing plantations have been established in Hungary. In these experiments, several spacing treatments were tested and the common black locust as well as its cultivars were compared.

In Helvécia (central Hungary, sand-soil region) an energy plantation was established using common black locust and its cultivars. The various spacings of the common black locust were: 1.5x0.3 m, 1.5x0.5 m and 1.5x1.0 m. At the age of 5 years the closest spacing (1.5x0.3 m) produced the greatest annual increment in oven-dry mass (6.5 t/ha/yr). This exceeded the increments of the two wider spacings by 33% and 51%, respectively. According to the results of the yield trial with black locust cultivars planted at 1.5x1.0 m spacing, at 5 years the highest yield was produced by the cultivar '*Üllői'* (8.0 t/ha/yr), followed by '*Jászkiséri'* (7.3 t/ha/yr) and the common black locust (6.7 t/ha/yr).

Black locust energy forests can also be established by coppicing. Advantages of energy forests of coppice origin are that the cost of establishment is low compared to that of soil preparation, plantation and cultivation. From the developed root system of the previous stand, a large dendromass can be produced within a short time period. Disadvantages of these forests are that the area distribution of trees in coppice stands is not as uniform as in plantations optimized for energy production. In coppice stands the quantity of the produced dendromass is lower and the length of growing time is highly influenced by the uneven distribution of stems.

The first peak of the annual increment in volume of black locust energy forests established from sprouts falls between the age of 3 and 5 years. Then, the annual increment declines and a new peak occurs between age of 9 and 12 years. A further maximum is

expected later on, at about 15 years because of an even higher degree of mortality. Approximately one-third of the stems are lost at age 7 and 8. By the 12-13 years, the stem numbers decreased to less than 50%.

The experiences from both the planted and the coppiced energy plantations and other stands indicate that it is not reasonable to harvest in the first three years, as the yield in oven-dry weight in the fifth year is 2-3 times higher than it is in the fourth year. Harvesting too early may also increase the population of biotic pests.

3 CONCLUSION

Black locust was the first forest tree species introduced from North America to Europe. Hungary has got much experience in black locust growing, as it has been grown for more than 250 years in the country. Being aware of the importance of black locust, forest research in Hungary has been engaged in resolving various problems of black locust management for a long time, and a lot of research results have already been implemented in the practice.

In the future there are two bigger regions, where the fast spread of black locust can be expected. In Europe the Mediterranean countries (Italy, Greece, Spain and Turkey), while in Asia China and Korea may become the most prominent black locust growers.

REFERENCES

HALUPA, L.- RÉDEI, K. (1992): Establishment of forests primarily for energetic purpose. Erdészeti Kutatások. Vol. 82-83: 267-286.

KERESZTESI, B. (1983): Breeding and cultivation of black locust (*Robinia pseudoacacia* L.) in Hungary. Forest Ecology and Management. 6: 217-244.

KERESZTESI, B. (ed.) (1988): The Black Locust. Akadémiai Kiadó, Budapest.

RÉDEI K. (1984): Akácosok fatermése. [Yield of Black Locust Stands]. FRI Research Report, Budapest. (in Hungarian)

RÉDEI K.(1986): Waldpflege in den ungarischen Robinienwäldern. Die Holzzucht, 40. 1-2:1-4.

RÉDEI K. (1991): Management of Black Locust Stands in Hungary. 10th World Forestry Congress. Voluntary Contributions. Paris, Proceedings 4:289-294.

RÉDEI K. (1992): Management of Black Locust Stands in Hungary. Proceedings: International Conference on Black Locust. East Lansing (MI), 38-43.

RÉDEI K. (1996): Yield study relations of regeneration of Robinia (*Robinia pseudoacacia* L.) stands. In: Skovsgaard. J. P. &V. K Johannsen (eds.) 1996. Modelling Regeneration Success and Early Growth of Forest Stands. Proceedings form the IUFRO Conference. Hoersholm, 105-111.

RÉDEI K. (2000): The Role of Black Locust (*Robinia pseudoacacia* L.) in Establishing Wood Energy Plantation. Hungarian Agricultural Research, 9.4:4-7.

RÉDEI, K. – MEILBY H. (2000): Effect of thinning on the diameter increment in black locust stands (*Robinia pseudoacacia* L.). Silva Gandavensis, 65:115-127. Gent, Belgium.

RÉDEI, K. – OSTVÁTH-BUJTÁS, Z. – BALLA, I. (2001): Vegetative Propagation Methods for Black Locust (*Robinina pseudoacacia* L.) Improvement. Hungarian Agricultural Research, 10.2:6-9.

RÉDEI, K.(2001): The main characteristics of black locust (*Robinia pseudoacacia* L.) management in Hungary. Third Balcan Scientific Conference. Proceedings, Sofia, 293–300.

RÉDEI, K. – OSTVÁTH-BUJTÁS, Z. – LEE, J. (2002): Selection and management of black locust (*Robinia pseudoacacia* L.) in Hungary for timber and honey production and landscape. Journal of Korean Forestry Society, 91:156-162.

RÉDEI, K. (2002): Improvement of Black Locust (*Robinia pseudoacacia* L.) in Hungary. IUFRO Meeting on the Management of Fast Growing Plantations. Izmit, Turkey, Proceedings, 166-173.

RÉDEI, K. – OSVÁTH-BUJTÁS, Z. – BALLA, I. (2002): Clonal approaches to growing black locust (Robinia pseudoacacia) in Hungary: a review. Forestry, Vol. 75, (5): 548-552.

RÉDEI, K. (ed.) (2003): Black Locust (*Robinia pseudoacacia* L.) Growing in Hungary. FRI Publication, Budapest.

RÉDEI, K. – OSTVÁTH-BUJTÁS, Z. – VEPERDI, I. (2006): Black locust (*Robinia pseudoacacia* L.) clonal seed orchards in Hungary. For. Stud. China, 8(4): 47-50.

RÉDEI, K. – OSTVÁHT-BUJTÁS, Z. – VEPERDI, I. – BAGAMÉRY, G. – BARNA T. (2007): La gestion du robinier en Hongrie. Foret enterprise. No 177, 5: 44-49.